October 2011

Explosives Dissolved from Unexploded Ordnance

Prepared by:

U.S. Army Environmental Command
Fort Sam Houston, TX 78234-7664

U.S. Army Corps of Engineers, Engineer Research and Development Center
Cold Regions Research and Engineering Laboratory
Hanover, NH 03755

Report Documentation Page

Form Approved
OMB No. 0704-0188

1. REPORT DATE	2. REPORT TYPE	3. DATES COVERED
31 MAY 2012		

4. TITLE AND SUBTITLE	5a. CONTRACT NUMBER
Explosives Dissolved From Unexploded Ordnance	5b. GRANT NUMBER
	5c. PROGRAM ELEMENT NUMBER

6. AUTHOR(S)	5d. PROJECT NUMBER
Susan Taylor; Susan Bigl; Carrie Vuyovich; Jeanne Roningen; Anna Wagner	5e. TASK NUMBER
	5f. WORK UNIT NUMBER

7. PERFORMING ORGANIZATION NAME(S) AND ADDRESS(ES)	8. PERFORMING ORGANIZATION REPORT NUMBER
Cold Regions Research and Engineering Laboratory,US Army Engineer Research and Development Center,72 Lyme Road,Hanover,NH,03755-1290	

9. SPONSORING/MONITORING AGENCY NAME(S) AND ADDRESS(ES)	10. SPONSOR/MONITOR'S ACRONYM(S)
	11. SPONSOR/MONITOR'S REPORT NUMBER(S)

12. DISTRIBUTION/AVAILABILITY STATEMENT

Approved for public release; distribution unlimited.

13. SUPPLEMENTARY NOTES

The original document contains color images.

14. ABSTRACT

For this work we: 1) sampled soil below unexploded ordnance (UXO) found in situ and noted the conditions of the rounds, 2) conducted laboratory tests to help us estimate high explosive (HE) dissolution from different sized holes in corroded rounds, and 3) used the modeling program Hydrus-1D and weather records to predict the ownward movement of the explosives into the soil. Although most of these UXO looked highly corroded, our laboratory tests on the metal casings show that iron oxides quickly seal any small holes. Consequently, we think that pitting is not an important release route for HE. However, if the holes are large enough-such as cm-sized perforations caused by fragmentation hits-dissolution of the fill occurs, and over time, hollows out a cavity in the fill increasing the surface area of the fill available for dissolution.

15. SUBJECT TERMS

16. SECURITY CLASSIFICATION OF:			17. LIMITATION OF ABSTRACT	18. NUMBER OF PAGES	19a. NAME OF RESPONSIBLE PERSON
a. REPORT	b. ABSTRACT	c. THIS PAGE			
unclassified	**unclassified**	**unclassified**	**9**	**103**	

Explosives Dissolved from Unexploded Ordnance

October 2011

Susan Taylor, Susan Bigl, Carrie Vuyovich, Jeanne Roningen, Anna Wagner, Nancy Perron, Steven Daly, Marianne Walsh, and James Hug

Cold Regions Research and Engineering Laboratory
Hanover, New Hampshire

Prepared for U. S. Army Environmental Command

Cover: A 60-mm mortar (CS-09-8) found at ERF in 2009 and thought to have been fired during a 2006 training exercise showing the (top) visible side and (bottom) side in contact with the soil.

Table of Contents

List of Figures and Tables

Figures

Tables

Terms and Acronyms

C4	Composition C4, plastic explosive with 91% RDX
CAS#	Chemical Abstracts Service numerical identifiers
Comp B	Composition B, a 39:60 mix of TNT and RDX that contains ~1% wax
CRREL	Cold Regions Research and Engineering Laboratory
ERDC	Engineer Research and Development Center
ERF	Eagle River Flats (impact area within Fort Richardson, near Anchorage, Alaska)
HE	High Explosives- chemical compounds that combust so rapidly that the resulting supersonic shock wave causes the mass to detonate.
HMX	A high explosive, 1,3,5,7,-octahydro-1,3,5,7-tetranitrotetrazocine (often a bi-product of RDX production)
HPLC	High performance Liquid Chromatography
IC	Ion conductivity
MMR	Massachusetts Military Reservation
NCDC	National Climatic Data Center, a division of the National Ocean and Atmospheric Administration
Octol	70:30 mix of HMX and TNT
PET	potential evapotranspiration
RDX	A high energy explosive, 1,3,5-hexahydro-1,3,5-trinitro-1,3,5-triazine
RMS	Root mean square
TNT	2,4,6-trinitrotoluene, a high energy explosive
Tritonal	70:30 or 80:20 mix of TNT and aluminum powder
USDA	U.S. Department of Agriculture
USEPA	U.S. Environmental Protection Agency
UXO	Unexploded ordnance

Acknowledgements

The authors thank the U. S. Army Environmental Command (AEC) for their financial support as well as Robert Kirgan, the project manager. We are grateful to Bonnie Packer and Kim Watts, of AEC, for their advice and assistance during the 2009 sampling campaign in Vieques, PR. We also appreciate the support provided by several personnel with CH2MHill Inc., the Environmental Restoration Contractor cleaning up the Vieques Naval Training Range, in particular Philip Fitzwater, Tim Garretson, and Billy Capstick. Madeline Riviera, the Navy coordinator at Vieques, also supported our efforts. Our UXO technician Christopher Graber, of USACE Fort Worth District, excelled in his duties during the 2010 Vieques sampling trip. And finally, we thank Jae Yun, the Parsons site manager who helped us with access to the San Luis Obispo, CA site.

Executive Summary

For this work we: 1) sampled soil below unexploded ordnance (UXO) found *in situ* and noted the conditions of the rounds, 2) conducted laboratory tests to help us estimate high explosive (HE) dissolution from different sized holes in corroded rounds, and 3) used the modeling program Hydrus-1D and weather records to predict the downward movement of the explosives into the soil.

We sampled soils beneath and near UXO at three sites, Eagle River Flats, Alaska, Camp San Luis Obispo, California and Camp Garcia on the island of Vieques, Puerto Rico. We sampled below 42 UXO found *in situ* that were at various stages of corrosion and ranged in size from 60 mm to 155 mm. Of these, seven (16%) were found to be leaking HE into the surrounding soil. We found explosives in soils both below the round and also laterally away from the round. Concentration levels ranged from < 1 to 110 mg kg^{-1}. For cores we found the highest concentrations nearest the round and decreasing concentrations with depth. We were able to recover and analyze dissolved explosives in the pore water with concentrations around 1 mg L^{-1}.

Our field observations indicate that much more HE is released into the soil from partially detonated rounds, or rounds where loss of the casing exposed the explosive fill. If the UXO had exposed HE fill, the soil beneath it contained HE and the concentrations were higher than those measured for the corroded rounds– 26,000 mg kg^{-1} in the highest case–due to the presence of particles in the soils. We sampled beneath one round that had only partially detonated; many other partially detonated rounds were observed, but they had been moved to collection points to be blown in place.

Both at Camp Luis Obispo and at Vieques we found that oxidation of the metal casing caused the metal to swell, forming both longitudinal and circumferential cracks in the casing. At Vieques, many of these rounds had shed their metal casing leaving their entire HE fill exposed. Often the HE cores were quite smooth and not pitted suggesting that the casing failed quickly. In a few instances we saw cracks in the casing reflected in the underlying fill, indicating that water had penetrated and dissolved some of the HE.

Although most of these UXO looked highly corroded, our laboratory tests on the metal casings show that iron oxides quickly seal any small holes. Consequently, we think that pitting is not an important release route for HE. However, if the holes are large enough—such as cm-sized perforations caused by fragmentation hits—dissolution of the fill occurs, and over time, hollows out a cavity in the fill increasing the surface area of the fill available for dissolution.

Introduction

Unexploded ordnance clearly present an explosive hazard but they also present a contamination point source if the casing is breached and the explosive fill is dissolved by water and transported to surface or groundwater. Restricting access to a site or blowing UXO in place

mitigates the explosive hazard, but does little to mitigate contaminating the site; UXO will eventually leak explosives and blown-in-place operations can spread HE particles onto nearby soil. The costs of finding and removing or detonating the UXO, however, are high. For this reason it would be helpful to know how many UXO can be left in an acre of land without contaminating the groundwater above drinking water levels. The answer to this question entails knowing the mass of HE available for dissolution, the dissolution rate as a function of HE mass and water flow rate, the local precipitation rate, the depth to groundwater and how the HE breaks down in the local soil. The local precipitation and depth to groundwater are easy to determine, the dissolution rate of explosives has been measured and modeled (Lever et al. 2005, Taylor et al. 2009) and some information exists on the breakdown rate of HE in different types of soils. The largest uncertainty, however, is the mass of HE available for dissolution, which depends on the number, type and condition of the UXO present at the site. This information, in turn, depends on multiple variables such as how long the site has been used, the number of rounds fired into the site, the dud and partial detonation rate of munitions fired, the thickness and composition of round casing, mass and type of HE in the rounds, how long the UXO have been in the field, how many are intact, how many are corroded and leaking HE, and how many are broken and exposing HE directly to water. Many of these variables are poorly known.

Some of this information can be gleaned from range records and technical manuals. However, the condition of UXO is unknown unless they are on the surface. This information is critical for estimating the likelihood of HE release. If the UXO are intact and the range has desert-like conditions, the rounds will not corrode quickly; furthermore, any exposed chunks of HE would take a long time to dissolve due to the low precipitation rates. Conversely wet, oxidizing, or saline soils all increase corrosion and the likelihood that thin-skinned casings will be breeched quickly—on decade time scales. High rainfall rates and warm temperatures increase the dissolution of any exposed HE, be it from UXO that are corroded (pits, wholesale loss of casing or loss of the fuse by galvanic corrosion), broken upon impact or split by fragments from a nearby high-order detonation.

UXO Corrosion

Undamaged UXO casings corrode in the environment and, if the casing is corroded through, can release the high explosive fill into the surrounding soils. The rates at which the steel casings corrode depend on the composition of their constituent metal(s), on a host of soil characteristics, and on any coatings formed on, or applied to, the metal.

Taylor et al. (2004) compiled corrosion rates for the main steel types used to manufacture common military rounds. The lowest rates (<0.001 mm yr^{-1}) were reported for Stainless Steel or Aluminum in an aerobic water environment. The highest rates (1-1.5 mm yr^{-1}) were reported for steel containing carbon and manganese in flooded soils that were anaerobic and sulfidic.

Soil characteristic important for corrosion include: aeration, electrolyte content, pH, the type and number of soil bacteria, and moisture (Romanoff 1957, Nalbandian and Kalkian 2007). Gen-

erally, corrosion will occur more slowly in: aerated rather than anoxic soils, soils with high resistivity (above 30,000 ohm-cm) rather than low resistivity (less than 1,000 ohm-cm), and soils with pH between 4.5 and 9.0 rather than pH less than 4.5 or above 9.0. Soil bacteria can accelerate corrosion by locally increasing the electrical conductivity and decreasing the pH of the soil. Poorly drained soils (high moisture content) also result in higher corrosion rates especially if the moisture has high dissolved oxygen content (Manahan 1994).

Corrosion of metal is rarely uniform, but has been reported to occur in an extremely localized area resulting in holes (Nalbandian and Kalikian 2007). This phenomenon, called pitting, is caused by contact with soil, organic material, or salt (Szklarska-Smialowska 1986). The pits, in most cases, occur on the sides of the round in contact with soil where moisture can collect. Over time more pits form but the pit diameter does not significantly increase in size. More commonly, the pits are fouled by oxidation products resulting in a narrowing of the pit diameters and decreased HE leakage. Oxidation rinds developed on the metal surface result in a slower corrosion of the underlying metal (Nalbandian and Kalkian 2007). Corrosion-protective paint also slows the corrosion rate of the surface; however, these paint coatings are often damaged during ground impact.

Nalbandian and Kalikian (2007) estimated corrosion rates and examined the types of corrosion occurring on inert items removed from the Massachusetts Military Reservation (MMR). They measured pit densities from fifty projectiles and cartridges and found between 2 to 7 pits cm^{-2} and pit sizes ranging from 0.8 to 6.4 mm. These values are similar to those found by Chendorain et al. (2004) who examined 161 UXOs and determined a pit density of 7.3 pits cm^{-2} and a typical pit diameter of 1 mm. From the pit depth and the age of the round, Nalbandian and Kalikian (2007) estimated a corrosion rate between 0.015 and 0.048 mm yr^{-1} and a time to perforation between 97 and 662 years. It was noted that despite more than 50 years of exposure, corrosion had perforated none of the items (Nalbandian and Kalikian 2007).

Dissolution rates of high explosives

Dissolution is the first step in environmental transport of explosives from high explosives. Factors affecting the dissolution rate of the explosive fill in a UXO include: the solubility of the explosive, the HE surface area 'seen' by the water, the refresh rate of the water interacting with the explosive, and the type and concentration of ions present in the water.

Dissolution rates of explosives were studied using laboratory column and batch tests (e.g. Monteil-Rivera et al. 2010; Lynch et al. 2002 a, b; Morley et al. 2006; Furey et al. 2008). The column tests place known amounts of HE on or in the soil and measure the HE exiting the soil column under different flow conditions. The batch tests measure dissolution of a known mass of RDX, TNT, or HMX or Comp B in fixed water volumes, stirred at constant rates, and maintained at constant temperatures. The latter tests are applicable to underwater UXO if the stirring rate can be related to flow rate past the opening in the UXO and if the surface area of HE exposed to the water can be estimated. The dissolution rate of totally exposed HE (batch test) is faster than HE

placed in soil columns where only a fraction of the surface might be wetted at any given time (Furey et al. 2008). This was also the case for gypsum under saturated and unsaturated water conditions where only 2.2 % of the surface was dissolving in the unsaturated experiment (Kuechler et al. 2004). HE dissolution rates in unsaturated soils should be much lower due to the small portion of HE surface that is being wetted and should increase with increasing flow rates.

Lever et al. (2005) took a different approach and dripped water on an HE piece at a known rate, a process that simulates rainfall. The concentration of the water interacting with the HE pieces was measured and used to parameterize a dissolution model. The model has a simple physical interpretation: all rainfall captured by the particle flows off it fully saturated in HE (Lever et al. 2005). Taylor et al. (2010) validated the drop impingement model using three years of outdoor dissolution data collected from different types and sizes of HE pieces supplemented with concurrent rainfall and temperature records. Temperature is an important input parameter because HE solubility is temperature dependent. Model results for two TNT and Tritonal chunks are shown in Figure 1. A nearly linear relationship exists between dissolution rate and rainfall rate, which makes it possible to link average annual HE influx to average annual rainfall. They predict that, in the absence of breakage and disaggregation, 1–10 g pieces should last 30–100 years. As the data were collected in an area with a ~100 cm yr^{-1} rainfall rate, the dissolution would be higher at wetter and warmer sites and lower at drier and colder sites.

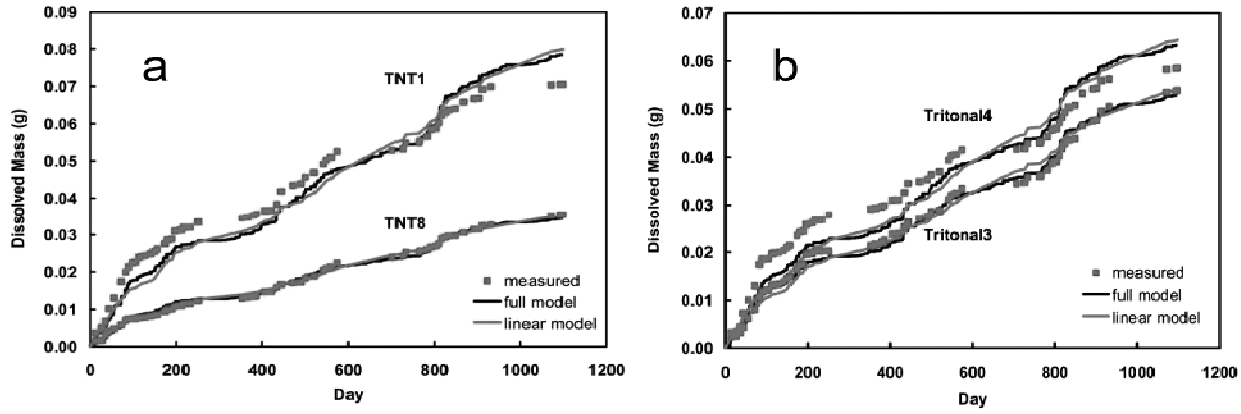

Figure 1. TNT mass loss versus time for a) TNT-1 and TNT-8 and b) Tritonal-3 and Tritonal-4 including predictions from the drop impingement model. The full model used the temperature and rainfall records as input parameters, the linear model used the yearly rainfall and temperature average (Taylor et al. 2010).

Although dissolution rate changed as the HE pieces became smaller, an average value for each of the explosive pieces used by Taylor et al. (2010) was calculated by dividing the mass lost by the estimated surface area of the piece (assuming the initial particle had a spherical shape) multiplied by the number of hours (Table 1). Because Tritonal (80%TNT and 20% aluminum) and C4 (91% RDX) are not 100% HE, their dissolution rates have been adjusted to account for the percent that is HE. The dissolution value for Comp B is lower than that for TNT because it contains 60% RDX, which has a lower solubility than TNT.

The rates determined from Taylor et al. (2010) outdoor test data are much lower than those estimated from the column or batch tests. The lower rates are reasonable given that the HE pieces were not immersed in water that was being stirred. Also some of the batch and column experiments crushed the HE to obtain particles of a given size range. Scanning electron images of similarly crushed explosives show they are covered in submicron grains, which quickly dissolve and account for the higher initial dissolution rates found in those experiments.

Because UXO can be found in saline environments, Brannon et al. (2005) measured TNT dissolution rates in salt water and found it was lower than in freshwater. The solubility of many organic compounds is reduced in saltwater due to the "salting-out" or "salt" effect. Prak and O'Sullivan (2006) also found lower solubilities of 2,4-DNT and TNT in seawater than in freshwater.

Table 1. Dissolution rates for HE exposed to outdoor conditions calculated from data in Taylor et al. (2010). C4 pieces were outdoors for 964 days; all other high explosive (HE) pieces were exposed for 1100 days.

Type	# HE pieces	Initial masses (g)	Masses dissolved (g)	Surface area (cm^2)	Average dissolution rate ($\mu g\ cm^{-2}\ hr^{-1}$)
TNT	10	0.4 to 2.0	0.10 to 0.22	1.3 to 4.0	2.5 ± 0.7
Comp B	11	0.3 to 5.1	0.07 to 0.37	1.2 to 6.7	2.3 ± 0.8
Tritonal	4	2.2 to 5.3	0.20 to 0.33	4.2 to 7.7	1.4 ± 0.2*
C4	6	0.2 to 4.9	0.04 to 0.33	0.8 to 7.3	1.8 ± 0.1*
* Mass adjusted for percent of HE in composition.					

Transport of HE through the vadose zone

Different explosives interact with various soil types differently; they can bind to soil and break down chemically or biologically while in solution (Brannon and Pennington 2002). Geo-sorbents and reactive minerals greatly affect HE transport rates. For example, RDX was found to be persistent and mobile in comparison with TNT, which photo-degrades rapidly and is aerobically bio-transformed to 2-Am-DNT and 4-Am-DNT (McCormick et al. 1976). Among six soil types, Larson et al. (2008) found that Ottawa Sand (with the smallest value for total organic carbon, surface area, and percent fines) sorbed the least amount of RDX and TNT. Larson et al. (2008) also reported that the dissolution rates for soil column experiments using Ottawa sand were one or more orders of magnitude lower compared to water-only batch tests, consistent with the fact that the HE in soil column studies are not "seeing" all of the water passing through the column.

Study description

For this study we focused on: 1) determining if HE was leaking from UXO and the conditions under which this occurs, 2) estimating the rate at which the HE dissolves from holes in UXO, and 3) estimating dissolved HE transport in soils. To accomplish our goals we: 1) sampled soil below UXO found *in situ* in the field and noted the conditions of the rounds, 2) conducted

laboratory tests to help us estimate HE dissolution from different sized holes in corroded rounds, and 3) used Hydrus-1D and rainfall records to predict the downward movement of the explosives into the soil.

We sampled below UXO at two sites where UXO were being cleared (Camp San Luis Obispo, California and Camp Garcia on the island of Vieques, Puerto Rico); we also sampled below UXO at Eagle River Flats, Alaska. Two of these sites, Eagle River Flats and Vieques, have soil and climate conditions that accelerate corrosion (poorly draining soils, high rainfall). Here thin-skinned rounds were most likely to corrode through to the fill providing us the highest chance of detecting and quantifying any HE dissolving from the round. We took the opportunity to sample landmines being exhumed at CRREL and although we do not discuss the results in the body of the report we have added the findings in Appendix A.

Since we could not control the variables affecting the rate of HE leakage from UXO in the field, we measured and modeled the dissolution rate of gypsum, a non-explosive filler, from practice rounds. We then scaled the dissolution rates based on solubility differences between gypsum and the HE fill and exposed surface area.

Given HE surface concentrations, we used Hydrus-1D, a one-dimensional aqueous transport model, to predict of explosives could reach ground-water. Many factors determine the fate and transport of HE from UXO. Since we know the values for these factors with less or greater degrees of certainty the resulting HE dissolved loads will have large uncertainties associated with them.

Field and Laboratory Experiments

Site Descriptions

The three chosen locations have diverse climates and moisture regimes – a tidally influenced estuarine salt marsh in south central Alaska near Anchorage, an upland site in San Luis Obispo, California about 7 miles inland from the central coast shoreline, and the Caribbean island of Vieques off the eastern coast of Puerto Rico (Figure 2). The objective of the field sampling was to document the extent of UXO corrosion in different environments and, if these were leaking explosives, to measure the lateral or vertical concentration of energetic compounds in the soils adjacent to the round.

The diversity of the study site climates is evidenced by their long-term precipitation and temperature trends (Figure 3). Anchorage Alaska has a subarctic climate, but with strong maritime influences that moderate temperatures. Average daytime summer and winter temperatures range from about 47–58 °F and 15–25 °F, respectively). The frost-free growing season is about 120 days. Precipitation averages 16 inches a year, with around 60 inches of snow. Because of Anchorage's high latitude (61 °N), daylight hours during summer days are very long and during winter are very short.

Figure 2. Location of UXO sampling sites.

Camp San Luis Obispo has a Mediterranean climate, characterized by warm to hot, dry summers and mild, wet winters associated with influence from the North Pacific subtropical high-pressure cell. The seasonal difference in temperatures is not extreme. The relatively low latitude and proximity of the ocean result in mean winter temperatures in the mid to upper 50s (°F) and mean summer temperatures in the mid to high 60s (°F) (Figure 3). Minimum daily winter temperatures rarely dip below freezing. Annual precipitation totals 62 cm (24 in). An extremely dry period occurs between June and August with less than 0.25 cm (0.1 in) of rainfall per month. In the fall, precipitation increases to the two wettest months of January and February, which have greater than 13 cm (5 in), then in spring decreases to the summer dry period. This site has a climate with average temperatures and total annual precipitation between the other sites.

Vieques has a tropical climate that is predominantly maritime, typical of small Caribbean islands. Temperatures are quite warm and humidity is generally high, due to the presence of warm ocean waters (Figure 3). The seasonal temperature variation is small, from being near the equator (latitude 18 °N); average daytime temperatures are in the high 70s (°F) in the winter and low 80s (°F) in the summer. Precipitation averages 132 cm (52 in) per year. The months between May and November are relatively wet. Precipitation during this time is produced mainly by easterly waves, disturbances embedded in the generally east-to-west trade winds across the region. December through April, most precipitation is brought to the island by cold fronts coming from the eastern US seaboard. Precipitation at this time is somewhat drier, but some of the largest fronts that are able to reach the island can produce significant precipitation. The frequent rains in this tropical environment keep the soil damp. High humidity also contributes to maintaining high soil moisture levels.

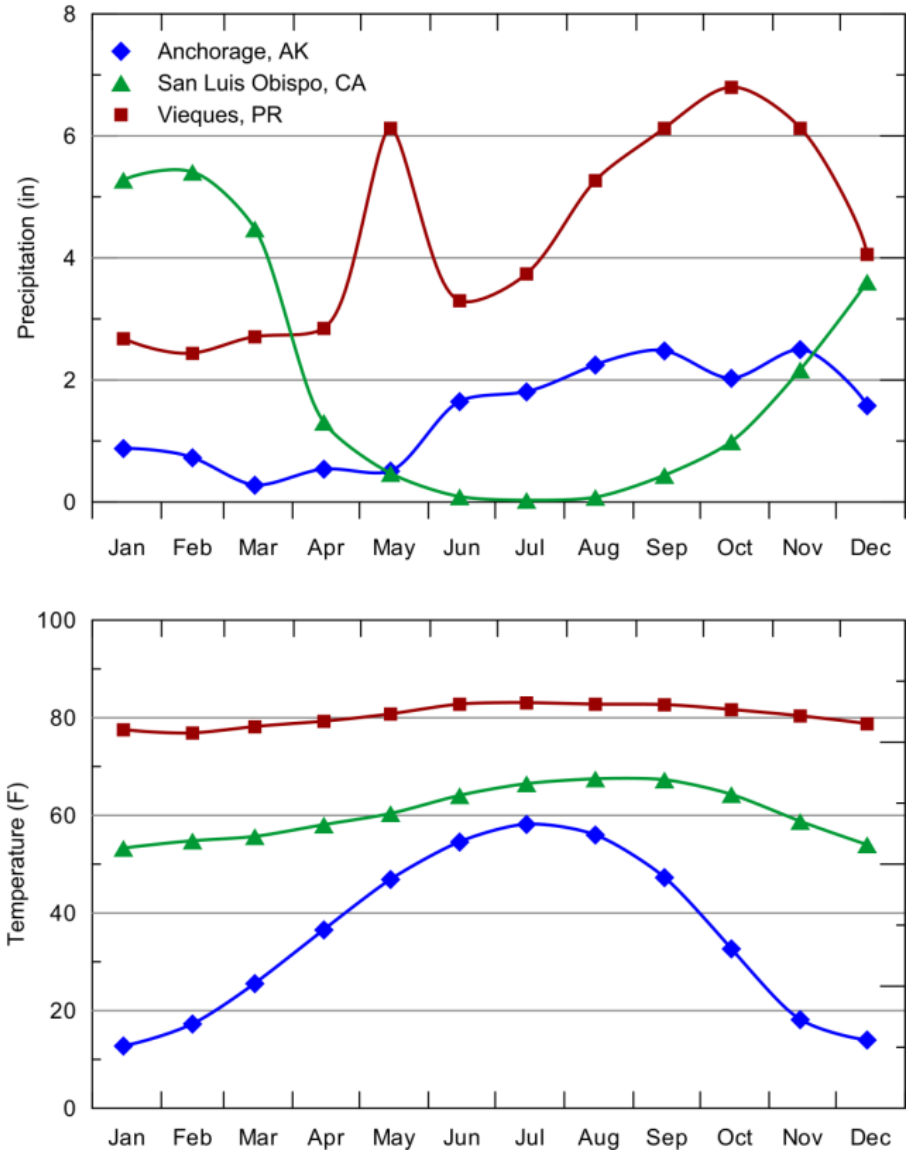

Figure 3. Thirty year (1971-2000) average monthly precipitation (upper) and temperature trends at the three sampled locations (NCDC 2010).

Eagle River Flats, Alaska

The Alaskan salt marsh we sampled is an active impact area on the Army's Fort Richardson just east of Anchorage, a site into which howitzer, mortar, and rocket rounds have been fired since around 1950 (Figure 4). It is referred to as Eagle River Flats; since it is a tidal flat at the mouth of the glacially fed Eagle River where it meets the Knik Arm, which ultimately flows into Cook Inlet and the Gulf of Alaska). Tidal height variations are extreme here and the salt marsh, which has flat relief at about 4.5 m (15 ft) above sea level, is flooded often several times a month. Thus, it is a very wet environment that experiences a complex interaction with mixtures of saline and fresh water. This particularly wet soil and the presence of saline water accelerates the rate of casing corrosion.

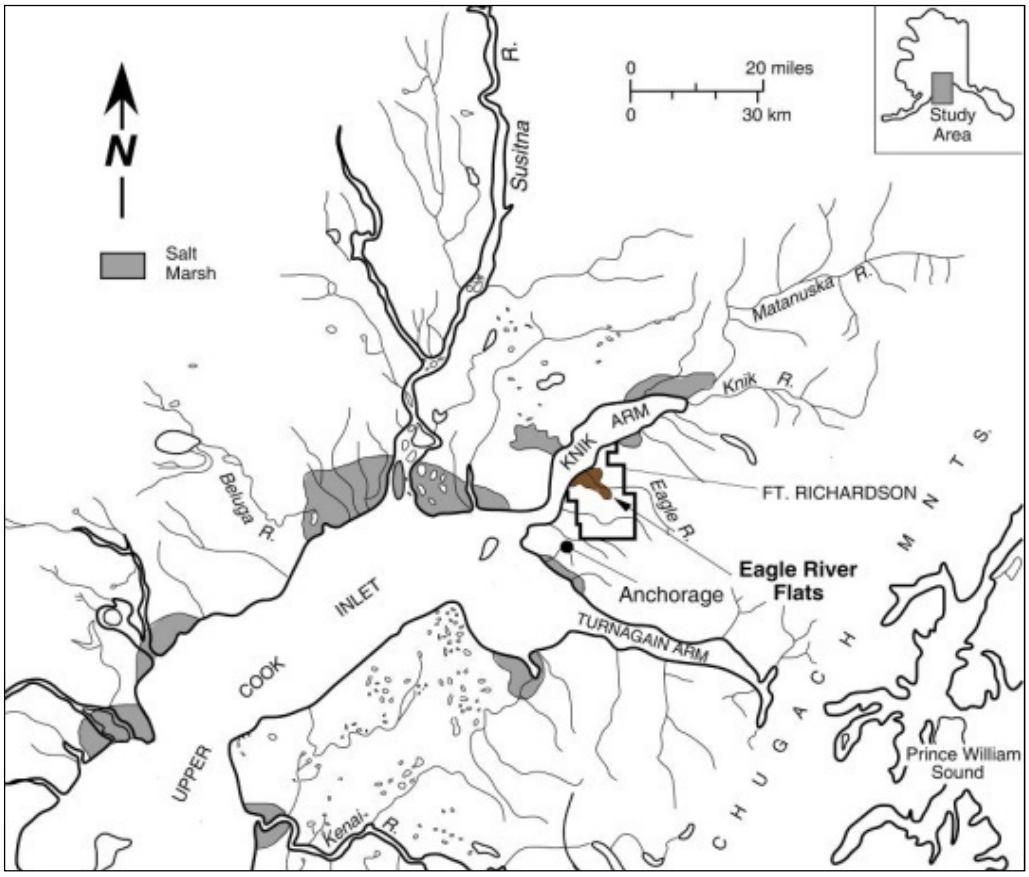

Figure 4. Location of Eagle River Flats (ERF, in the center, shown in brown) within the Anchorage area and south central Alaska (inset).

The specific area search was in the southeastern corner of Eagle River Flats, an area referred to locally as "Area B" (Figures 5 and 6). This location was targeted during a March 2006 training exercise using 60-mm M888 mortar rounds (Walsh et al. 2006). Observers at the exercise noted that several rounds did not detonate, so our chances of finding unexploded ordnance at this site were good. The searching and sampling was done between 18 and 26 May 2009.

Soils in the area are typic cryaquents and typic cryaquepts, found on tidal flats and beach terraces, respectively (USDA Web Soil Survey). They consist of dark gray silt loam, with weak very fine granular structure; they are friable, non-sticky, and non-plastic. The cryaquepts, found on the slightly elevated locations adjacent to small erosion gullies have slightly coarser silt to fine sand grain size. The "crya-" prefix indicates that the soils were formed in cold climates with a mean annual air temperature between 29 and 43 °F and a frost-free period of 105 to 135 days. Due to their fine-grained nature, these soils drain very poorly and thus hold moisture a long time.

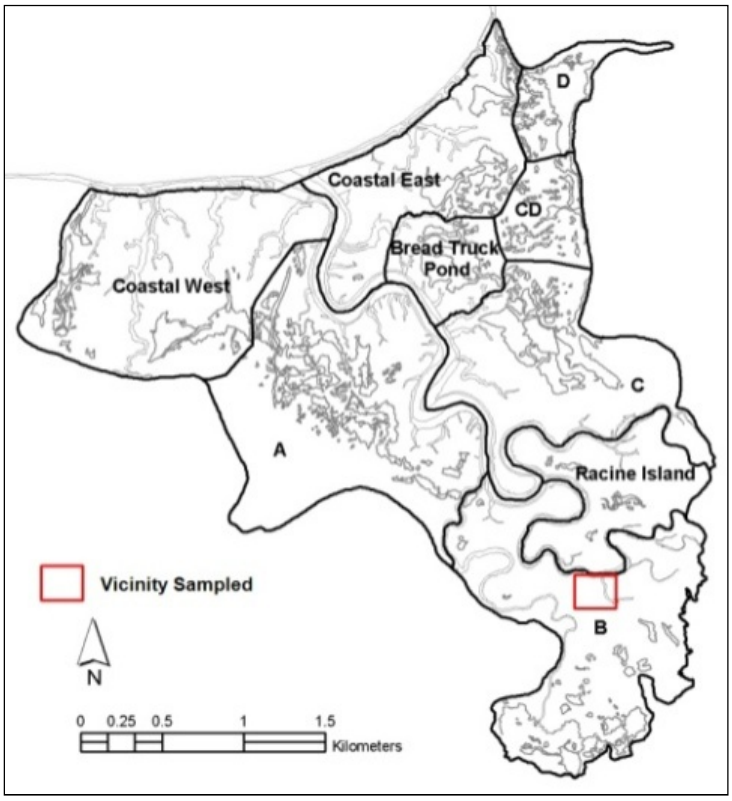

a. Sketch of ERF with named areas. Sampling was done in Area B. Red rectangle shows extent of air photo shown below.

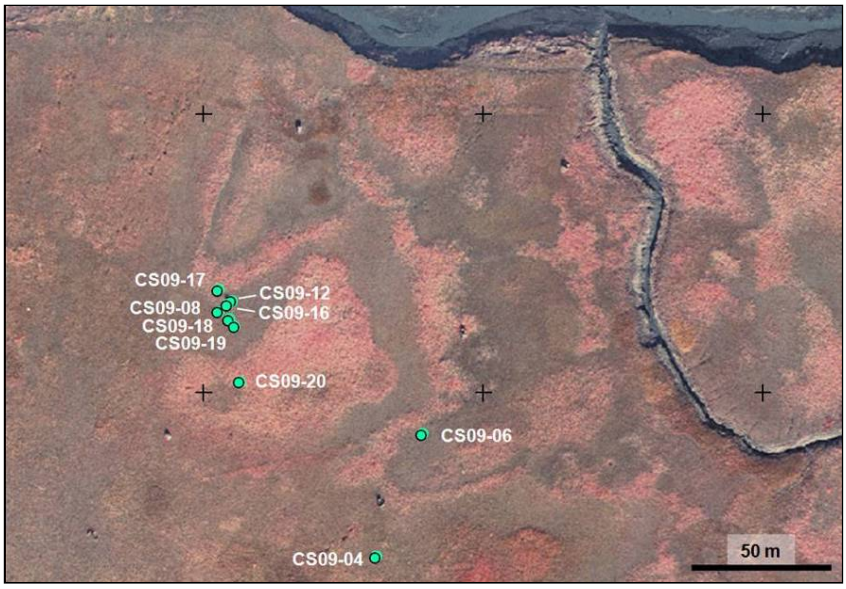

b. Sample locations within the vicinity sampled.

Figure 5. Area searched within ERF.

Figure 6. Northeast-looking view of the ERF sampling area. Two lines of target jeeps are seen in the photo's center.

Camp San Luis Obispo, California

Camp San Luis Obispo is in central California at 37 °N latitude and about 12 km (7 mi) inland from the Pacific Ocean (Figure 7). The camp was formally known as Camp Merriam when established after World War I as a state owned training area for the California National Guard. During World War II, the U.S. Army leased the facility for infantry division training with artillery, small arms, mortar, rocket, and grenades (Parsons 2009). After a period of inactivity, the Army trained at the camp again during the Korean War from 1951–1953. Our sampling was conducted within Rifle Range #12 of the Munitions Response Site 05 Range Complex.

The terrain here includes rolling hills and canyons classified as grassland, wooded grassland, or brush (Figure 8). The hills are south-southwest trending finger ridges with streams between that drain into the west-northwest flowing Chorro Creek from the higher 760-m (2600-ft) spine of the Santa Lucia Range in the Los Padres National Forest. Samples were collected on a south-facing hillside at about 110 to 145 m (360 to 480 ft) elevation.

Sampling at this site was coordinated with Corps personnel testing geophysical techniques for detecting UXO. As the study was in the intrusive investigation phase and UXO were being exhumed. Between 4 and 13 August 2009, we sampled five rounds within the central portion of the study area (Figure 7); one was further south, and the others were about 100 m north-northeast in a cluster within about 40 m. Soil in this area is dry, very compacted clay (USDA Web Soil Survey), so much so that a corer could not penetrate unless we pounded on the handle. For other samples we used a pick and scraped the material onto a flat scoop. In some cases, the exhuming process had disturbed the soils with the greatest probability of containing any leaked compounds.

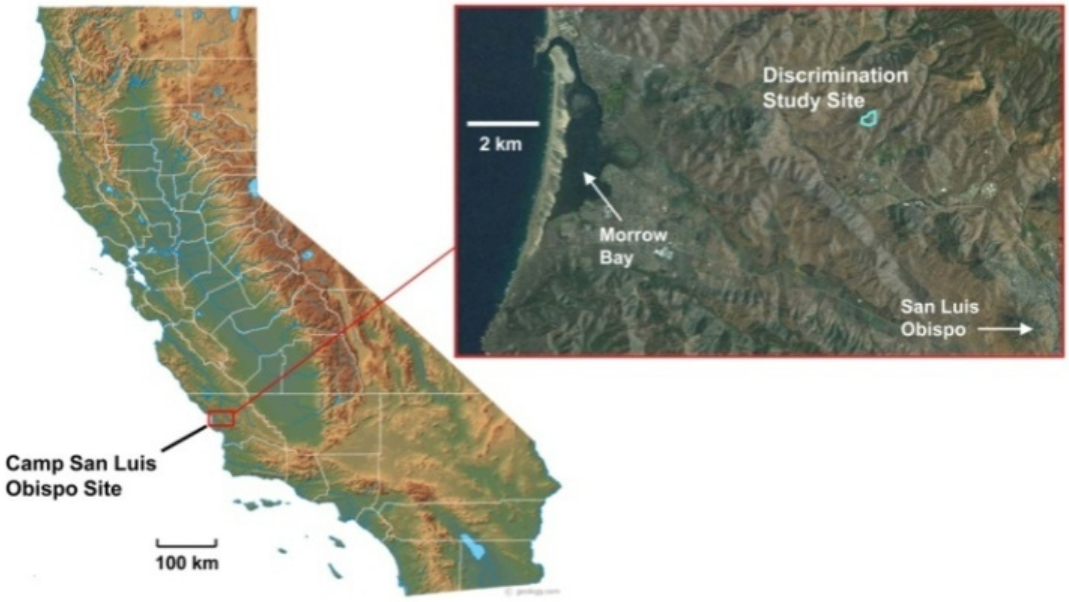

a. Location along California coast (left) and relation to coastline (inset). The cyan polygon in the upper right shows the area covered by the geophysical technique discrimination study.

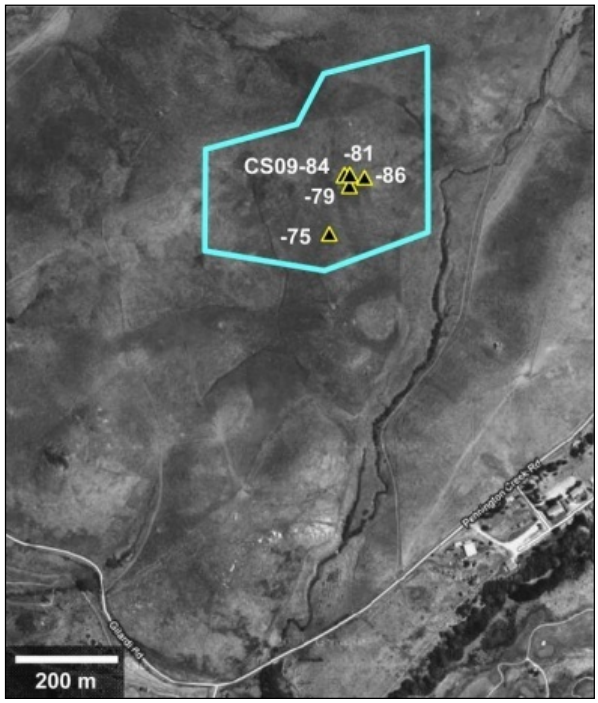

b. Location of samples collected within the discrimination study site.

Figure 7. San Luis Obispo, California site maps.

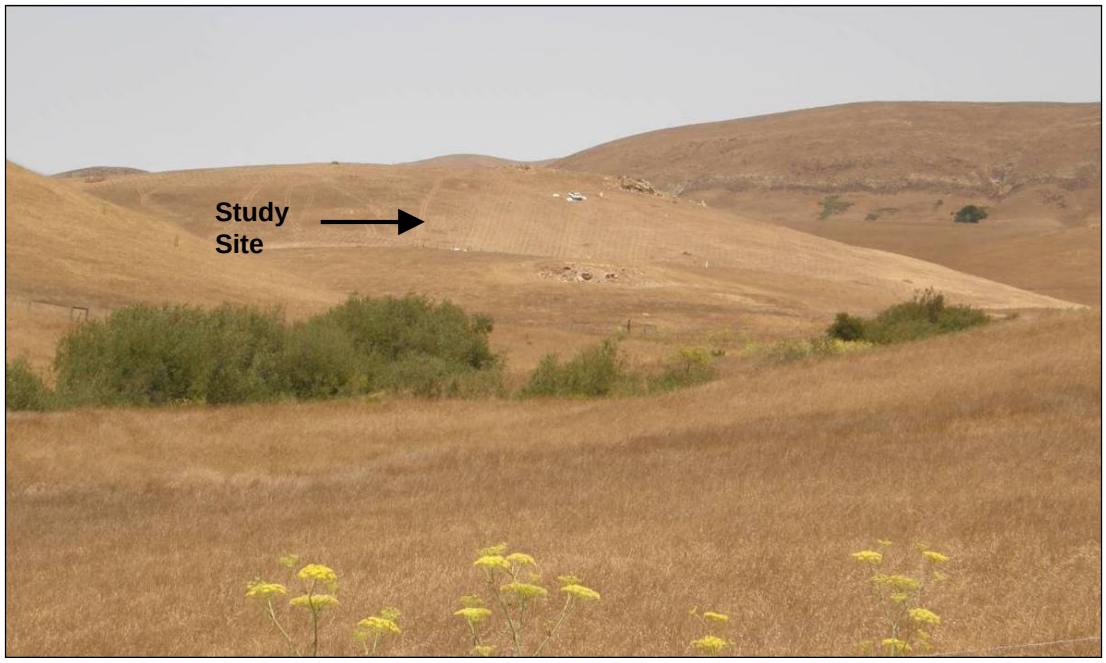

Figure 8. North-northwest view of hillside searched for UXO at Camp San Luis Obispo, CA.

Camp Garcia, Vieques, Puerto Rico

We sampled at the Vieques site once in 2009 and once in 2010. Vieques is a small island, 34 km (21 mi) long, 6 km (4 mi) wide at the northern end of the Lesser Antilles in the Caribbean Sea and about 20 km (12 mi) southeast of Puerto Rico (Figure 9). The Navy used the former Vieques Naval Training Range on the eastern end of the island for ground warfare and amphibious training, naval gunfire support training and air-to-ground training after World War II and until 2003 (CH2MHill 2007). Relief within the training range is mostly quite low [less than 45 m (150 ft) above sea level]; however, several higher peaks up to 90 m (300 ft) are scattered around and one highest peak rises to 138 m (450 ft, Figure 10).

Two trips to Vieques for sampling soil happened from 16 – 23 June 2009 and 13 – 17 September 2010 (Figure 11). The Navy is clearing UXO from the area and we were able to coordinate with the contractor performing the work to sample soil under UXO before these were removed. This gave us the opportunity to collect closely spaced samples adjacent to undisturbed rounds. However, we could only sample when the contractor teams were not in the immediate area and sample under rounds found during or just before the weeks of our travel.

In 2009, the contractor located seven rounds containing explosive fill near both the northern and southern shorelines. Three rounds were found on the northern coastal beach approximately 50 m (165 ft) from the water (CS09-34, -41, -55). Here the USDA Web Soil Survey maps the soil as sand; our analysis of bulk samples collected near the rounds further classified the material as poorly sorted, tan-colored medium to fine sand. The fourth round in the northern area was found about 250 m (820 ft) from the shore in an area mapped as clay by the USDA. However,

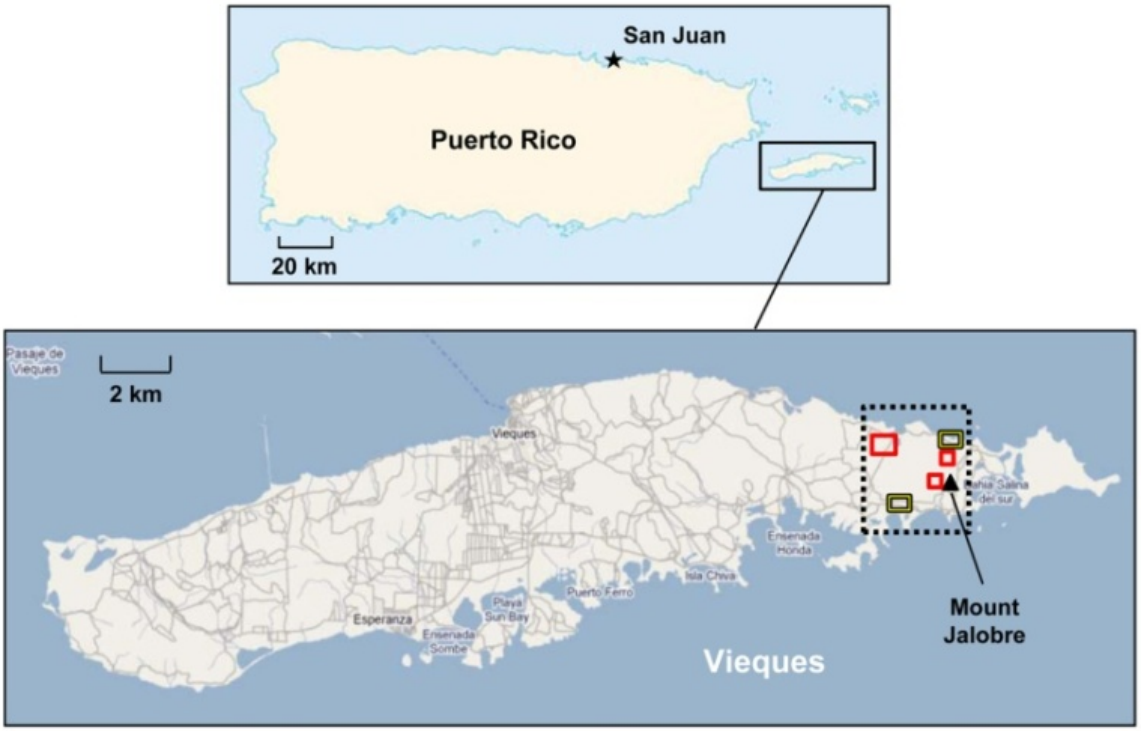

Figure 9. Vieques Island map showing the location of areas sampled in 2009 (yellow rectangles) and 2010 (red rectangles). Area enclosed by a dashed rectangle is shown in Figure 11.

Figure 10. The eastern section of Vieques Island as viewed to the west from Mount Jalobre.

our analysis of a bulk sample collected near the round classified the material as organic-rich medium brown loamy fine sand with gravel. The other three rounds located in 2009 were on the south side of the island and a bit further from the shore, at approximately 200–300 m (640–980 ft) inland. This area is mapped as gravelly clay loam; our analyses also classified these soils as organic-rich medium brown loamy fine sand, one of which also included some gravel.

In 2010, we collected soil samples near 21 rounds at locations further inland than the 2009 sampling – about 0.5 to 1.0 km from the shoreline (Figure 11). They were from four general vicinities all of which had more clay-rich soils. We collected 135 samples from in situ locations adjacent and under rounds.

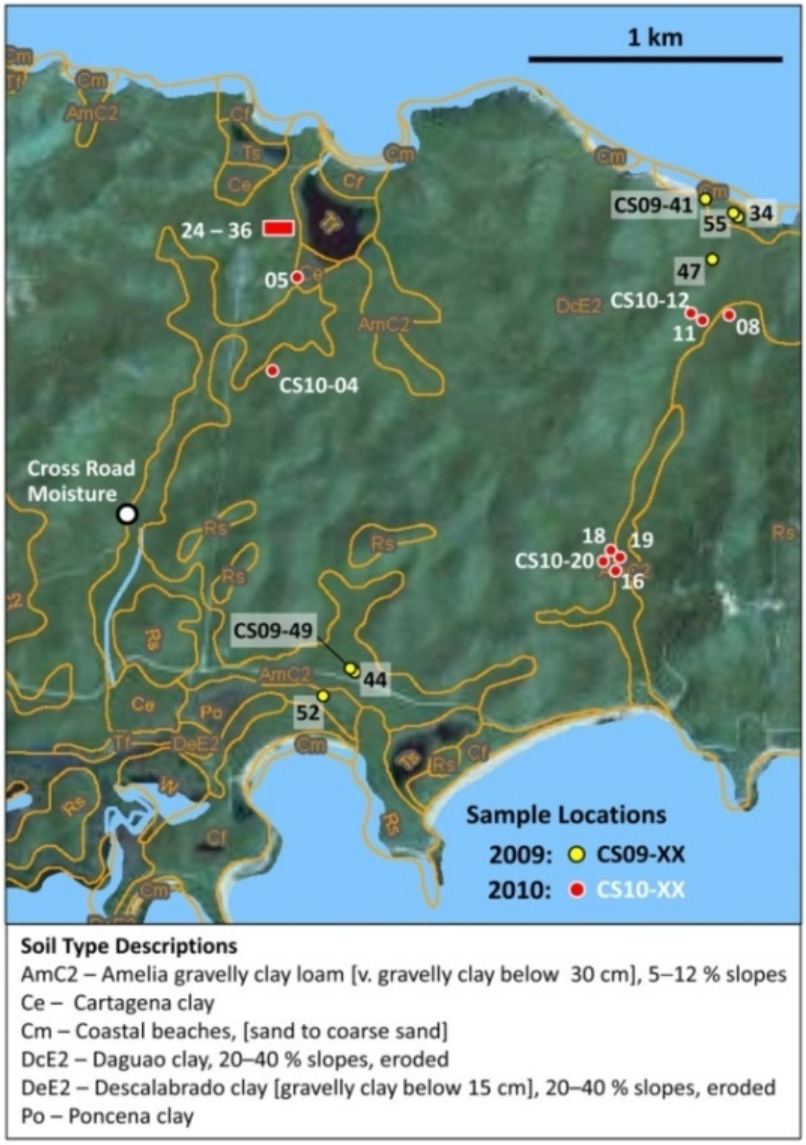

Figure 11. Locations sampled in 2009 and 2010 on the eastern part of Vieques Island. Extent of figure is shown by dashed rectangle in Figure 9. Background air photo and soil overlay from USDA Web Soil Survey.

In addition, during the 2010 trip we had the opportunity to conduct an *in situ* dissolution test. We found a 105-mm round that was partially detonated and had strewn chunks of HE on the surface nearby. We weighed the chunks and positioned them at a nearby site that had no UXO. Fortunately, rain fell overnight and the following day we collected soil core samples beneath and a short distance away from the HE chunks.

Methods

Field sampling

We started by photographing and describing the condition of the round, noting if the round was intact, if not what portion was missing, the size of any holes or cracks, and the extent of cor-

rosion. We then used a field-screening test to determine if energetic material was leaking from the shell. This was done with an Expray™ Explosives Detection Kit[1]. The kit includes three aerosol cans, each of which contains reagents that react with explosives residues and give an easily discernable color change. To conduct the test, we first swabbed the area where energetic material was suspected to be with an acetone-saturated piece of filter paper, or we dripped acetone over the area and collected it on the filter paper. We then sprayed the aerosol on the filter and recorded any observed color change.

Next we collected soil samples. We used a variety of tools, depending on the soils, including stainless steel short-nosed and flat rectangular scoops, and an Oakfield corer with a 2-cm (0.8-in) inner diameter. Samples were placed in clean plastic bags and labeled.

At ERF we used a scoop to collect the entire layer of material underneath the round from the surface to 1 cm deep and from 1 cm to 2 cm deep (Figure 12). When the rounds were obviously damaged (cracked or punctured), we took a core sample beneath the round. To measure the lateral concentration of HE we aggregated 30 multiple increments, collected using a 2-cm (0.8-in)-ID corer penetrating 4 cm deep, into one sample. One of these multi-increment samples was collected between the edge of the round extending outwards 15 cm. A second sample came from the perimeter of that area and extending 15 cm further away. In two cases the rounds located were close to the edge of a target jeep; here, the lateral samples extended only half way around the round on the outer side.

At Vieques and San Luis Obispo, we collected 2-cm (0.8-in)-ID cores directly below the round (Figure 13). For UXO that looked intact we generally took three cores from under the round and combined the core portions from the same depths. For UXO with a crack or hole we took a core directly beneath this feature. Some of the vertical core samples extended to 50 cm beneath the round. The lateral samples were collected from a 10-cm wide swath in about a 3-cm deep lift at a position perpendicular to the center of the round's long axis. Samples were collected from 5- or 10-cm sections from the farthest location inwards. The top of the 3-cm lift was positioned to be either level with the top of the round (if buried) or along the soil surface.

Sample preparation

The Eagle River Flats (ERF) Alaska samples were stored in clean plastic bags and refrigerated (4°C). Within a day or two of collection, samples were spread out on sheets of aluminum foil in the Fort Richardson laboratory to air dry. Once completely dry, in another day or two, they were returned to their sample bags. At the end of the sampling trip, we sent the dried samples by contracted carrier to the ERDC-CRREL laboratory in Hanover, New Hampshire.

The ERF samples were prepared following the standard procedures recommended in EPA Method 8330B (US EPA 2006). The step in the method that calls for sieving samples through a

[1] Plexus Scientific Inc, Alexandria, VA; www.plexsci.com

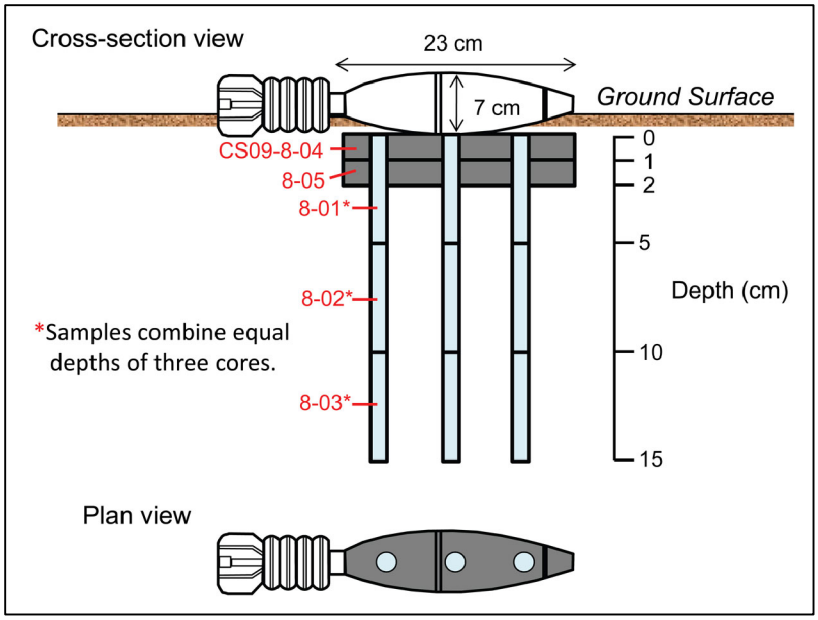

a. Vertical core samples.

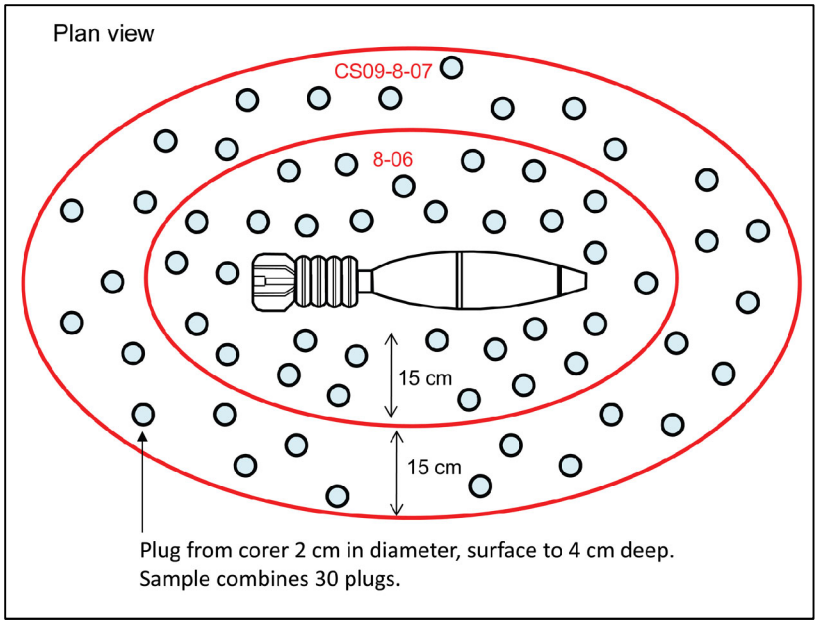

b. Lateral samples.

Figure 12. Example of sampling collection pattern used at Eagle River Flats, Alaska.

10-mesh (2-mm) sieve was skipped because the silty soil from ERF did not include any particles larger than 2 mm. The next procedure in the method is grinding samples thoroughly in a puck mill grinder. Grinding was performed only on samples with adequate mass – samples heavier than 300 g were ground for 90 seconds and those between 100 and 300 g were ground for 60 seconds. The ground sample was then spread out on a large sheet of aluminum foil. Subsamples of 10.0 g (±0.1 g) were obtained by combining at least 30 increments from the entire sample into 2-oz (59-mL) amber wide-mouth glass bottles with Teflon-lined lids. Subsample triplicates were

removed from the midpoint and end of the >300g and 100-300g sample groups. Once subsampling was completed, the remaining sample was returned to the bag and archived at CRREL. Each 10.0 g (±0.1 g) subsample was extracted with 20.0 mL of acetonitrile on a platform shaker overnight (18 hours at 150 rpm).

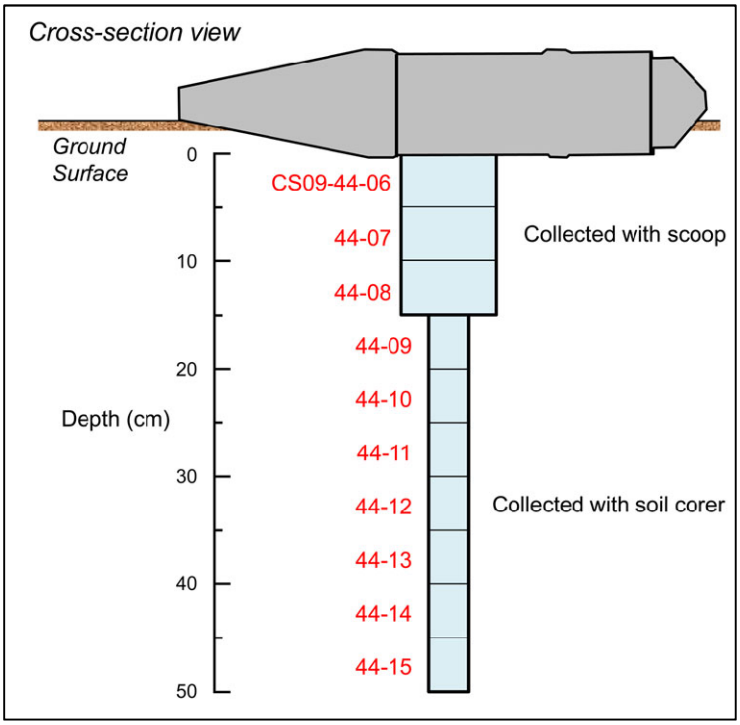

a. Vertical distribution samples.

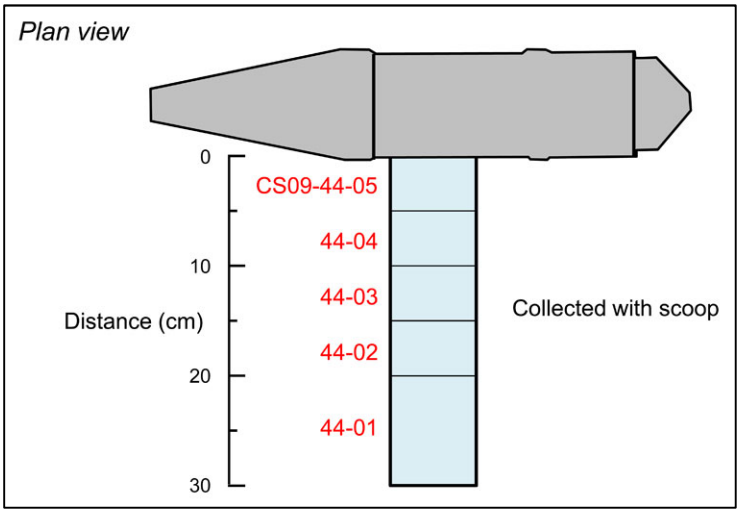

b. Lateral distribution samples.

Figure 13. Example of sampling collection pattern used at Vieques and CSLO.

Samples from ERF with less than 100 g (e.g. plugs from vertical core samples) were processed using whole sample extraction. The entire un-ground sample was placed in an 8-oz (239 mL) sample jar with a Teflon-lined lid. It was then extracted with a volume of acetonitrile (in milliliters) approximately double the mass (in grams), also conducted by shaking overnight (18 hr at 150 rpm).

Because we hoped to detect dissolved explosives in the soil pore water we wondered if the standard extraction procedure used in Method 8330B, which involves drying the soil, would lower the detection of HE. The standard procedures were developed to measure the soil concentration of energetic compounds, which are usually found as particles. Furthermore, the aqueous solubilities of the TNT, RDX and HMX are low, and pore water volumes are also generally low ~10%.

To test the recovery of energetic compounds in the soil pore water we added 400 mL of a Comp B spiked aqueous solution (3.21mg L^{-1} RDX, 1.32 mg L^{-1} TNT) to 977 g of dry, explosives free, soil collected in Vieques. The slurry was left to homogenize for two weeks in a cold room at 4 °C (40 °F) and stirred every few days. The sample was then divided in half. One half was split into five samples, which were extracted as whole samples without drying. The other half was processed according to Method 8330B—the sample was dried, ground and 10-g samples built by combining 30 increments taken from the ground material. Data from these tests are in the results section, but based on our findings we altered our sample preparation for the San Luis Obispo and Vieques soil samples.

The Vieques and San Luis Obispo samples were placed clean plastic bags and refrigerated (4°C) until shipped to CRREL in coolers with ice packs. We did not air dry these samples but kept them in their field moist condition until the entire sample was extracted. This procedure minimized loss of dissolved explosives due to drying or sub-sampling. The sample was extracted using a volume of acetonitrile (in milliliters) approximately double the mass (in grams), and the mixtures shaken overnight on a platform shaker (18 hours at 150 rpm). Different size jars (4, 8, or 16 oz; 120, 239, or 478 mL) were used depending on the size of the original sample. A few samples were too large to be totally extracted. In this case the sample was spread on a sheet of aluminum foil and about 30 increments were collected to amass an 80-g subsample, which was placed in an 8-oz sample jar with a Teflon-lined lid and extracted.

Analytical procedures

All samples were analyzed at CRREL following the procedures outlined in Method 8330B. Briefly, following the 18-hr extraction period on a tabletop shaker, each sample was vigorously hand shaken and the soil was allowed to settle for one hour. An aliquot of each extract was then passed through a Millex FH filter unit[2] and transferred to a 7-mL glass amber vial. These sample extracts were stored in a freezer until the day of analysis.

[2] Millipore, PTFE, 0.45 µm; Millipore, Billerica, MA; www.millipore.com

We typically analyzed 20 to 50 samples at a time and included at least one laboratory control sample and a sample preparation blank. On the day of analysis the sample extracts were allowed to warm to room temperature. The extracts of samples from rounds that had positive results from Expray™ Kit[3] field screening, were pre-screened again. The procedure involved removing a small portion with a disposable glass pipette, placing a drop on special paper, and spraying with the Expray™ Kit aerosol reagents. This screening step identified a few samples that should be diluted 10-fold prior to analysis, so as to keep the concentration estimates within the linear range of the calibration. The final preparation step prior to high performance liquid chromatography (HPLC) analysis was to mix one part of the acetonitrile extract (or diluted extract) with three parts reagent-grade water.

Determinations were made on a modular system[4] that included a SpectraSYSTEM® Model P1000 isocratic pump with a 100 µL sample loop, a UV2000 dual wavelength UV/Vis absorbance detector set at 210 and 254 nm (1 cm cell path), and an AS3000 auto-sampler. Primary separations were achieved on a 15 cm × 3.9 mm (4-µm) NovaPak C-8 column[5] maintained at 28°C and eluted with 15:85 isopropanol/water (v/v) at 1.4 mL min^{-1}. Secondary (confirmation) separation was made on a 25 cm × 4.6 mm (5-µm) Supelcosil Liquid Chromatograph-Cyanopropyl (LC-CN) column[6] maintained at 30°C and eluted with 65:12:23 reagent-grade water, methanol, and acetonitrile (v/v) at 1.3 mL min^{-1}. Concentrations were estimated from peak height measurements compared to commercial multi-analyte and single analyte standards[7].

Laboratory dissolution tests

For safety reasons we could not drill holes into un-fuzed HE ordnance or use HE ordnance for these tests. Instead, we used six empty 60-mm shells. In one, we drilled a 3.16-mm-diameter hole; in the five others, we made a 6.32-mm-diameter hole (Figure 14). The hole diameters were selected based on pit sizes measured in the field. A 3.16-mm-diameter hole equals the cross-sectional area of ten 1-mm-diameter holes, the average pit size determined in the study by Chendorain et al. (2004). The 6.32-mm-diameter hole is similar to the maximum pit size (6.4 mm) found in the study by Nalbandian and Kalikian (2007).

To prepare the rounds, we plugged the holes and filled the rounds with a slurry made of water and calcium sulfate hemihydrate (calcined gypsum with CAS# 10034-76-1), then dried the shells in the oven for 48 hours. Calcined gypsum, $CaSO_4 \cdot 0.5H_2O$, was used because: 1) it is an inert filler used in practice rounds, 2) its dissolution rate in water can be measured using ion chromatography or electrical conductivity, and 3) it has a high water solubility (on the order of 2,400 mg L^{-1}). Its high solubility ensured that we could measure its dissolution but is an order of

[3] Plexus Scientific Inc, Alexandria, VA; www.plexsci.com

[4] Thermo Electron Corporation, Waltham, MA; www.thermo.com

[5] Waters Chromatography Division, Milford, MA; www.waters.com

[6] Sigma-Aldrich Company, St. Louis, MO; www.sigmaaldrich.com

[7] Restek Corp., Bellefonte, PA; www.restek.com

magnitude higher than the solubility of TNT (130 mg L^{-1}) and RDX (46 mg L^{-1}), the explosive compounds of interest.

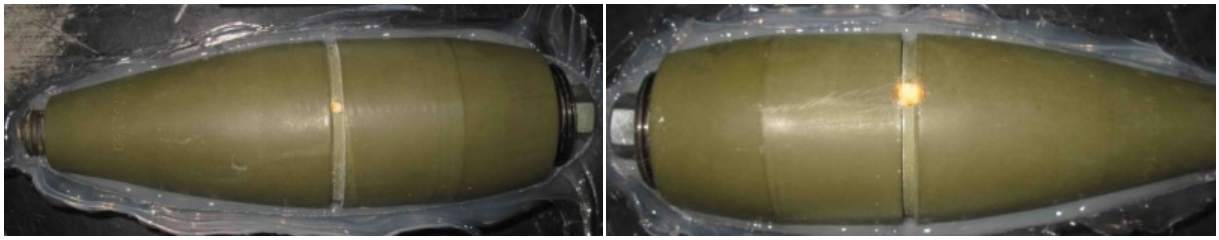

Figure 14. Two 60-mm ordnance glued to Plexiglas lids. Two hole-diameters were tested in this study, 3.16 mm (left) and 6.32 mm (right).

One half of each 60-mm mortar casing, the half into which the hole was drilled, was then submerged in deionized water using the following experimental set up. A 38-L glass aquarium (50 cm L × 25.4 cm W × 30 cm H) was divided into two compartments using a Plexiglas partition and was then filled with deionized water run through a Milli-Q purification system. The ordnance were glued to Plexiglas lids (Figure 14) and the lids placed on top of the tanks. The lid was sealed to the glass aquarium to minimize interaction between water and air and thus limit the formation of HCO^{-3} ions in the water.

We tested all six gypsum-filled casings. Because metal rusts and adds Fe to the water we set up two control tests using gypsum-filled Nalgene™ bottles, one with a 3.16-mm-diameter and the second with a 6.32-mm-diameter hole. The electrical conductivity sensors were placed about 10 cm below the ordnance. Figure 15 shows the experimental setup with a Nalgene bottle and a 60-mm mortar casing.

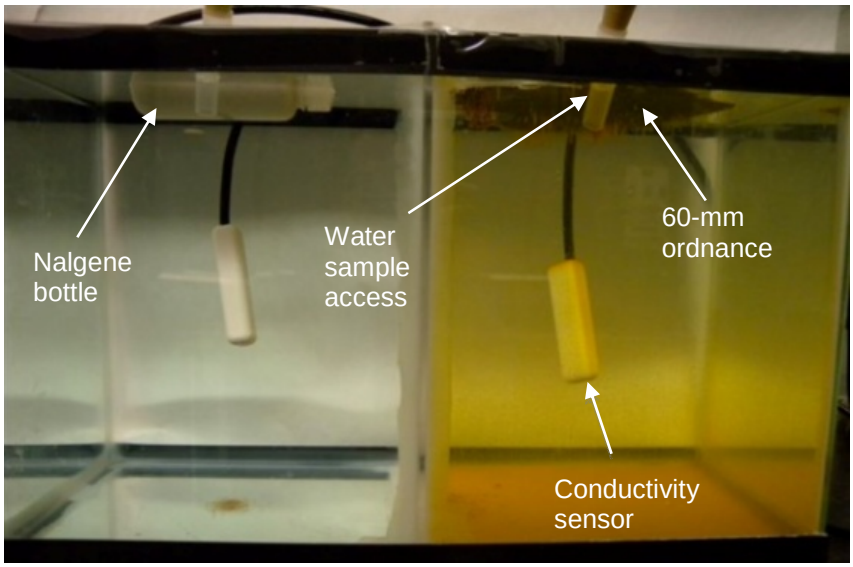

Figure 15. Glass aquaria setup with a Nalgene test (left) and 60-mm casing (right). Note that the metal casing rusts quickly and colors the water orange.

The water samples were analyzed with an ion chromatography system[8]. The conductivity of each solution is measured and compared to conductivities of prepared standards to quantify the concentration for the ion or ions of interest. The electrical conductivity was continuously measured with a temperature-corrected conductivity meter[9] attached to a data-logger[10]. We checked to be sure that only the gypsum was releasing ions, Ca^{2+} and SO_4^{2-}, into the water as the electrical conductivity measures the sum of the ion conductivities and cannot distinguish between the different types of ions present. If other ions were present it could lead to an underestimation or overestimation of the gypsum content.

Results

Aqueous analyte extractions

Because we are trying to detect explosives dissolved in small volumes of soil pore water, we tested to see if the standard soil preparation technique that involves drying and grinding the soil to homogenize it would decrease our detection. To determine this we homogenized a soil sample, spiked with a known concentration of RDX and TNT, and extracted half of the sample using whole sample extraction (moist) and the other half of the sample using the standard drying and grinding technique. Some of the key parameters and the results are presented in Table 2.

Table 2. High explosive (HE) compounds recovered from spiked pore water.

Sample ID	Sample Mass (g)	AcN (mL)	HE concentration (mg L^{-1})		HE mass	% RDX
			RDX	TNT	RDX (mg kg^{-1})	
Moist Samples						
VS-M1	147	290	0.432	0.012	1.23	94
VS-M2	134	270	0.427	0.009	1.24	95
VS-M3	145	290	0.443	0.011	1.28	98
VS-M4	151	300	0.443	--	1.27	97
VS-M5	119	240	0.449	--	1.32	101
Dried Samples						
VS-D1	10	20	0.460	--	0.92	70
VS-D2	10	20	0.452	--	0.90	69
VS-D3	10	20	0.456	--	0.91	70
VS-D4	10	20	0.446	--	0.90	69
VS-D5	10	20	0.473	--	0.95	73
Spike			3.21	1.32	1.31	

[8] Model ICS-3000, Dionex Corporation, Sunnyvale, CA; www.dionex.com

[9] Model CS547A, Campbell Scientific, Inc., Logan, UT; www.campbellsci.com

[10] Model CRX1000, Campbell Scientific, Inc., Logan, UT; www.campbellsci.com

Data for the whole sample extractions (moist samples) show that RDX is recovered and that TNT is poorly retained. When the samples are dried, about 70% of the RDX is recovered but none of the TNT. These important data show that we can indeed recover and analyze dissolved explosives in the pore water with concentrations around 1 mg L^{-1}. The data also indicate that TNT will be underestimated in all samples and that drying the samples will decrease the RDX concentration. For our data, these results suggest that our RDX values are 30% low in the ERF samples as these were dried before extraction. Note that these data are for RDX and TNT in pore water and the results do not pertain to most range soils where explosives are in particle form.

HE concentrations in soils under UXO

We collected soil samples from under 42 corroded UXO (Table 3) that were found *in situ*. The UXO ranged in size from 60 to 155 mm and we think most were HE-filled. Although most of these UXO looked highly corroded, only seven were found to be leaking HE into the surrounding soil. Analyses of soil cores taken at training ranges generally show a high surface concentration that decreases exponentially with depth (Taylor et al. 2011) and we expect to see this type of pattern.

Table 3 lists the *in situ* rounds found to be leaking HE. Concentrations in samples containing energetic compounds are tabulated in Appendix B. Photographs of the rounds sampled that had no explosives in the surrounding soil are compiled in Appendix C.

Table 3. Corroded rounds sampled at Eagle River Flats (ERF), San Luis Obispo (SLO), and Vieques.

Location	Munition Type	# UXO Sampled	# Leaking HE	Comment
ERF	60-mm	9	2	1 Fuse failed; Cracked on impact with target jeep 2 Punctured by fragments
SLO	60-mm (Korean)	5	1	Fuse missing; HE exposed at nose
Vieques	60-mm	5		--
	81-mm	9	1	Corroded and missing fins
	90-mm	1		--
	105-mm	6		--
	106-mm	2	1	Casing split, HE exposed in 9 x 15 cm
	4.2 in.	2	1	Crack in casing with exposed HE
	5 in.	1		--
	155-mm	1	1	Casing has scaling on top and sides
Total		**42**	**7**	

Because all of these sites are impact ranges, it is possible that soil contamination found near a UXO derives not from the UXO but from some prior range activity (false positive). Because many UXO were heavily weathered, obliterating surface markings and altering the rounds' shape, absence of HE in the soil under a round need not indicate that the UXO had not perforated. It is possible that the round was a practice or smoke round and contained no HE (false

negative). We kept these possibilities in mind while we were examining and sampling the UXO. Fortunately, the ratio of the different explosive compounds or their degradation products provides information we can use to determine false positives. For example, for dissolved Comp B (a 60-39 RDX-TNT mix and HMX concentrations ~3%- a byproduct of RDX manufacture) we would expect mainly RDX and HMX in the soils beneath Comp B-filled UXOs that are leaking, since the TNT readily photo- and bio-degrades. If dissolved Comp B has not entered the soil recently we would expect that, over time, the ratio of HMX to RDX would increase as RDX is more soluble than HMX. However, particles of Comp B should contain TNT in roughly the same proportion as in Comp B ~40%. For TNT-filled rounds, we would expect the dissolved TNT to biodegrade in the soil to 2 am-DNT and 4 am-DNT. Particles of TNT, on the other hand, would have a high TNT concentration relative to the degradation products.

Eagle River Flats, Alaska

The soil adjacent to nine unexploded 60-mm M888 mortars was sampled at Eagle River Flats. As mentioned previously, these UXO likely resulted from a training event in March 2006 and so had been in the tidal flats for about three years. Although not in place very long, the rounds were quite corroded, although none of them had corroded through to the fill.

Two mortars were leaking explosives. The fuse on CS09-12 was badly damaged and the body was cracked along its length (Figure 16). We think both the damage to the fuse and the crack formed when the fuse impacted the ground (or the adjacent jeep target) but did not initiate a detonation. The fuse on CS09-16, on the other hand, was intact and the round was not badly corroded (Figure 17). However, the round had been damaged by flying fragments from a nearby high order detonation as evidenced by the ding marks on the body (Walsh et al. 2011). One piece of frag pierced the casing through to the HE fill and it is through this hole, located near the tail of the round, that HE is leaking.

A soil core taken beneath the cracked round contained the compounds TNT, RDX and HMX and degradation products in the top 5 cm of soil (Figure 16). We think this round was filled with Comp B and that the low concentrations of TNT result from degradation while the concentrations of RDX (10 mg kg^{-1}) and HMX remain. Multi-increment samples taken horizontally away from the round contain only small amounts of HMX. Ongoing dissolution of Comp B from this round, coupled with the degradation of the TNT, would produce the sub-surface profile we see. The surface concentration of HMX could result from Comp B that dissolved some time ago leaving only its HMX.

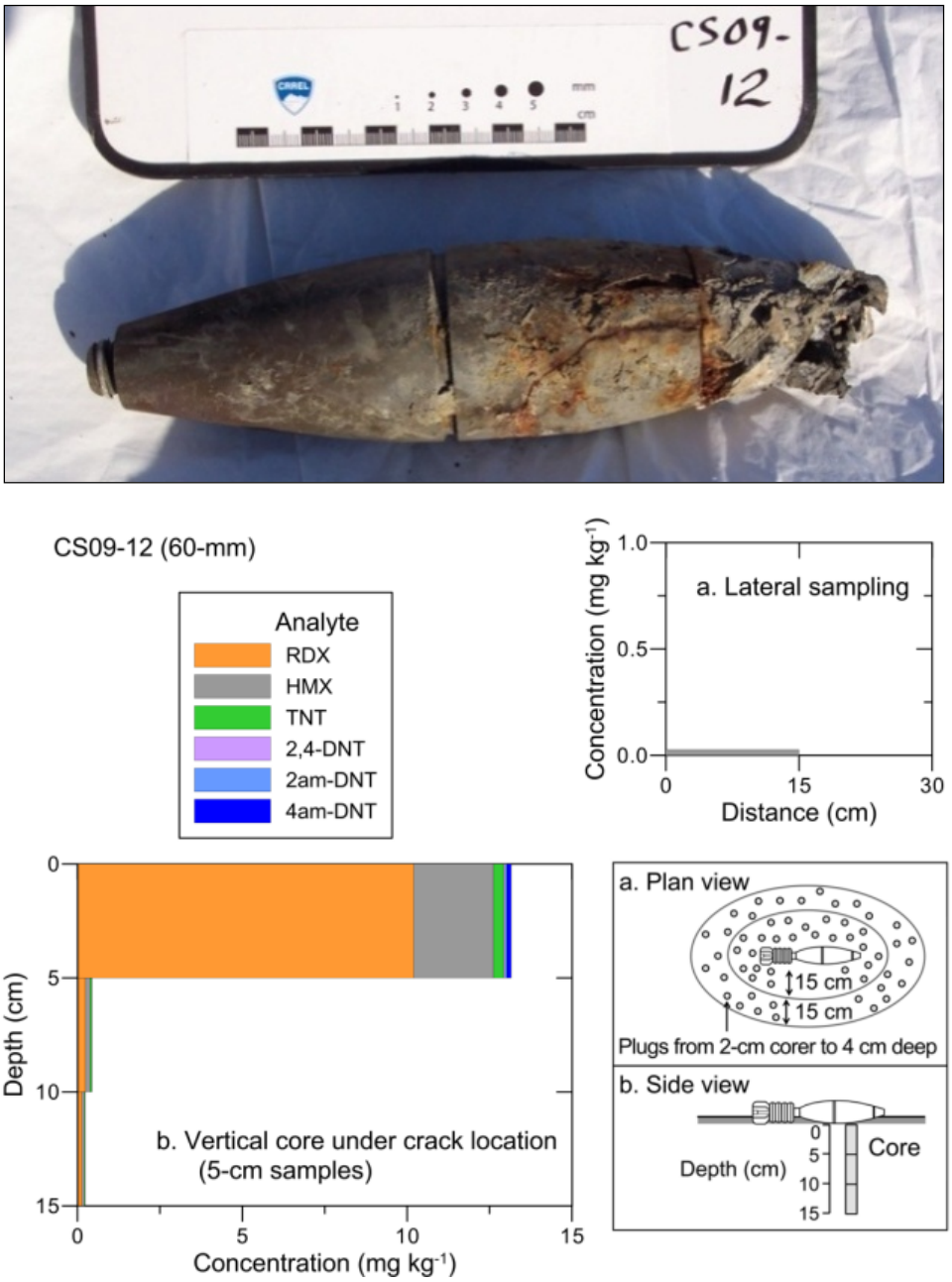

Figure 16. Image of CS09-12, a 60-mm UXO with a large longitudinal crack (upper), and high explosive compounds and breakdown products in soil samples lateral to and beneath the round.

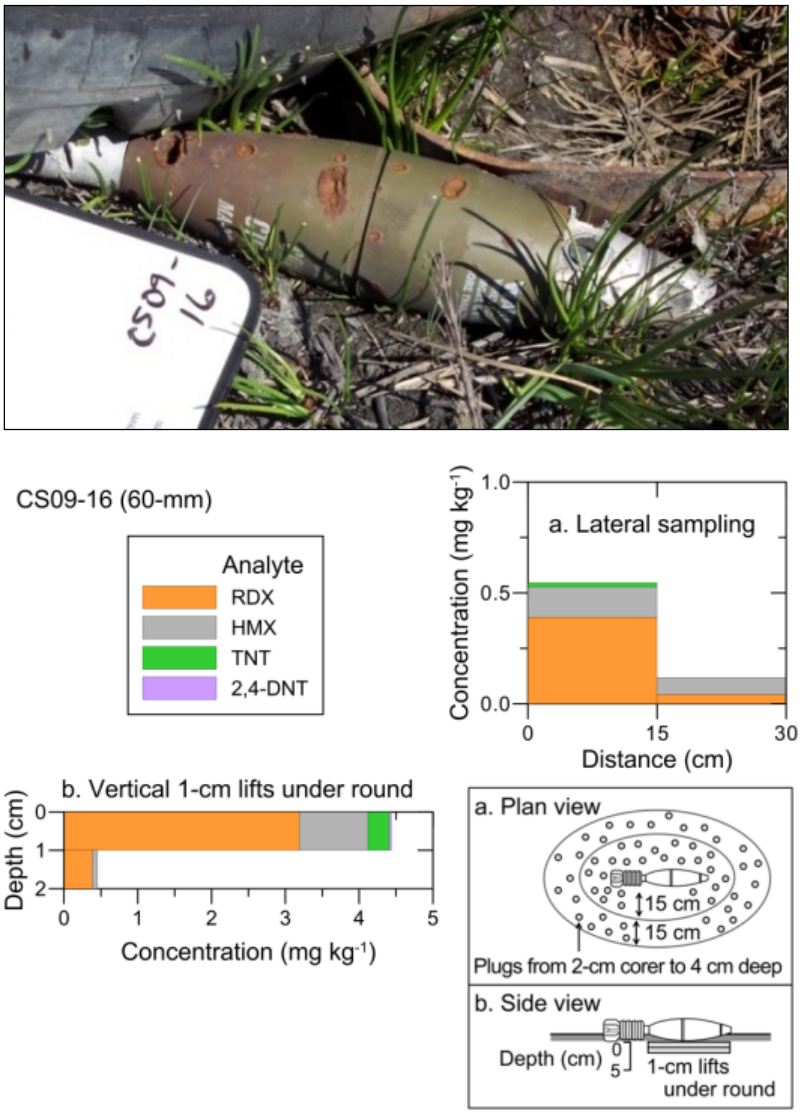

Figure 17. Image of 60-mm mortar CS09-16 punctured by fragmentation from a nearby detonation (upper) and high explosive compounds in soil samples lateral to and beneath the round.

Figure 17 shows the concentration of explosives in the soil beneath the holed round filled with Comp B. Samples taken beneath the round show fairly high levels of RDX and low levels of TNT consistent with preferential dissolution, transportation and degradation of TNT. Multi-increment samples taken horizontally away from the round show RDX and HMX concentrations decreasing with distance; TNT is present only in the first 15 cm. Note, too, that more HMX than RDX is present in the 15–30 cm sample indicating that most of the RDX has been transported away. We think the lateral HE concentrations are due to wetting fronts that move water-containing explosives away from the round. The water concentration should decrease with distance as the area wetted increases but if the distal areas are not wetted as frequently their HE would not be replenished providing the time needed to transport away some of the RDX.

Camp San Luis Obispo, California

Only one of five 60-mm rounds sampled at Camp San Luis Obispo was leaking HE. This round was missing its fuse but looked similar to the others we studied (Figure 18, Appendix C). We collected a core beneath the nose of the round and lateral surface samples downhill from the nose (Figure 18, lower). The only compound detected in the core samples was tetryl, a component used in the boosters of these Korean-era rounds. The lateral samples included tetryl and 2,4-DNT in the closest sample. The origin of the 2,4-DNT is not known: either the original round contained 2,4-DNT or we sampled some propellant residues.

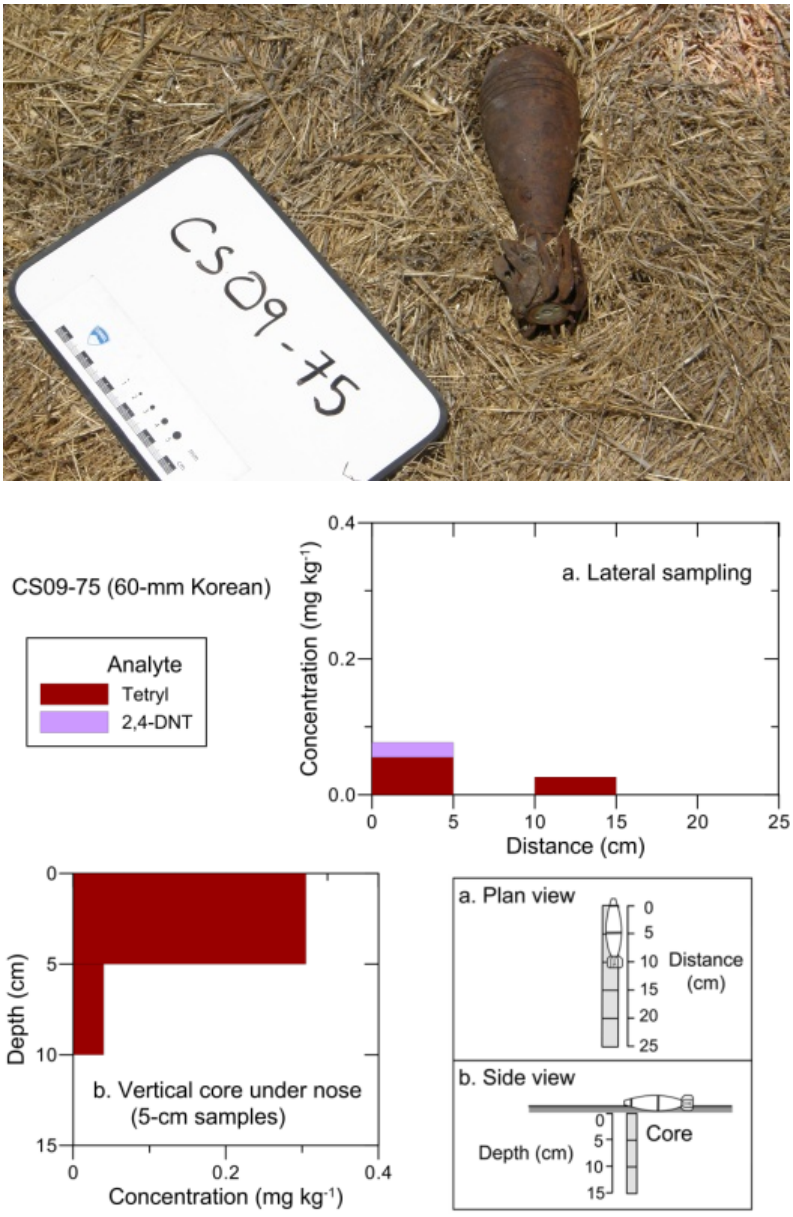

Figure 18. Image of 60-mm mortar sampled at San Luis Obispo that was leaking HE (upper) and high explosive compounds and breakdown products in soil samples lateral to and beneath the round.

Vieques Island, Puerto Rico

We collected soil samples adjacent to 27 UXO, four were found to be leaking HE and are described below from the smallest to the largest caliber, and one was a low-order detonation which we sampled next to and beneath (Table 4).

CS10-25 was an 81-mm mortar with its nose pointed downward into a sloping hillside (Figure 19). Its surface was highly corroded and the fins were missing. We took a core sample from beneath the nose. The near surface samples (0-5 and 5-10 cm) contained high concentrations of tetryl (up to 60 mg kg^{-1}); the tetryl concentration in the deepest (10–15 cm) sample decreased to 2 mg kg^{-1}.

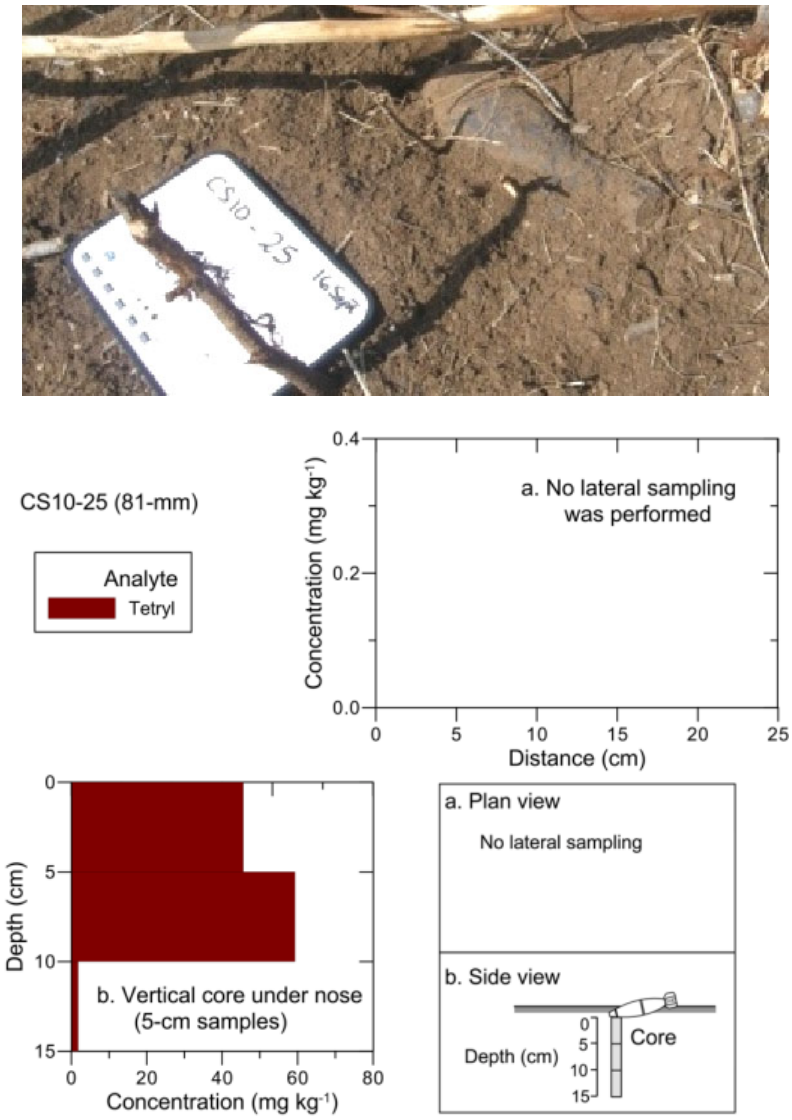

Figure 19. Image of 81-mm mortar sampled at Vieques that was leaking HE (upper) and high explosive compounds in soil samples collected beneath the round.

CS09-55 was a 106-mm HE anti-tank round that was partially buried in sandy soils near the northern coastline (Figure 20). It was corroded to the point that the metal casing was missing in a rectangular patch (9 × 15 cm) on the upper side, exposing the HE fill inside. A scoop was used to collect lateral samples to a distance of 30 cm and vertical samples to a depth of 21 cm.

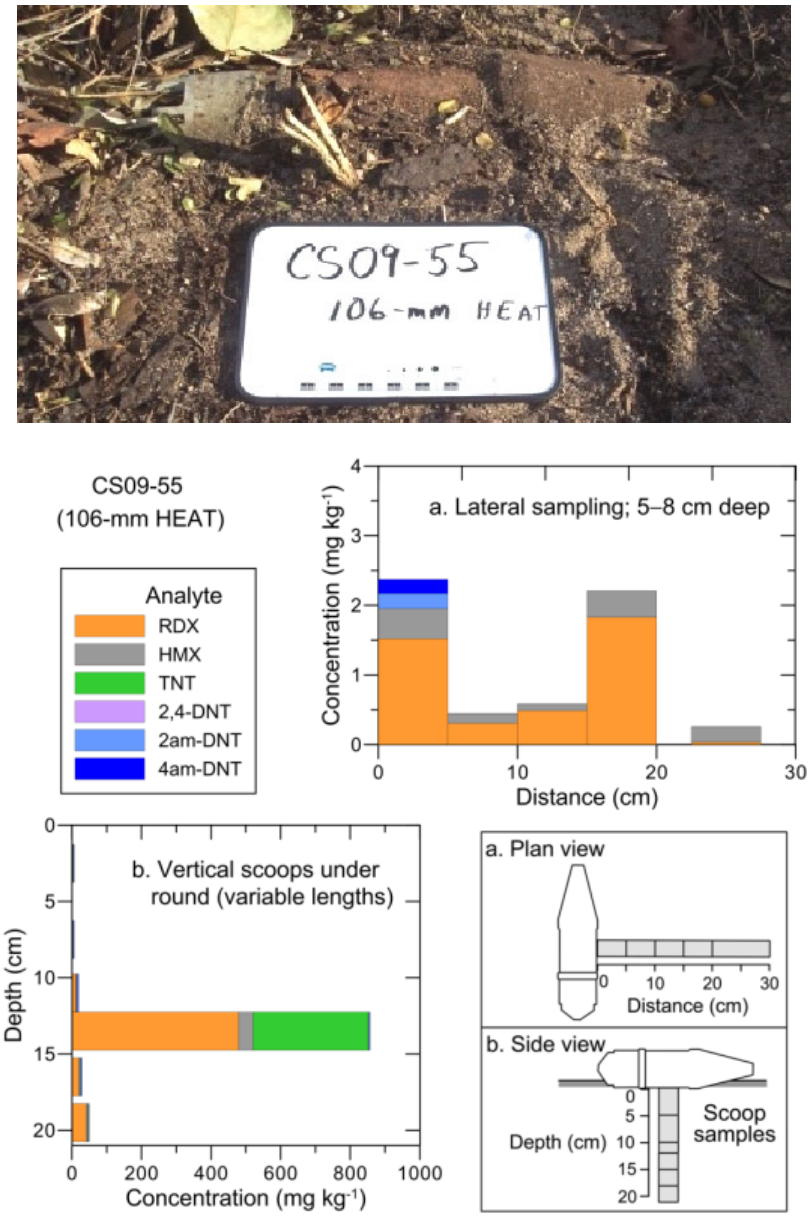

Figure 20. Image of the 106-mm HEAT round CS09-55 (upper) and HE compounds and breakdown products in soil samples taken lateral to and beneath the round.

Lateral samples contained mainly RDX and HMX in concentrations < 2 mg kg^{-1}. The sample closest to the round also had small amounts of 2am- and 4am-DNT (<0.5 mg kg^{-1}) that are TNT breakdown products. Note that the sample taken furthest from the round has mainly HMX suggesting that the other HE compounds had dissolved. The vertical samples contain RDX, TNT,

DNTs and HMX and are similar in concentration to the lateral samples (range <0.5–11 mg kg^{-1}; note change in scale from lateral samples). The concentration of explosives increases dramatically in the soil between 12-15-cm, with RDX at ~ 500 mg $kg^{-1}$and TNT at 300 mg kg^{-1}. Samples deeper than 15 cm had concentration levels less than 50 mg kg^{-1}but higher than surface concentrations.

This concentration profile was surprising given that we expect the concentrations to be highest near the surface and to decrease quickly with depth. The high concentrations of RDX and TNT have ratios similar to those we would expect for Comp B, and strongly suggest that Comp B particles are present. Interestingly, it looks as if dissolved HE is being generated by this layer and moving into the underlying soil. We think this high concentration layer was once a contaminated surface that was buried either by material lofted by a nearby detonation or more likely by wave deposition given that the sampling location was on the beach. We favor this explanation over cross contamination of the sample because the surface concentrations are much lower than the concentration in the buried layer.

CS09-49 was an extremely corroded a 4.2-in mortar with a crack that exposed HE material (Figure 21). It was sitting on the surface and had not indented the organic-rich soil beneath. Lateral samples were collected using scoops to a distance of 30 cm. We collected three sets of vertical samples – two with the corer, both to a 15 cm depth, and a third using scoops to 19 cm and then coring from the bottom of the hole to 21.5 cm depth.

Figure 21 shows the explosive compounds contained in the lateral samples and in the core with the highest concentration. TNT was the primary compound in the lateral samples. The closest sample had a high concentration (~60 mg kg^{-1}) indicating that particles were present and the more distant samples had lower concentrations (~2 mg kg^{-1}). TNT breakdown products, 2am- and 4am-DNT, were also present in all the samples, at levels ~2 mg kg^{-1}in the near sample and <0.5 mg kg^{-1}in the other samples. Core #2 had much less TNT (~1.5 mg kg^{-1}) than the horizontal samples, but much higher amounts of 2am- and 4am-DNT, ~20 mg kg^{-1}in the top increment of the core and <1 mg kg^{-1}in the deeper increments. The high concentration of breakdown products and the low concentration of TNT in the core samples indicate biotransformation of the dissolved TNT. The core samples also contained 2,4-DNT, 1.3 mg kg^{-1}at the surface to 0.5 mg kg^{-1}at depth.

Figure 22, which compares the results from the three sets of vertical samples, demonstrates the variability in energetic compound concentrations within a distance of less than 0.5 m. Core #1 and Core #2 (discussed above) mainly contain 2am- and 4am- DNT, while Core #3, collected with scoops, has primary TNT with smaller amounts of 2am-DNT, 4am-DNT and 2,4-DNT. We interprete the concentration patterns in Core #1 and #2 as due to dissolved TNT that has had time to bio-transform. Core #3, on the other hand, is sampling TNT particles as evidenced by the high TNT concentrations. The large concentration spike at 15 cm depth has the signature of TNT particles and probably results from cross contamination with the surface. Cores may be a better

method of collecting samples than scoops, which loosen more soil and increase the chance of cross contamination from surface soils.

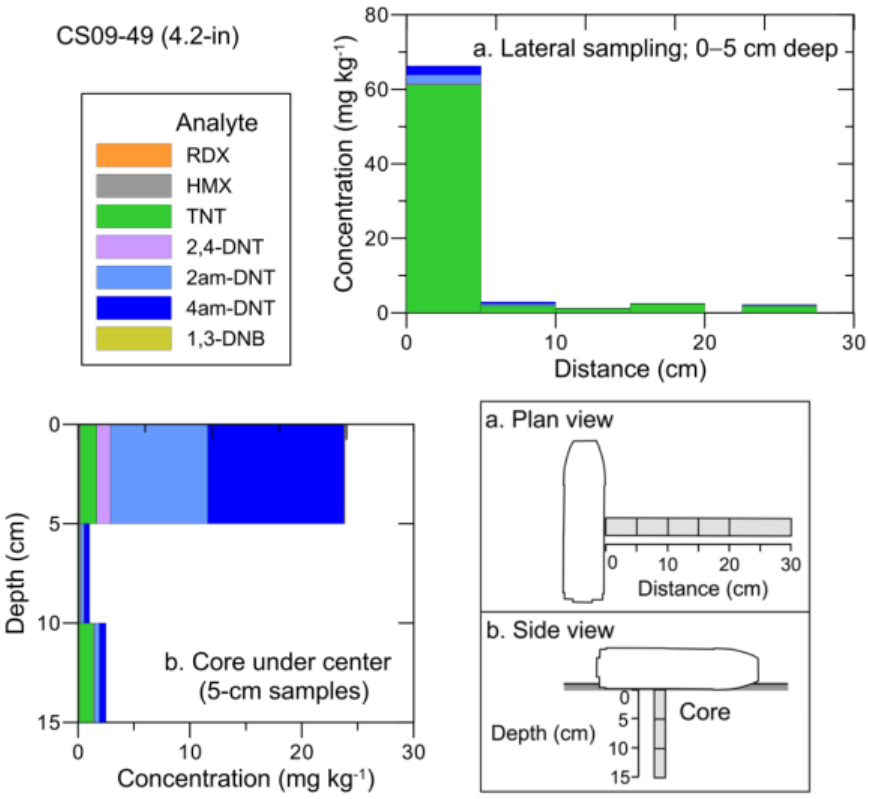

Figure 21. Image of the 4.2-in mortar CS09-49 (upper) and HE compounds and breakdown products in soil samples taken lateral to and in one core beneath the round.

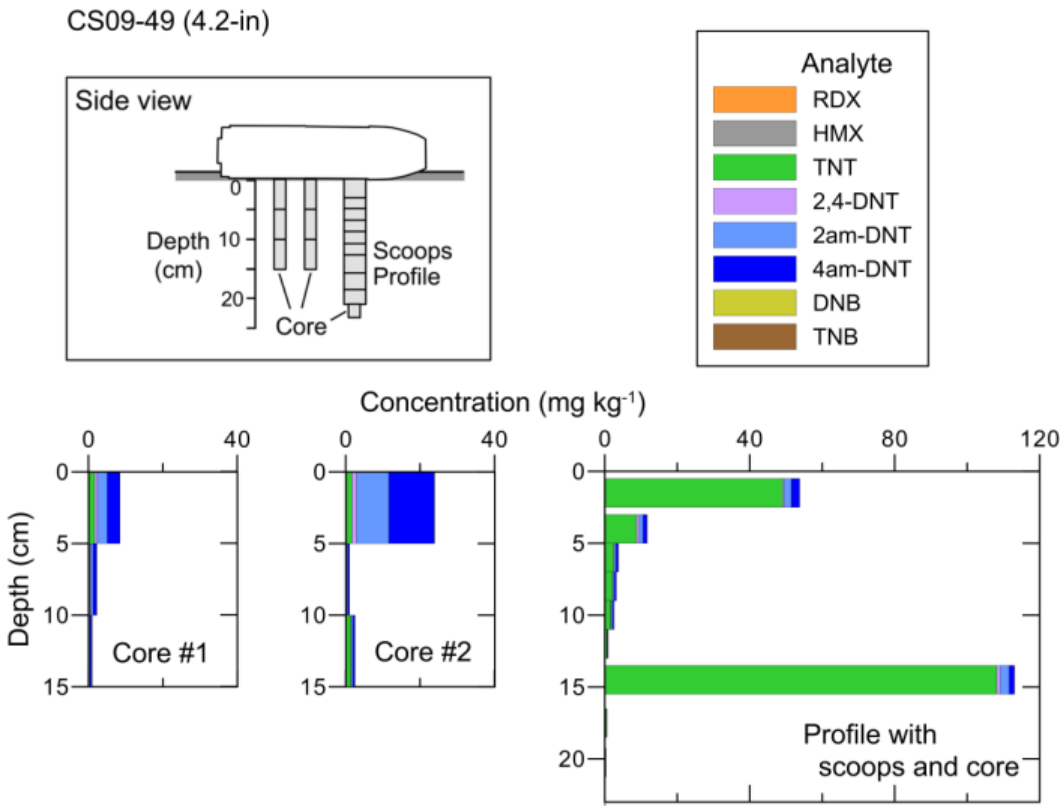

Figure 22. HE compounds and breakdown products in three sets of vertical samples beneath the 4.2-in mortar CS09-49.

CS10-11 was a 155-mm projectile, the largest round we sampled in Vieques. It was located in silty soils on a sloping hillside with its nose pointed in the uphill direction (Figure 11, 23). The metal casing was scaled on the top and sides. The nose was dented and the rotation band was missing. Lateral samples were collected of the surface soil from the tail end downhill to a distance of 25 cm. Vertical samples were collected in a single core located beneath the tail.

The lateral samples contained primarily TNT at concentrations from <0.5 to 2 mg kg^{-1}, along with trace amounts of 2,4-DNT (< 0.05 mg kg^{-1}). The highest concentration was found 10–15 cm from the tail. The upper two core samples also had mainly TNT, at concentrations less than 0.5 mg kg^{-1}, along with trace amounts of RDX (in the surface sample) and 2,4-DNT. No compounds were present in the deepest core sample (10–15 cm).

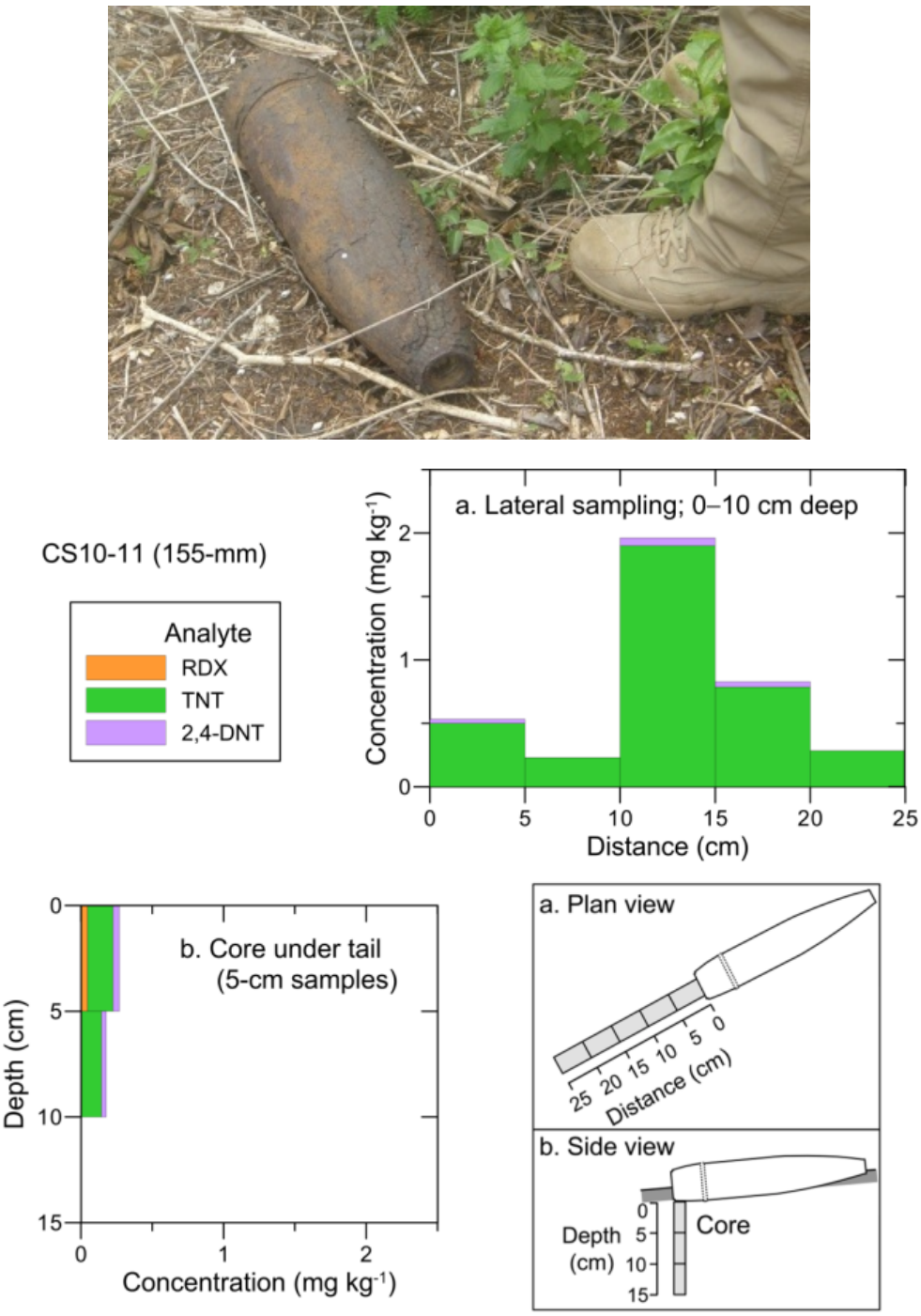

Figure 23. Image of the 155-mm mortar CS10-11 (upper) and HE compounds in soil samples taken laterally from and beneath the round.

Explosive concentrations in soils under breached rounds and HE pieces

CS10-16 was a 105-mm that had partially detonated. It contained visible exposed HE chunks inside the casing; another group of HE chunks were spread on the ground surface about 30 cm away from the opening (Figure 24, 25). The chunks were somewhat protected by a thin layer of leaf litter.

Figure 24. Images of a 105-mm round that had only partially detonated. Chunks of HE were visible inside the casing (right).

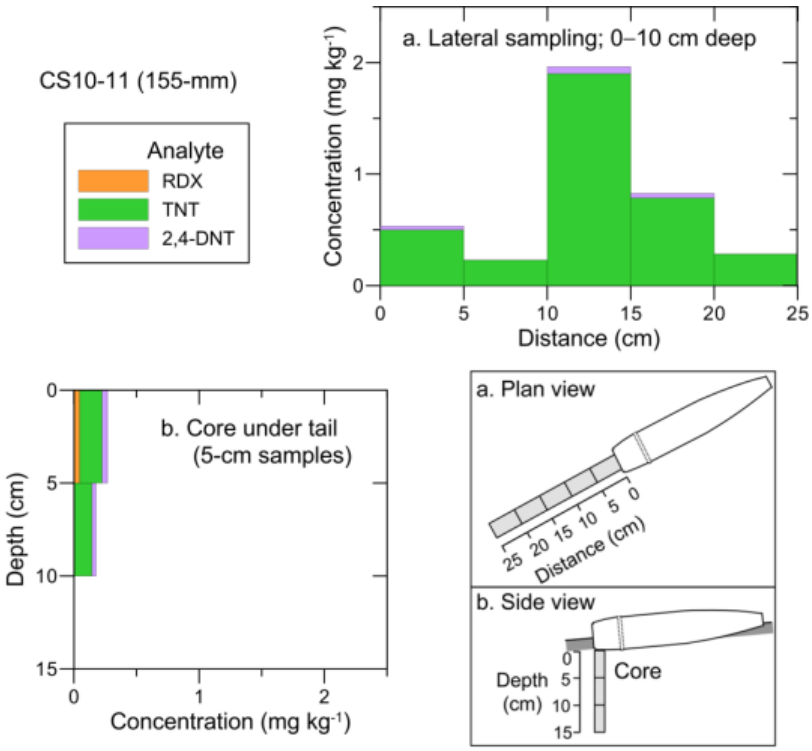

Figure 25. High explosive compounds and breakdown products in soil samples lateral to and beneath the broken 105-mm round CS10-16.

We collected a core underneath the round and two lateral soil samples adjacent to the base of the split in the casing (Figure 25). Analyses identified explosive compounds in both the vertical and lateral samples. Beneath the round, only RDX was present; its concentrations were less than 1 mg kg^{-1} and decreased to undetectable amounts below 10 cm. The lateral surface samples near the round included RDX, HMX, and TNT, along with the TNT breakdown products 2am- DNT and 4am- DNT. Their concentrations were two orders of magnitude higher 10-100 mg kg^{-1}. The

high levels of explosives in the surface soil, and the proportion of the explosives (60%-40% RDX to TNT split) indicate we are analyzing small particles of Comp B and not dissolved HE.

To measure any downslope movement of energetic compounds in the soil, we also collected a surface soil sample under the HE chunks (we moved the chunks first) and two 25-cm vertical cores, one about 10 cm away at the same elevation as the chunks and the other was 10 cm away in the down-gradient direction (Figure 26). The surface sample under the HE chunks had extremely high concentrations of RDX, HMX, and TNT, the highest being 26,000 mg kg^{-1} (26 g kg^{-1}) of RDX, indicating the presence of particles. The adjacent and down-gradient core samples had RDX (primary), HMX, and TNT in concentrations less than 10 mg kg^{-1} (Figure 26). The down-gradient core had higher explosive concentrations at the surface than the adjacent core suggesting some downhill surface transport. The high concentration of RDX relative to TNT indicates that the latter has been preferentially degraded or dissolved.

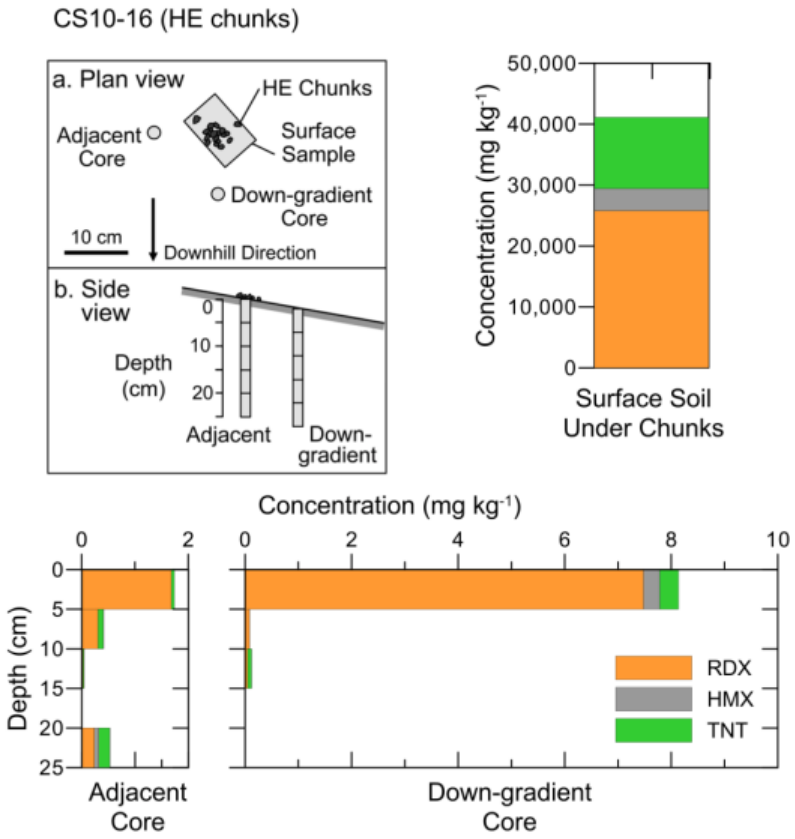

Figure 26. High explosive compounds in core samples taken near chunks of HE spilled from the broken 105-mm round CS10-16.

We conducted a short dissolution study by setting out 21 HE chunks that were collected near CS10-16 on a nearby level soil surface before a rain event. The chunks ranged in size from 0.1 to 1.2 g for a total of 7 g. It did rain and we captured 2.4 mm in our improvised rain gauge, an open-mouthed jar set nearby. We collected two 25-cm cores – one directly underneath the HE pieces and one about 10 cm away (Figure 27).

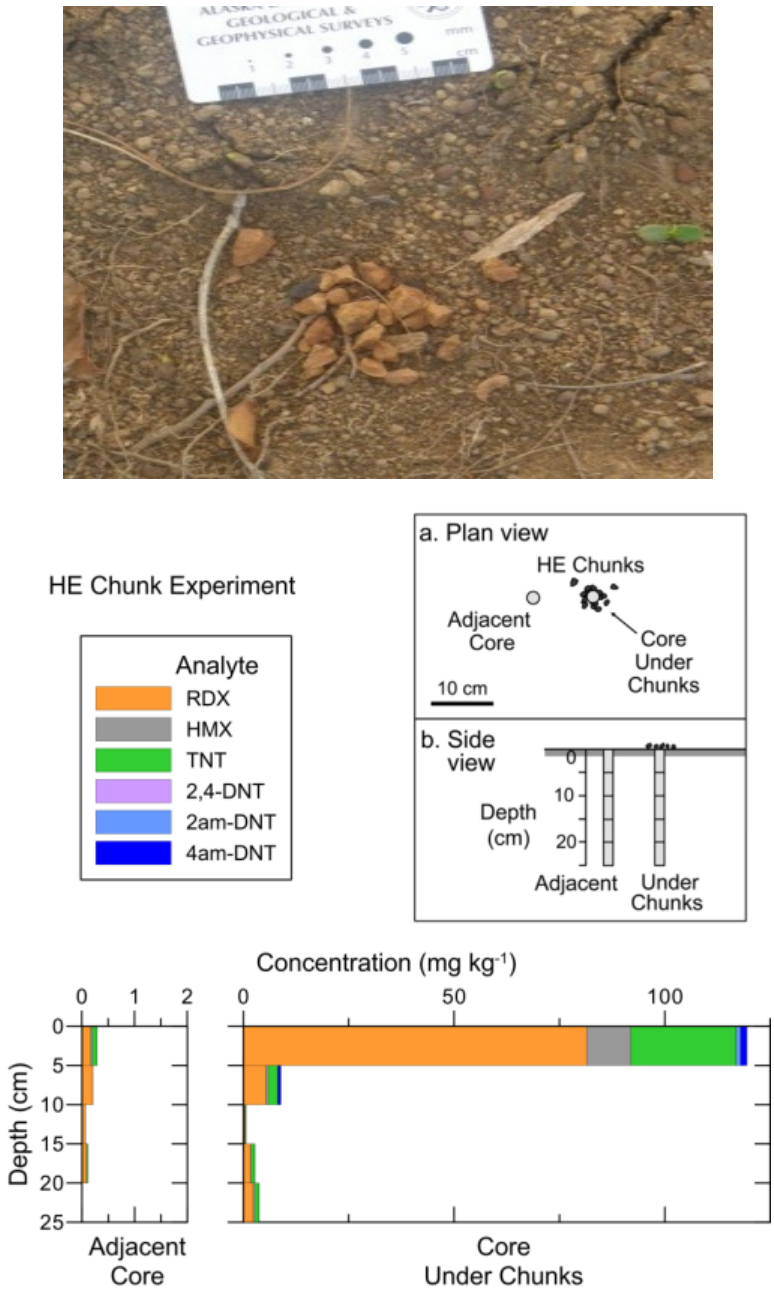

Figure 27. Image of 21 Comp B pieces placed on soil for a dissolution experiment (upper) and concentrations of HE compounds beneath Comp B chunks exposed to a single rain event.

The samples contained the full suite of high explosive compounds (Figure 27). In the 0 to 5-cm sample underneath the chunks, RDX was present at the highest concentration (81 mg kg^{-1}), followed by TNT (25 mg kg^{-1}) and HMX (10 mg kg^{-1}), with minor amounts (<2 mg kg^{-1}) of 2,4-DNT and the 2am- and 4am-DNTs. Although we cannot be certain that the explosives in the soil core derived from the single rain event, the much higher concentrations in the core directly beneath the Comp B pieces compared to the second, nearby core, indicate that this is the case.

We estimated the amount of dissolved HE entering the soil by assuming that the 2.4 mm of rainfall left the HE particles saturated with respect to TNT and RDX. We used the mass of each particle to calculate its equivalent spherical diameter and the collective surface area seen by rain, 12 cm^2. Using the values listed in Table 1 we estimate that the rain hitting these particles would have introduced 50 mg of dissolved HE to the soil. Since the core barrel had a 1-cm radius, it sampled a 3.14-cm^2 area of the surface. If the HE were evenly distributed, we would predict a total of 8 mg kg^{-1} dissolved HE in the area sampled by the core. What we measured was over 100 mg kg^{-1} in the 0–5-cm interval, about 10 mg kg^{-1}in the 5–10-cm section, and lower values with depth. The large surface concentration cannot be accounted for by dissolved HE, so small explosive particles must have been present. Consistent with our interpretation is the ratio of TNT to RDX in the 0–5-cm interval, which is similar to those of Comp B particles. The lower concentrations with depth could result from dissolved HE in the pore water.

Table 4 summarizes the UXO that were leaking HE into soil and the peak concentrations of compounds detected. Of the 43 UXO (42 corroded rounds and one partial detonation), eight were found to have leaked HE into the soils.

Table 4. Summary of HE concentrations found under leaking UXO rounds.

Site [1]	Round type	Highest concentration		Next highest concentration		Sample ID
		(mg kg^{-1})	Compound	(mg kg^{-1})	Compound	
ERF	60-mm	10.2	RDX	2.42	HMX	CS09-12
	60-mm	3.2	RDX	0.93	HMX	CS09-16
SLO	60-mm	0.31	Tetryl			CS09-75
VQS	81-mm	59	Tetryl			CS10-25
	105-mm	**26,000**	**RDX**	**12,000**	**TNT**	**CS10-16***
	106-mm	1.8	RDX	0.43	HMX	CS09-55
	4.2-in	110	TNT	12	4am-DNT	CS09-49
	155-mm	1.9	TNT	0.06	2,4-DNT	CS10-11

[1] ERF - Eagle River Flats, AK; SLO - San Luis Obispo, CA; VQS - Vieques, PR.
*** Partial detonation**

Examples of UXO not leaking HE

Some rounds we thought would leak HE were not leaking. CS09-41 was a 105-mm round that appeared to be found *in situ*, but which could not be moved because of its proximity to a 5-in round (Figure 28). The round was extremely corroded with longitudinal cracks and flaking metal. Using scoops, we collected one vertical profile beneath the round and lateral soil samples from a trench (Figure 29). Analyses of the samples taken beneath the round show no explosives. The lateral samples contain RDX and HMX (Figure 29). The lack of HE under the round suggests that the round was not leaking and the high concentration of HMX relative to RDX in the lateral samples closest to the round suggest that the HE was not released recently. We think, therefore, that the surface soil was contaminated. The presence of the 5-in round suggests this location is a collection point where blow-in-place operations have taken place.

Figure 28. Image of 105-mm round found near the northern shoreline at Vieques (below sign in upper photo) and another showing the trench created by removing the lateral samples collected adjacent to this round.

Three other UXO appeared to have exposed HE. CS10-24 was a 60-mm UXO with large chunks of exposed fill at the nose (Figure 30a). One of these chunks weighed 34g (Figure 30b) and we moved it to a nearby flat area and, after a rain event, took a core directly below this piece. We found no HE under the chunk or under its parent round, suggesting that CS10-24 was an inert round with a non explosive fill. Similar negative results were found for cores taken below the 81- and 60-mm mortars pictured in Figure 31. We think these rounds are also inert practice rounds. Expray can be used to check potential HE pieces such as these

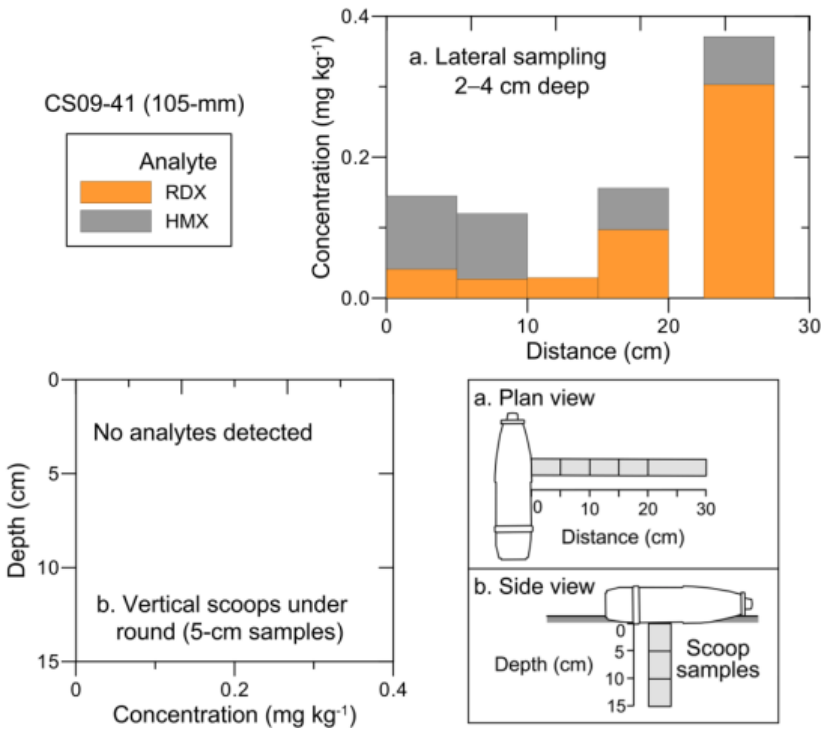

Figure 29. High explosive compounds in soil samples lateral to and beneath the 105-mm round CS09-41.

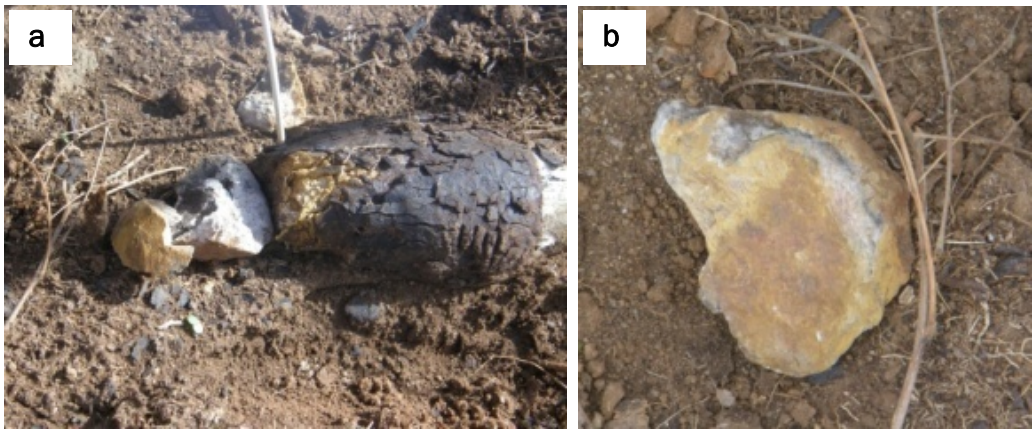

Figure 30. A 60-mm round (CS10-24) with apparent exposed HE in position as found (a), and a 34-g chunk from this round that we moved and sampled beneath after a rainstorm (b).

Figure 31. Rounds with exposed fill and no HE compounds in the soil below: 81-mm CS10-33 (a, left); and 60-mm CS10-34 (b, right).

Number of UXO per acre

Contractors clearing UXO at Vieques have divided the island into a system of 30 × 30-m grids and record the number of items found on the soil surface in each grid. On 16 September 2011, we sampled from three adjacent grids (I3G3C9, I3G3D9, I3G3E9), which sized together total 30 × 90 m (Figure 32). Within them, the UXO team located sixteen 81-mm mortars and four 60-mm mortars, or 20 UXO in 2700 m^2. If this surface density is representative, we would expect 74 UXO on the surface per hectare (a hectare = 10,000 m^2), or 30 per acre (4047 m^2). We collected soil samples from nine of the 81-mm rounds and from all four of the 60-mm rounds. At the time we sampled, only one round (an 81-mm, CS10-25) was leaking energetic compounds into the soil (tetryl). If these data are representative, we would expect five or six leaking UXO per hectare (two per acre). The amount of HE dissolving from these rounds would depend on the amount of HE exposed and the amount of rainfall.

Figure 32. The cleared area of grid I3G3E9 searched and sampled for UXO in September 2010.

Corrosion Patterns

Although we sampled soil beneath 42 UXO, we examined many others and describe their corrosion patterns.

The rounds sampled at ERF had been sitting in the salt marsh environment for three years. Generally the visible metal casings of the 60-mm mortars were in good condition and still coated with paint. The aluminum fins and fuses of the rounds showed some pitting and oxidation (Figure 33a). The sides of the rounds that had been in contact with the soil were more heavily weathered and had sections where the iron casing had pitted and was corroding (Figure 33b).

At Camp San Luis Obispo, UXO found on the surface were oxidized and pitted (Figure 34); rounds that were buried were very corroded. The casings of the corroded rounds were mainly iron oxides that flaked off when touched (Figure 35). Oxidation of the iron metal caused the casing to expand, forming longitudinal cracks and circumferential cracks, the latter similar to layers of an onion (Figure 35b), which flake off the round.

At Vieques, we saw pitting and oxidation on the upper surfaces of rounds lying on the soil and heavy corrosion on the undersides that were in contact with the soil (Figure 36a). Soil moisture and possibly bacterial action greatly accelerated the corrosion of the metal in contact with the soil and some UXO appear to have corroded through to the HE-fill via this mechanism (Figure 36b). As was observed for buried rounds at San Luis Obispo, metal in contact with soil oxidized and expanded forming longitudinal cracks and circumferential cracks (Figure 37). The iron casing sometimes had expanded so much that the aluminum rotating-band was no longer

Figure 33. A 60-mm mortar (CS-09-8) found at ERF in 2009 and thought to have been fired during a 2006 training exercise showing the (a) visible side and (b) side in contact with the soil.

Figure 34. Examples of 60-mm mortar rounds found on the surface at San Luis Obispo.

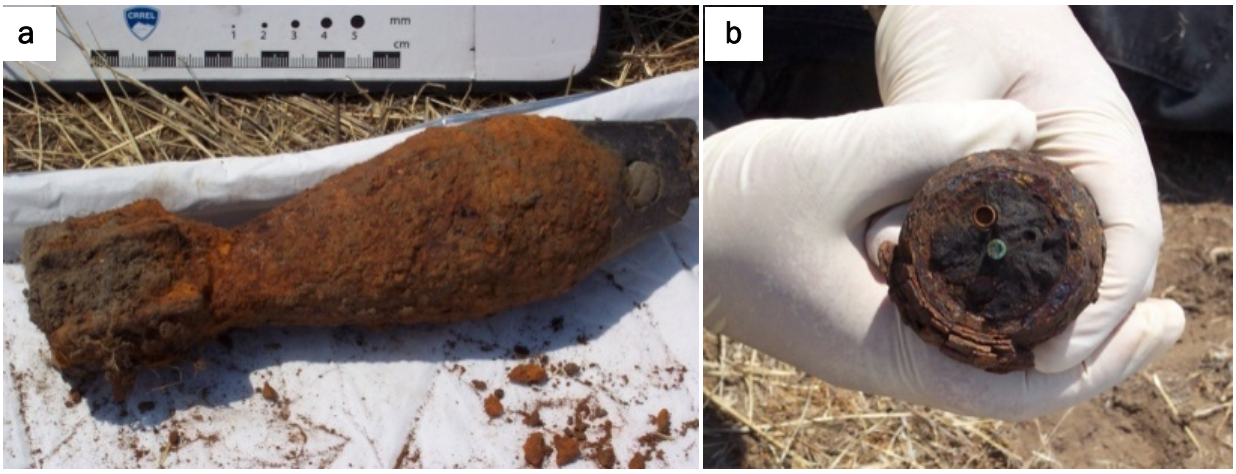

Figure 35. Buried rounds exhumed at Camp Luis Obispo: (a) 60-mm mortar with fuze; (b) 60-mm mortar without a fuze that shows the metal flaking in concentric layers.

flush with the surface but a centimeter below it (Figure 37a). Pieces of oxidized metal readily flaked off the rounds (Figure 38a) and examination of a metal piece from a 105-mm casing show a series of planes parallel to the inner and outer surfaces of the casing (Figure 38b). The casing readily splits along these planes facilitating flaking. In some cases, the entire casing has flaked off leaving the explosive fill totally exposed (Figure 39). When this occurs, the surface of HE is dissolved by precipitation and the explosive pieces are subject to mechanical breakage (Figure 39b). Interestingly, we saw chunks of HE-fill with smooth surfaces that retained the shape of the casing within which they were enclosed (Figure 39b). This indicates that even when highly corroded the casing protected the HE from dissolving until the casing fell apart completely. Figure 38a and 39c show groves in HE that appear to be extensions of cracks in the casing suggesting that, in these cases, water penetrated through the cracks and dissolved a small amount of the fill.

Figure 36. Examples of large-diameter UXO found at Vieques that were partially buried. (a) The surface of the UXO exposed to air was pitted and oxidized while the surface in contact with soil was highly corroded; (b) UXO carcasses showing large holes resulting from corrosion. What happened to the HE once in these rounds is not known.

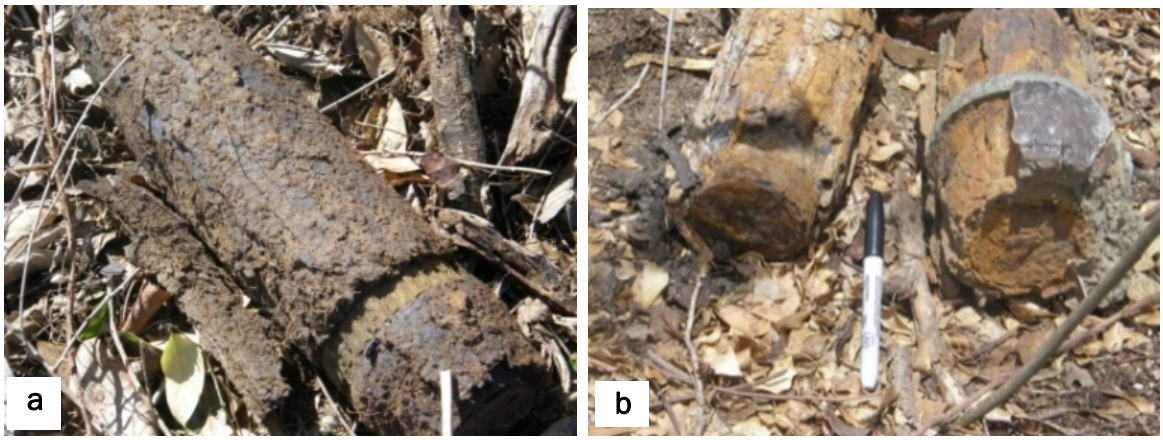

Figure 37. Corrosion patterns seen in Vieques in which metal in contact with soil oxidized and expanded forming longitudinal cracks and circumferential cracks.

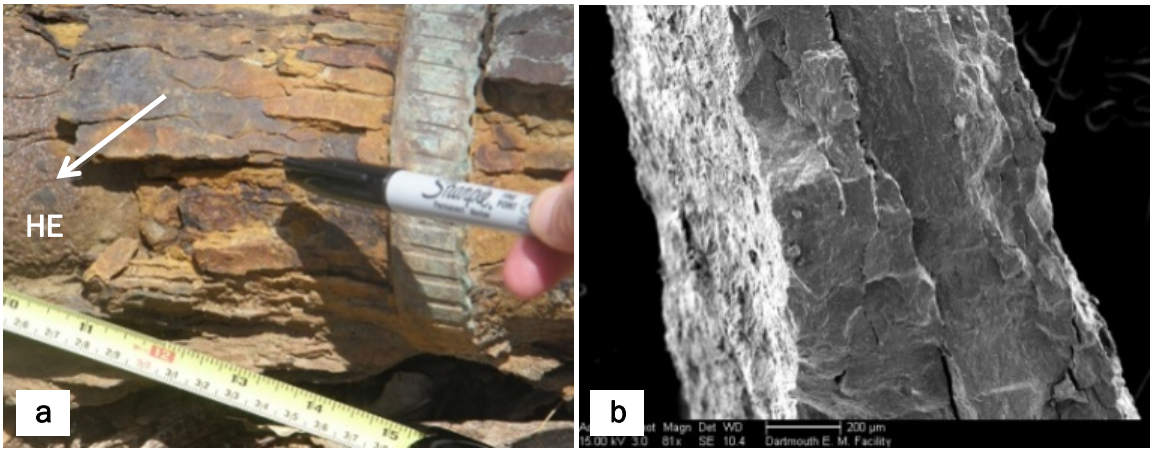

Figure 38. Oxidized metal flaking off on a corroded 105-mm round as seen (a) in full size and (b) magnified by a scanning electron microscope.

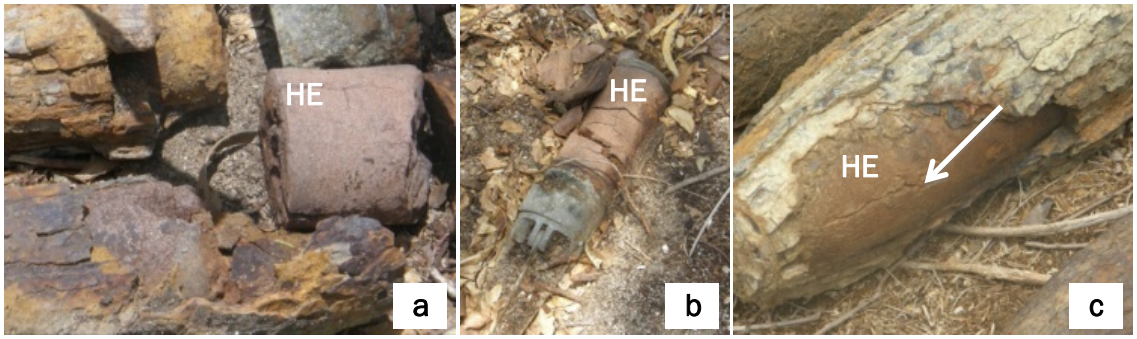

Figure 39. Rounds with explosive fill that has been totally exposed and retained the shape of its former casing.

Although we did not study UXO in the nearby ocean at Vieques, we were able to examine a 155-mm round that had been underwater (Figure 40). It was covered with a white crust, some type of carbonate, which we removed using a knife and a wire brush. While removing the carbonate, large pieces of the underlying metal also scaled off.


Figure 40. A 155-mm round that was pulled from the ocean in Vieques (left side of each image) along with one that had been on the island (a, left) before and (b, right) after scraping off the white crust layer.

At all three sites, surfaces of UXO not in contact with soil were pitted and oxidized; alteration of the metal to iron oxides occurred for the parts of casings buried in, or in contact with, the soil. We saw total corrosion of casings at SLO and Vieques and failure (leaking HE) in about 20% of these highly corroded rounds. Models that predict how quickly pinholes will widen and deepen until they penetrate the casing (Chendorain et al. 2005) will predict much longer times to UXO failure than if the effects of oxidation and swelling of the metal and loss of large pieces of the casing had been modeled. Since these researchers were not able to move the UXO they studied, they only observed the top pitted surfaces of their rounds.

Gypsum dissolution from 60-mm mortars

Before beginning these dissolution tests we tested the comparability of ion conductivity (IC) to electrical conductivity measurements for quantifying ions in solution (Figure 41). The two

methods produce similar results giving us confidence that both techniques could quantify the dissolved calcium and sulfate from the gypsum. In addition, the 1:1 calcium to sulfate ratio found by IC analyses indicates that no other cations or anions were in the water (Figure 42). As only calcium and sulfate ions were present continuously recorded electrical conductivity should accurately measure the gypsum concentration in long-term tests without the need to take water samples for IC analyses.

Figure 43 plots the gypsum dissolution, in mg, from the six pieces of ordnance and the two Nalgene bottles for first 25 days. The mass loss ranged from 1 to 51 mg and most of the ordnance items lost between 5 and 10 mg. The highest rate was measured from the Nalgene bottle with the large hole and the smallest mass loss was from the piece of ordnance with the small hole (purple line). The mass loss from this last item did not plot above baseline until after day 23.

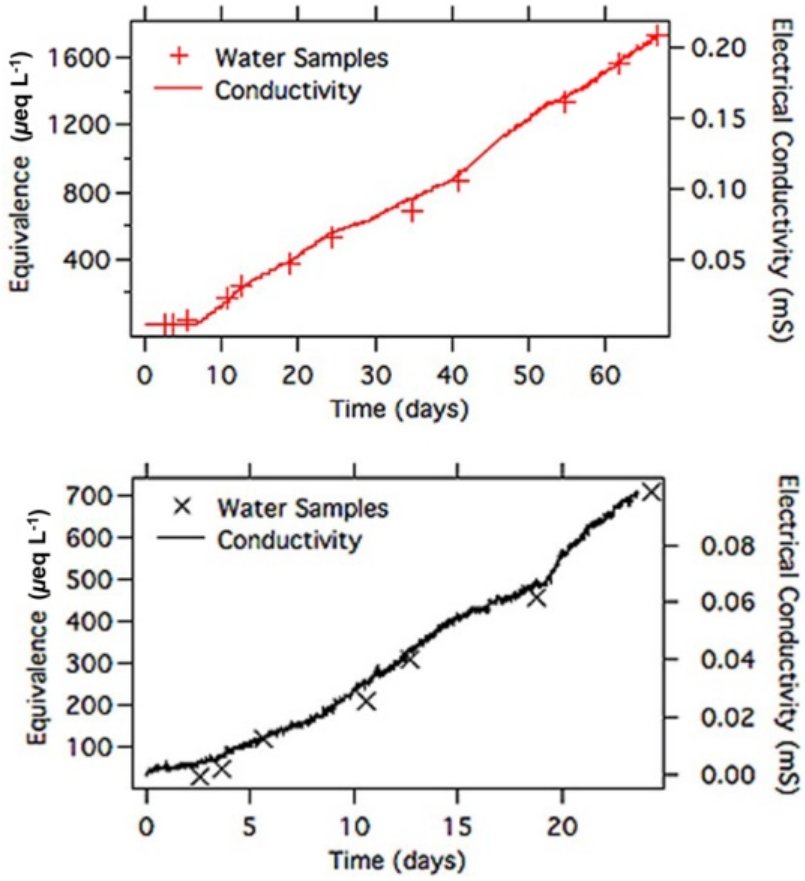

Figure 41. Relationship between the ion conductivity measurements made on water samples and electrical conductivity measurements for one of the Nalgene (red) and ordnance (black) tests.

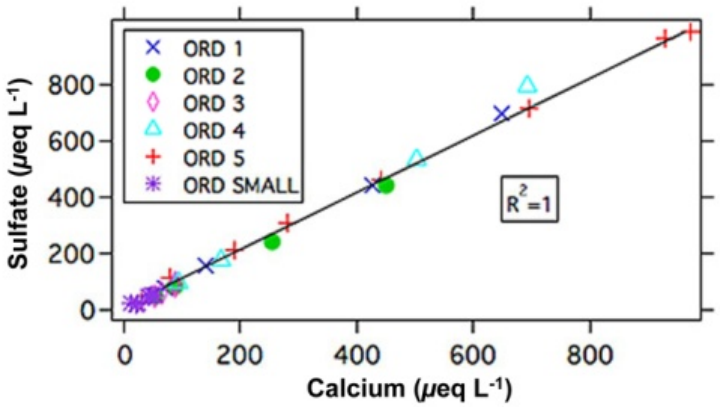

Figure 42. Measured calcium versus sulfate concentration for the six ordnance tests.

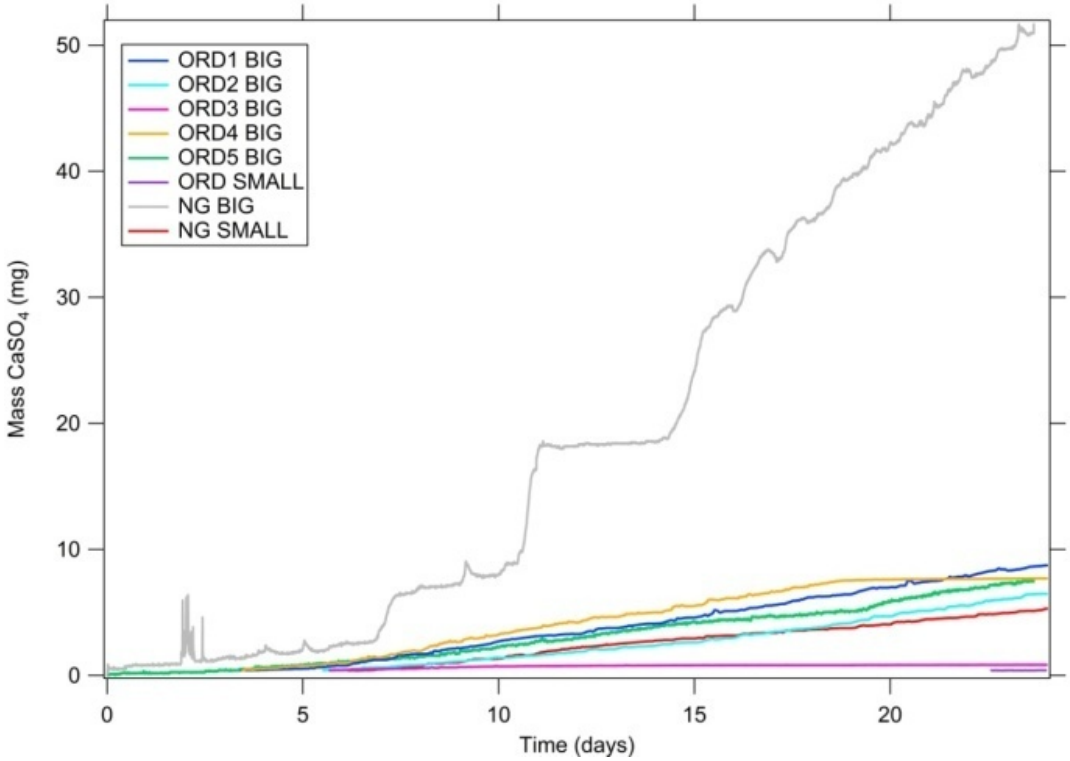

Figure 43. Gypsum mass loss results for the first 25 days from the ordnance (ORD) and Nalgene (NG) tests with big and small holes.

Figure 44 plots the gypsum mass loss over the duration of the longest test, 272 days. Mass loss was still highest for the Nalgene bottle with the large hole although this test was stopped after 25 days. Next came the Nalgene bottle with the small hole, which lost 48 mg of gypsum during the 272 days. Two of the ordnance items lost 19 and 20 mg, three others lost between 5.6 and 9.4 mg and the ordnance with the small hole lost the least amount of gypsum, less than one mg. Generally the dissolution from the steel ordnance and Nalgene bottles start off at similar rates but then slowed down for the ordnance, while the Nalgene bottles have linear loss rates. The rounds with the small holes always loose less gypsum than those with larger holes.

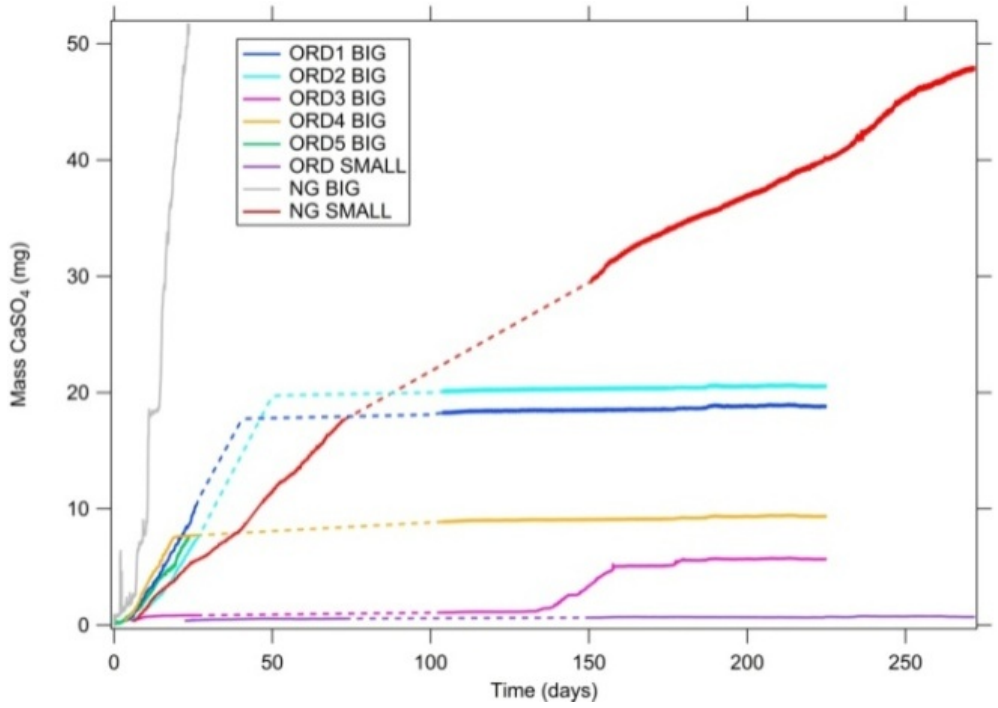

Figure 44. Dissolution results for 272 days. Unfortunately a problem with the data logger produced a break in what should be a continuous record. We have dashed in the missing data and added the sharp bends to ORD1&2 following the pattern seen in ORD3&4.

The gypsum dissolution rates between the ordanance and the Nalgene bottles are quite different and we think two reasons account for these differences. First, the walls of the Nalgene bottles are very thin compared to the 60-mm mortars, making it easier for water to contact and dissolve the gypsum. We saw cavities forming in the gypsum (Figure 45) and we hypothesize that the saw-tooth pattern seen in the record from the Nalgene bottle with the large hole derives from small pieces of gypsum falling out into the tank. The second, more important, reason is that iron oxide forms around the drilled holes in the ordnance (Figure 46). We think that rust blocks the opening and dramatically decreases the loss of gypsum. Our results indicate that iron oxides blocked a 6.32-mm hole in less than 50 days and that the 3.16-mm hole was never fully opened. Nalbandian and Kalikian (2007) also report iron oxides blocking holes in ordnance found in the field. We would expect pinholes and small pits in field UXO to be blocked by oxides as well, which would explain why highly corroded rounds were not leaking HE (Figure 47a). If the holes are large enough, such as those formed by a fragment from a high order detonation (Figure 47b), oxides cannot seal the opening and HE will leak from the round.

Figure 45. Pictures of the cavity formed in NG BIG. The depth of the cavity measured approximately 2.4 cm.

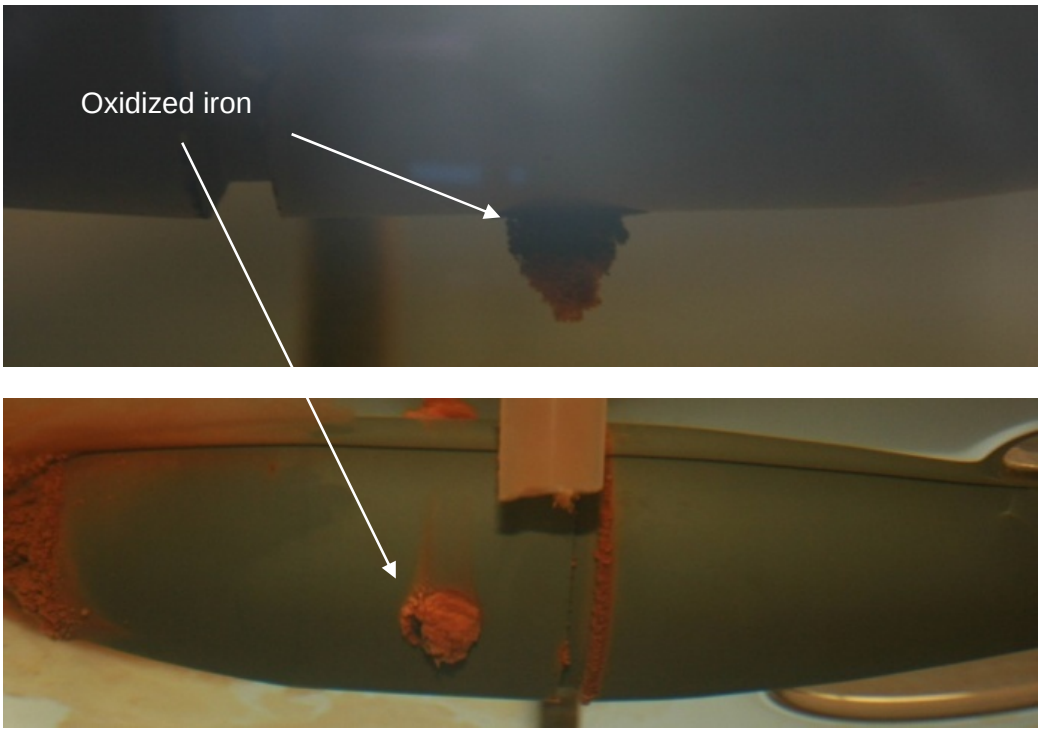

Figure 46. Oxidized iron surrounding the drilled hole in one of the munitions seen in (a, upper) side view and (b, lower) oblique view.

Figure 47. (a, upper) Very corroded 81mm round not leaking explosives and (b, lower) hole in a 81-mm mortar caused by a fragment from a nearby high-order detonation.

Table 5 lists the dissolution rates derived from these tests along with literature values for TNT and RDX. Gypsum leaked from the "big" 0.3-cm^2 holes in the 60-mm rounds at dissolution rates varying from 3 to 42 µg cm^{-2} hr. Less mass loss would occur from explosive-filled rounds because gypsum's solubility (2,400 mg L^{-1}) is much higher than those of TNT or RDX (130 mg L^{-1} and 46 mg L^{-1}). Also, any iron oxide build-up at the hole would decrease the area available for dissolution and lower the dissolution rate.

Table 5. Dissolution rate estimates for gypsum measured using a variety of experimental conditions. Note that the rate cannot be given by one value as the dissolution changes with surface area exposed: more mass will be dissolved when larger areas are exposed. Therefore, the given rates are averages over the duration of the experiment. The TNT and RDX rates are also averages derived for surface areas up to ~4cm^2, holes 1 mm to 2 cm in diameter. Many of the UXO holed by fragmentation pieces have holes in this size range.

Category	Item	Time	Gypsum dissolved	Hole dimensions		Dissolution rate
				Diameter	Area	
		(hrs)	(mg)	(mm)	(cm^2)	(µg cm^2 hr^{-1})
Current study	Ord1	5396	18.84	6.32	0.314	11.1
	Ord2	5396	20.54	6.32	0.314	12.1
	Ord3	5396	5.68	6.32	0.314	3.35
	Ord4	5396	9.38	6.32	0.314	5.53
	Ord 5	568	7.46	6.32	0.314	41.8
	Ord Small	6521	0.71	3.16	0.0785	1.38
	NG Big	568	51.73	6.32	0.314	289.86
	NG Small	6521	47.97	3.16	0.078	93.71
	Compound	**Test type**				
Taylor et al. 2010	TNT	Outdoor Tests			0.6 to 2.0	2.5 ± 0.7
	RDX				0.4 to 3.7	2.3 ± 0.8

The same sized hole in a Nalgene bottle had a dissolution rate two orders of magnitude larger than that measured for the ordnance. We think this resulted when a cavity formed in the gypsum, increasing the surface area exposed to water over time. Therefore, the dissolution measured from the Nalgene bottles does not reflect mass loss from a 0.3 cm^2 area but from a much larger area. Such cavities could form in HE filled rounds pierced by large holes, and have been seen in practice rounds collected in the field (Figure 48).

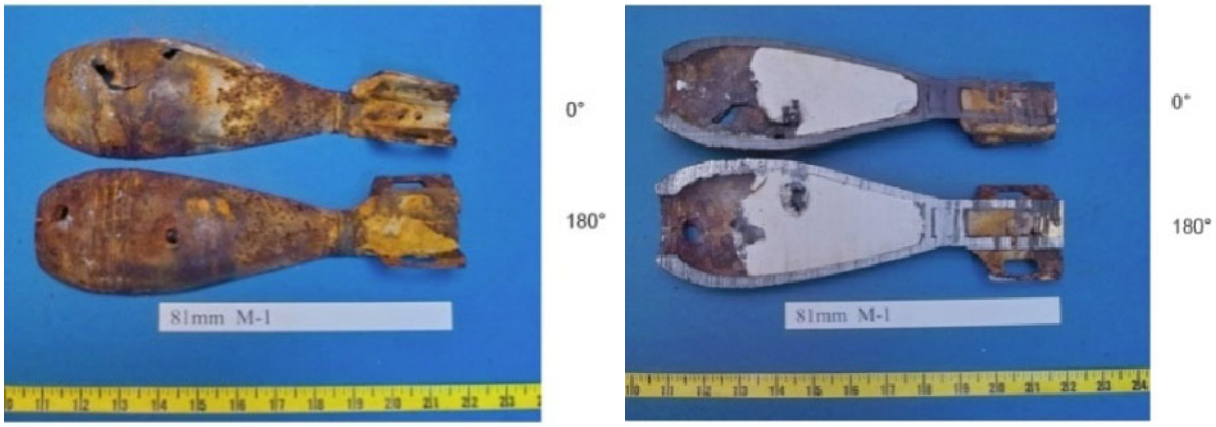

Figure 48. Practice UXO collected at MMR (from Nalbandian and Kalikian 2007).

Given a 2-cm^2 hole in an HE-filled UXO, we would predict ~2.5 x10^{-6} g to be dissolved each hour for a UXO in areas receiving ~ 100cm y^{-1} rainfall. If this were the only area of HE exposed to water, it would take ~2000 years to dissolve the 35g of HE from a 60-mm mortar. If larger areas of HE were exposed to water, by the formation of a cavity, the rate would be faster. Climate would also play a role: drier areas would have less dissolution, wetter areas more dissolution.

Numerical Modeling of HE transport

Transport of TNT and RDX through the soil was simulated with Hydrus-1D (Šimůnek et al. 2009), a one-dimensional numerical model for solving water and solute transport through variably saturated media. The groundwater infiltration model accounts for field conditions and calculates the rate at which dissolved explosives are transported vertically into the soil and groundwater. Several sources of data were used to develop the transport model. Local meteorological data determine boundary conditions that drive infiltration and account for evaporation and plant uptake. Soil hydraulic properties determine the rate at which water moves through the soil. Finally, source, transport, and reaction parameters govern the behavior of HE in the soil profile. The results from the simulation indicate that 1) all solute flux through the bottom of the soil profile occurs in the days following major seasonal precipitation events, and 2) to the extent that transformation occurs and flow does not pass through preferential pathways, it is possible that no TNT or RDX passes through the bottom of the soil profile.

Site data

Meteorological data

Local meteorological data are limited and are often quite variable, both spatially and temporally. Meteorological data are continuous for San Juan, Puerto Rico from 1973 to the present (NCDC). Limited meteorological data are available from a station in central Vieques Island from 1955–1976 and 1983–1994. More recent data for Vieques is available through the Citizen Weather Observer Program at station MVIEP4 and covers between 2007 and 2011, although 2010 is the only year of the dataset for which the data was found to be complete, and metadata was not supplied with this dataset. In addition, historical reports give annual estimates of the precipitation, temperature and evaporation on Vieques (Lugo-Lopez et al. 1953, Goyal 1988).

The San Juan data shows the average annual temperature is 26.6°C and the mean annual rainfall is 1252 mm. These estimates compare well with the historical Vieques data (Figure 49). Based on available meteorological data (NCDC 2010), Vieques has an average annual temperature of 24.3°C and mean annual rainfall of 1184 mm. Lugo-Lopez et al. (1953) estimated an average annual temperature of 26.4°C and a mean annual rainfall of 1242 mm, but cautioned, "…the eastern section of Vieques is extremely dry, total rainfall probably is not more than 20 or 25 inches (508–635 mm), as in eastern St. Croix." Another report notes similar findings of low precipitation amounts on the eastern side of the island (Baker Environmental 1999). However, due in part to intense rains registered in 2010 in July (325 mm) and October (462 mm), the rainfall was reported to be well above average at 1899 mm, which is 150 to 160% of the average rainfall from prior reports. Figure 50 shows the monthly total rainfall variability at Vieques and San Juan for comparison. Significant year-to-year variability in precipitation appears to occur in the late summer and early fall due to tropical storms and hurricanes in the Caribbean. Because increased precipitation is likely to be associated with a larger solute mass-loading of the system, use of rain data from this more recent above-average year may be justified.

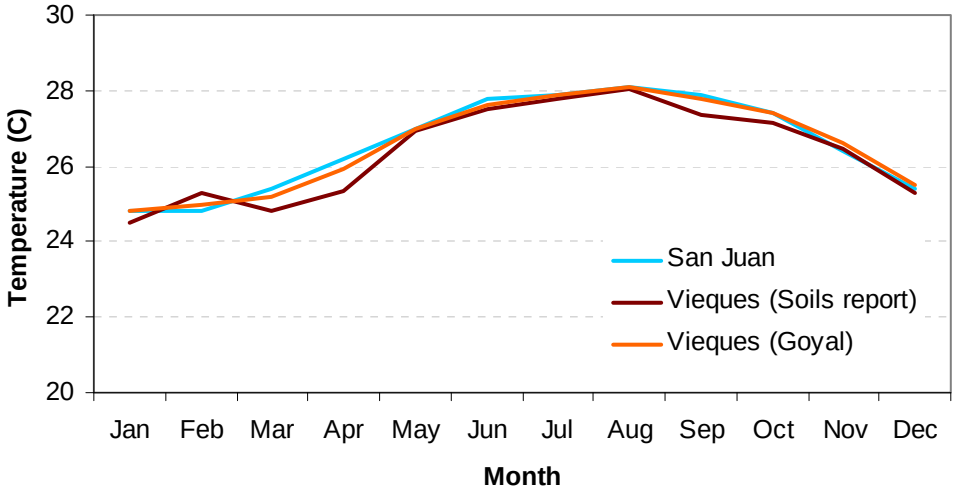

Figure 49. Average monthly temperature at San Juan and Vieques.

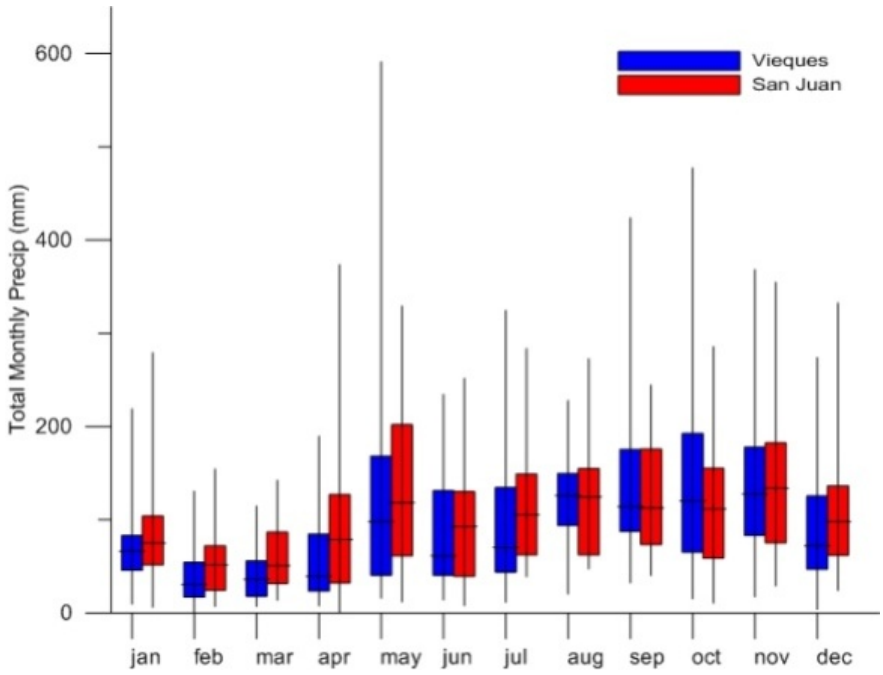

Figure 50. Monthly precipitation at San Juan and Vieques showing the median, 25th and 50th percentiles, and the historical maximum and minimum.

The Hargreaves formula (Maidment 1993) can be used to estimate potential evapotranspiration (PET) from daily air temperature data. The mean annual PET calculated for San Juan is 1387 mm. Goyal (1988) used the Hargreaves method to estimate evapotranspiration in Vieques and found monthly values ranging from 3.29 mm day^{-1} in December to 4.94 mm day^{-1} in July, and a total annual PET of 1556 mm (Figure 51). These values are slightly higher than the values estimated using the San Juan temperature data; 3.02 – 4.43 mm day^{-1}. Torres-Gonzalez (1989) noted that approximately 90 percent of precipitation on St. Thomas is lost to evaporation and that of the remaining 10 percent, approximately 3-5 percent infiltrates into the groundwater system and the remainder becomes surface runoff. These estimates were reported in Jordan and Cosner (1973), though the justification for the estimates was not clearly supplied.

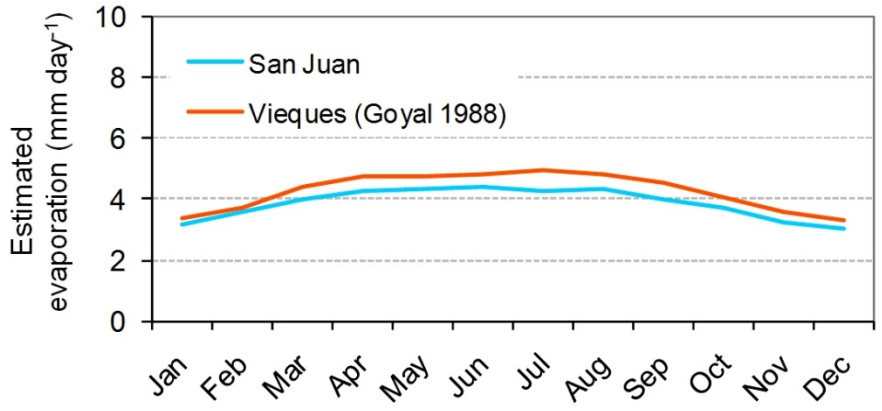

Figure 51. Average monthly evaporation at San Juan and Vieques.

Vegetation

Vegetation on the eastern portion of the island consists of mostly mesquite trees and guinea grass (CH2M HILL 2009, Lugo-Lopez et al. 1953). Site visits confirmed these descriptions (Figure 52). Mesquite trees are a hardy species that can survive under drought conditions. Average mesquite trees are about 3.6 m high. They have a shallow root system that extends 0.30 to 1.3 m beneath the surface, and a longer taproot that can extend as deep as 3 m. Vegetation properties used in the model are given in Table 6. The remediation plan calls for the removal of all vegetation smaller than 76.2 mm (3 in) in diameter (CH2M HILL 2009). This will have an impact on transpiration and net infiltration during remediation; however the climate of Vieques is such that plant growth occurs relatively quickly (Figure 53).

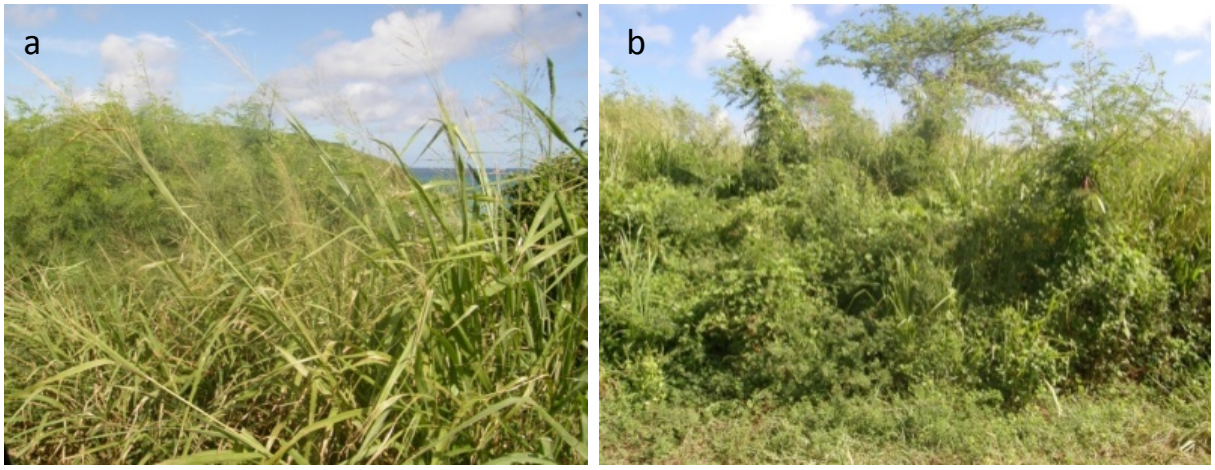

Figure 52. Typical vegetation at Camp Garcia, Vieques: (a) guinea grass in the foreground with mesquite trees covered in vines behind, and (b) closer view of mesquite trees.

Table 6. Properties of mesquite trees (Thompson 1986)

Leaf Area Index	1.25
Light extinction coefficient, k	0.34
Radiation use efficiency	1.61
Root depth	0.30 to 1.3 m, with tap root <= 3 m
Tree height	3.6 m

Figure 53. Example of vegetation growth rate on the southern shoreline. Scene soon after clearing in June 2009 (upper) and in September 2010.

Hydrogeology

The eastern half of the island largely overlies impermeable granodiorite bedrock and minimal non-saline groundwater is available (Baker Environmental 1999). Limestone underlies the easternmost isthmus of the island, and Lugo et al. (2004) notes that all Puerto Rican limestones have karst features, which may provide preferred flow pathways for recharge. Above the bedrock lies a layer of Guayama Clay (Torres-Gonzalez 1989), ranging in thickness from 1.5 to 4.75 m (Baker Environmental 1999). At the surface, a layer of silty topsoil is mixed with the clay. This was also noted in field measurements at sites inland from the shore, while at the shore the surface layer consisted mostly of medium to fine sands.

The two productive aquifers beneath the island of Vieques are the Resolucion aquifer in the west and the Esperanza aquifer in the south-central part of the island. Groundwater does not flow

from the eastern portion of the island to the western portion where the aquifers are located, based on a potentiometric surface that follows the shape of the terrain, partly confirmed in the field by Baker Environmental (1999). Torres-Gonzalez (1989) found groundwater levels in the Esperanza aquifer to be between 3 and 9 m beneath the surface depending on the distance from the shore. Earlier studies measured groundwater levels on the eastern side of the island to be 3 m below the surface (Baker Environmental 1999). No stream gauges have been installed at Vieques, but on St. Thomas in the nearby U. S. Virgin Islands "small rains that cause no rise in the water level in the bedrock cause a marked increase in spring discharge and base flow of the stream" (Jordan and Cosner 1973). This suggests that precipitation on St. Thomas moves laterally through the shallow subsurface before discharging in ephemeral streams, rather than running off as sheetflow or entering the deeper groundwater system.

Governing Equations used for Simulations

Hydrus-1D simulates 1) water flow through a soil profile over time, and 2) the fate of chemical species during that time. The purpose of building this model is to investigate how different processes may affect the delivery of TNT and RDX from UXOs into the soil and groundwater system present on Vieques. This information could subsequently be used to estimate the total TNT load in soil and groundwater for a larger area based on the total number and type of UXOs present. In its current form, the model includes analysis of TNT and RDX only, and does not follow the fate and transport of their transformation products. It also does not simulate physical or chemical behavior below the soil profile in weathered or unweathered bedrock, although some physical behavior can be inferred.

In Hydrus-1D, the physical flow and the chemical fate-and-transport subroutines each solve a governing equation given a set of boundary conditions and physical parameters. Physical flow is calculated with the Richards equation (Šimůnek et al. 2009), which describes flow behavior in variably saturated media as

$$\frac{\partial \theta}{\partial t} = \frac{\partial}{\partial x}\left[K\left(\frac{\partial h}{\partial x} + \cos\alpha\right)\right] - S \qquad (1)$$

where h is the pressure head [L], θ is the volumetric water content [L^3L^{-3}], t is time [T], x is the distance [L], α is the angle between the flow direction and the vertical axis (i.e., $\alpha = 0$ for vertical flow), and S is a sink term, which in the present case is a function that represents root water uptake by vegetation. K is the unsaturated hydraulic conductivity [LT^{-1}], which is a function of the head and reaches its maximum value when saturated.

The governing equation used to calculate chemical transport in this Hydrus-1D simulation is a version of the advection-dispersion equation, with a term that includes non-equilibrium sorption-desorption reactions and a sink term to include loss of HE through transformation. The equation presumes that flow is one-dimensional and the medium is rigid (Šimůnek et al. 2009).

$$\frac{\partial \theta c}{\partial t} + \rho \frac{\partial s}{\partial t} = \frac{\partial}{\partial x}\left(\theta D^w \frac{\partial c}{\partial x} - qc\right) - \gamma_w \theta \qquad (2)$$

where θ is the volumetric moisture content [L^3L^{-3}], c is the dissolved concentration [ML^{-3}], t is time [T], ρ is the soil bulk density [ML^{-3}], s is the sorbed concentration [MM^{-1}], z is vertical distance [L], D^w is the coefficient of dispersion [L^2T^{-1}] , q is the volumetric flux density [LT^{-1}], and γ_w is a zero-order rate constant used to represent transformation [$ML^{-3}T^{-1}$].

Flow inputs

First, daily meteorological data from Vieques (MVIEP4) from 8/8/2008 to 1/17/2011 were input to Hydrus-1D as a daily time step. Unfortunately, a significant data gap was present between August and November 2009. Based on similarities in the average weather parameters from both Vieques and San Juan, data was substituted during this time period from NCDC records from San Juan. The precipitation data entered into Hydrus-1D covered a period of 893 days (Figure 54). Sinusoidal variations of precipitation during each time step were implemented within Hydrus-1D. This feature may be advantageous in tropical areas because if hourly precipitation measurements are not available and fluctuations in intensity are not considered over the day, more precipitation may be calculated to infiltrate than can occur during the duration of the actual event.

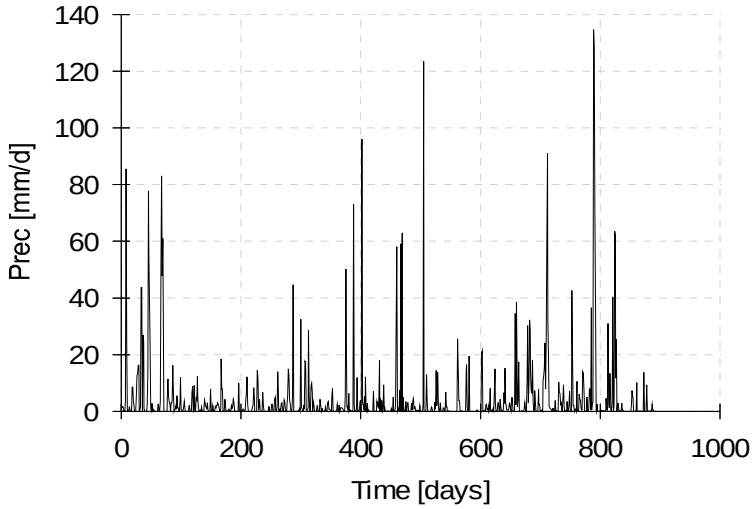

Figure 54. Precipitation on Vieques and San Juan, August 2008–January 2011. Data sources: Citizen Observer Weather Program (MVIEP4) and National Climactic Data Center (NCDC 2010).

Potential evapotranspiration is calculated internally to the model using the Hargreaves formula (Figure 55), and sub-daily variations of transpiration were also simulated internally. Root water uptake was calculated separately from surface evaporation based on the characteristics of mesquite trees (Table 6). Feddes' water uptake reduction model was used to account for presumed higher transpiration through roots located close to the surface.

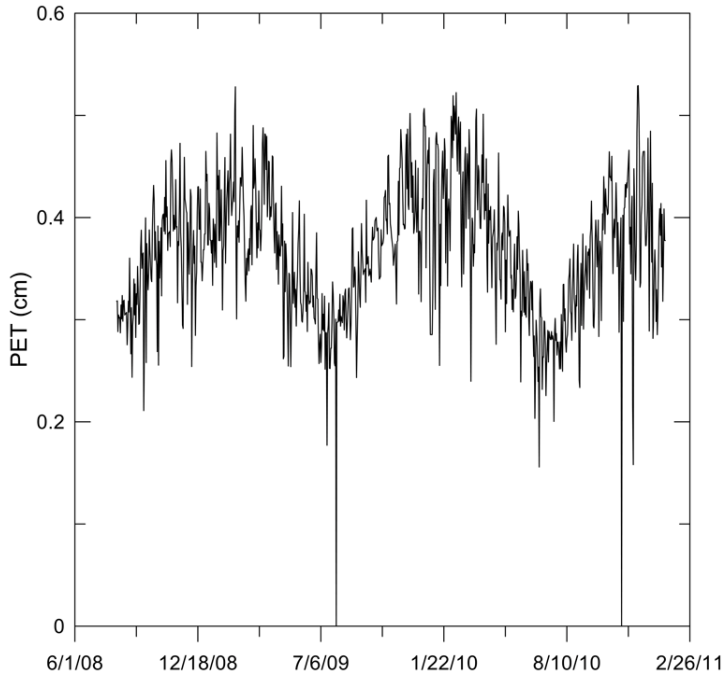

Figure 55. Potential evapotranspiration (PET) as calculated by the Hargreaves method. Days with PET of 0 indicate gaps in the temperature record.

Soil properties

Information for soil hydraulic properties was obtained from the typical soil profile of map units published in the USDA soil report and a grain-size classification database internal to Hydrus-1D that is based on laboratory soil testing (Carsel and Parrish 1988). According to the USDA Web Soil Survey, the locations of the UXOs on Vieques occur on five different soil profiles (Figure 56). Flow results are discussed in this report for the characteristic profiles AmC2, Ce, and Cm, and transport results are discussed for AmC2. The UXOs found on each soil type are given in Table 7. Table 8 lists input parameters used for soil hydraulic properties .

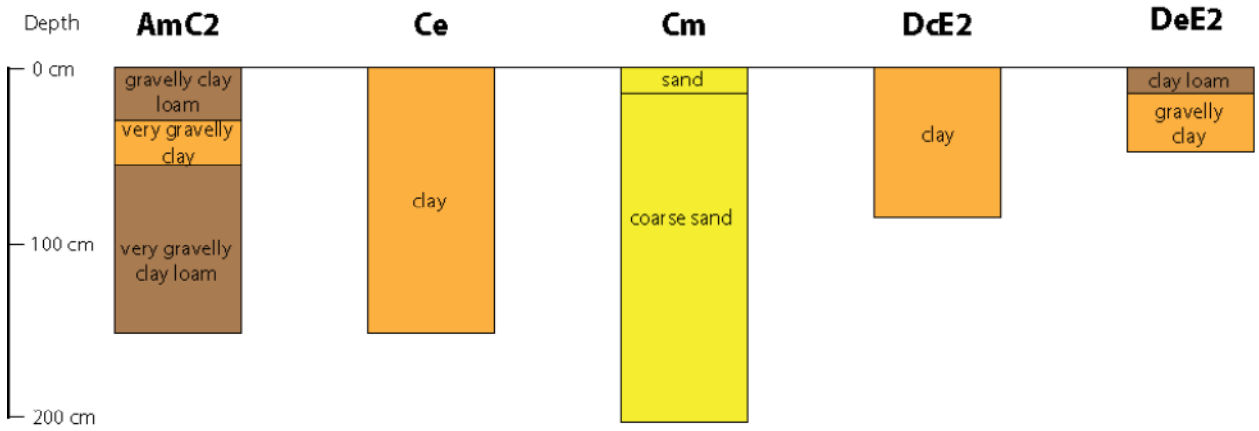

Figure 56. Typical soil profiles at locations of UXOs found in the field. Underlying weathered/unweathered bedrock and rock land not depicted. Source: USDA Web Soil Survey.

Table 7. Soil types at the locations of the UXOs found on Vieques. Map source: USDA Web Soil Survey.

Abbreviation	Soil type	UXO identification numbers		Number found
		CS09-	CS10-	
AmC2	Amelia gravelly clay loam	44, 49, 52	16, 19	5
Ce	Cartagena clay		05	1
Cm	Coastal beaches	34, 41, 55		3
DcE2	Daguao clay	47	04, 11, 12, 18, 20	6
DeE2	Descalabrado clay		24-36	13
Rs	Rock land		08	1
Total number of UXOs				29

The difference between the scale of the small sampling area around a UXO and the scale of larger area of the landforms mapped as a soil unit on the USDA maps means that a particular field observation may not match the larger mapped soil unit, which is only representative at the scale at which it was drawn. However, excavation of soil pits for site-specific profiles is neither practical due to safety protocols when sampling in the vicinity of UXO nor desirable when this process is used to estimate solute transport on a wider scale. As such, the map unit profiles are representative of the larger area. All soil profiles were limited to unconsolidated soils. No data were available on the porosity or storage characteristics of underlying weathered bedrock, and storage in unweathered bedrock was presumed to be minimal. The van Genuchten-Mualem single porosity model was implemented for the hydraulic solution (van Genuchten 1980).

Table 8. Soil hydraulic properties

Depth (cm)	Soil layer	Saturated soil water content (dimensionless)	Residual soil water content (dimensionless)	K_{sat} (cm day^{-1})
AmC2: Amelia Gravelly Clay Loam				
0-30	gravelly clay loam	0.41	0.095	6.24
30-56	very gravelly clay	0.38	0.1	2.88
56-152	very gravelly clay loam	0.41	0.095	6.24
Ce: Cartagena clay				
0-152	Clay	0.38	0.068	4.8
Cm: Beach Sand				
0-152	Sand	0.43	0.045	712.8

Flow results

The flow simulations show that soil hydraulic properties have an effect on the overall water balance of a given profile for the 893-day study period. In particular, the Cm sand induces no runoff, somewhat reduced evapotranspiration, and higher flux through the bottom of the soil profile as compared to the AmC2 loam/clay profile and the Ce clay profile (Figure 57).

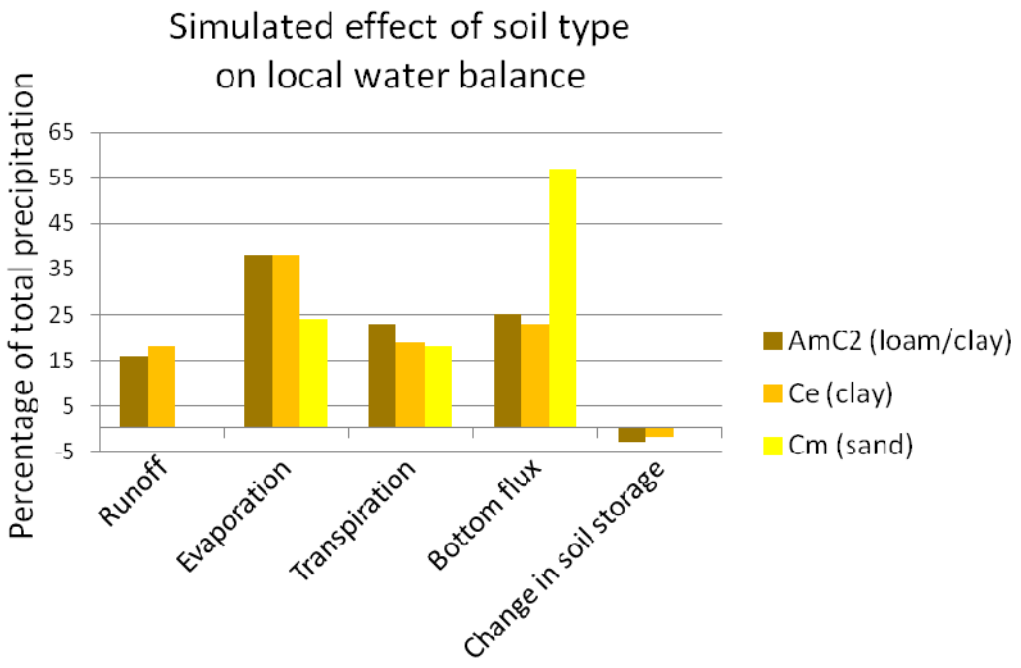

Figure 57. Simulated effect of soil type on local water balance in the flow simulations for AmC2, Ce, and Cm soils, as a percentage of total precipitation during the study period (8/8/2008 to 1/17/2011). Errors in water balance are 0.4%, 3.7%, and 0.1% of total precipitation, respectively.

For all three profiles, flow through the bottom of the soil profile occurs during discrete recharge periods immediately following periods of significant and repeated rainfall (Figure 58). This flow analysis suggests that much of the water that feeds ephemeral streams in the days following a rain (Torres-Gonzalez 1989) has previously passed through the soil profile, allowing for soil-solute interactions to take place.

Transport inputs

After the flow regime was established, Hydrus-1D was used to solve a version of the advection-dispersion equation (Šimůnek et al. 2009) for transport of TNT and RDX. The processes represented in the transport simulation are mass loading through dissolution of the explosives in the UXO, one-dimensional advective-dispersive flux through the soil profile, sorption-desorption, and aerobic transformation. Parameters were chosen based on previous research and site conditions.

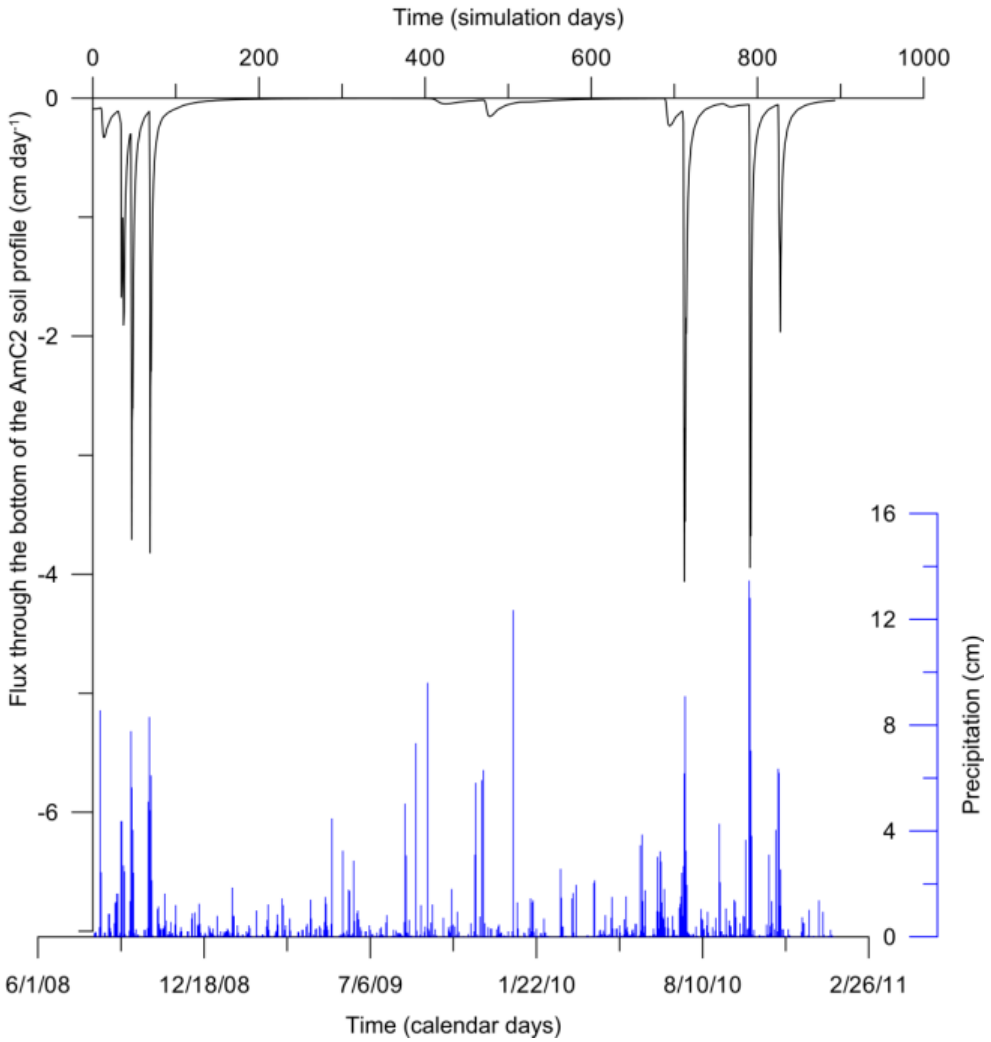

Figure 58. Flux through the bottom of the AmC2 soil profile (vBot) occurs during discrete recharge periods associated with the rainy season. Precipitation events are shown in the lower graph.

Initial mass loading of the surface of the soil due to dissolution of broken or exposed UXO was calculated using the result of the drip experiments. The solubility rates per square centimeter of HE exposed to long-term precipitation were 2.5 (TNT) and 1.8 (RDX) µg per hour (Table 1). These rates were converted to concentrations of incoming rainfall at the top of the soil profile of 21.9 and 15.8 µg mm^{-1} precipitation for TNT and RDX, respectively. This rate is equivalent to incoming precipitation concentrations of 219 and 158 mg L^{-1}, respectively. It is important to note that according to these calculations, precipitation from an area of 1.7 (TNT) and 3.4 (RDX) square centimeters would need to be funneled on to the 1 cm^2 of UXO in order for the concentration in that millimeter of precipitation to remain at or below solubility (130 mg L^{-1} TNT and 46 mg L^{-1} RDX). This may occur via temporary ponding at the surface or by a funneling of the artillery shell itself. It could also indicate that the assumption of a 1:1 relationship between precipitation and dissolution may be incorrect in this situation, and that, for example, during high-intensity tropical rain, not all precipitation falling on the UXO surface becomes saturated. Kinetic properties of dissolution of both TNT and RDX could also be a factor.

Other parameters and boundary conditions were chosen as follows: A low longitudinal dispersivity of 5 cm was chosen because of the relatively short distances involved in transport through the soil profile (Vanderborght and Vereecken 2007), although results were somewhat insensitive to changes in this value. The upper boundary condition was defined by the concentration flux proportional to rainfall from the UXO source as described above, and the lower boundary condition was set to a concentration gradient of zero, although the transport results were not found to be sensitive to this lower boundary condition. Soil bulk density was estimated at 1.5 kg L^{-1}. Although plant uptake and subsequent biotransformation of TNT has been observed (e.g. Best et al. 1999), root solute uptake was not included in the simulation.

One-site non-equilibrium sorption was modeled with a linear isotherm (Dontsova et al 2006):

$$\frac{\partial s^k}{\partial t} = K_D c - s^k \qquad (3)$$

where s^k is the sorbed concentration of the kinetic sorption sites [ML^{-3}], t is time [T], K_D is an empirical sorption coefficient [-], and c is the dissolved concentration of HE [$M\ L^{-3}$]. It is this time derivative of the sorbed concentration that appears in the transport governing equation (2). Sorption coefficients K_D were estimated from Brannon and Pennington (2002) using aerobic soils with similar clay contents (Figure 59).

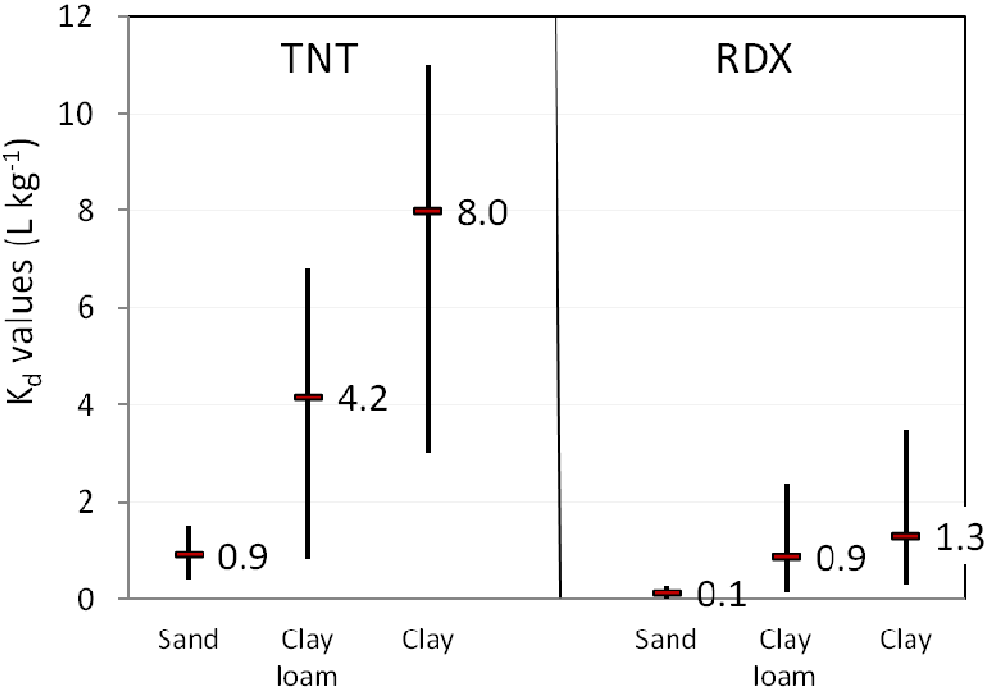

Figure 59. Experimental sorption coefficient (K_d) values from soils that approximate soil layers found in AmC2, Ce, and Cm soil profiles (Brannon and Pennington 2002, surface soils only). Label indicates median used in simulation, and vertical bars indicate range. Sands were explicitly named (n=4 for TNT, n=2 for RDX), clay loam category averages values from soils with 20-40% clay content (n=10 for TNT, n=9 for RDX), and clay category averages values from soils with 40-60% clay content (n=3 for TNT, n= 6 for RDX).

Transformation of TNT can occur through a variety of mechanisms, and transformation products and pathways have been defined and observed in the laboratory (Brannon and Pennington 2002). These pathways may depend on soil conditions such as oxidation state, pH, and temperature. In this simulation, first-order equilibrium transformation was modeled with

$$\gamma_w = \mu_w c \qquad (4)$$

where γ_w is the transformation rate (M L^3 T^{-1}), μ_w is the coefficient of transformation from the dissolved state [T^{-1}], and c is the concentration [M L^{-3}]. The transformation rate coefficients used in the simulation are given in Table 9.

Table 9. Average experimental transformation coefficients from soils that approximate soil layers found in AmC2, Ce, and Cm soil profiles (Brannon and Pennington 2002, Table 21).

Solute	Transformation coefficients μ_w, from dissolved state (hr^{-1})		
	Sand	Clay loam	Clay
TNT	0.0055	0.0072	0.0163
RDX	0	0.0080	0.0081
Sands were explicitly named (n=2 for TNT, n=1 for RDX), clay loam category averages values from soils with 20-40% clay content (n=3 for TNT, n=2 for RDX), and clay category averages values from soils with 40-60% clay content (n=1 for TNT, n= 3 for RDX).			

Saline environments may have an effect on the quantity of TNT found dissolved in soil water and ground water, both because with increasing salinity, dissolution rates are lower (Brannon et al. 2005) and sorption is stronger (Brannon and Myers 1997). On Vieques, salinity may be present both in aerosol loading of precipitation and in tidal effects in proximity to the ocean. However, effects of salinity have not been included in the numerical simulation.

Transport results

Using the governing equations and parameters described above, 30 monthly TNT and RDX concentration profiles were derived for the study period (Figures 60 and 61). The green line indicates the concentration profile after the first month of the simulation (day 29) and the peach line indicates the profiles at the end of the simulation (day 893). The figures show total concentrations, which are the sum of the sorbed and dissolved concentrations. All concentration values are presented here in mg kg^{-1}. Total concentration is given by

$$c_{total} = \theta c_{dissolved} + \rho c_{sorbed} \qquad (5)$$

where c_t is the total concentration [M L^{-3}] (total mass present in either the solid or dissolved phase per volume of sample), θ is moisture content [L_{water}^3 L_{soil}^{-3}], c_d is dissolved concentration [$M_{dissolved}$ L^{-3}_{water}], ρ is soil bulk density [M_{soil} L_{soil}^{-3}], and c_s is sorbed concentration [M_{sorbed} M_{soil}^{-3}]. To convert from a total concentration given in M L^{-3} to equivalent sorbed concentration, the total concentration was divided by the bulk density used in the simulation (1500 mg cm^{-3}) to yield a concentration in mg_{solute} mg_{soil}^{-1} which was then converted to the same units as the concentrations measured in the field [mg_{solute} kg_{soil}^{-1}].

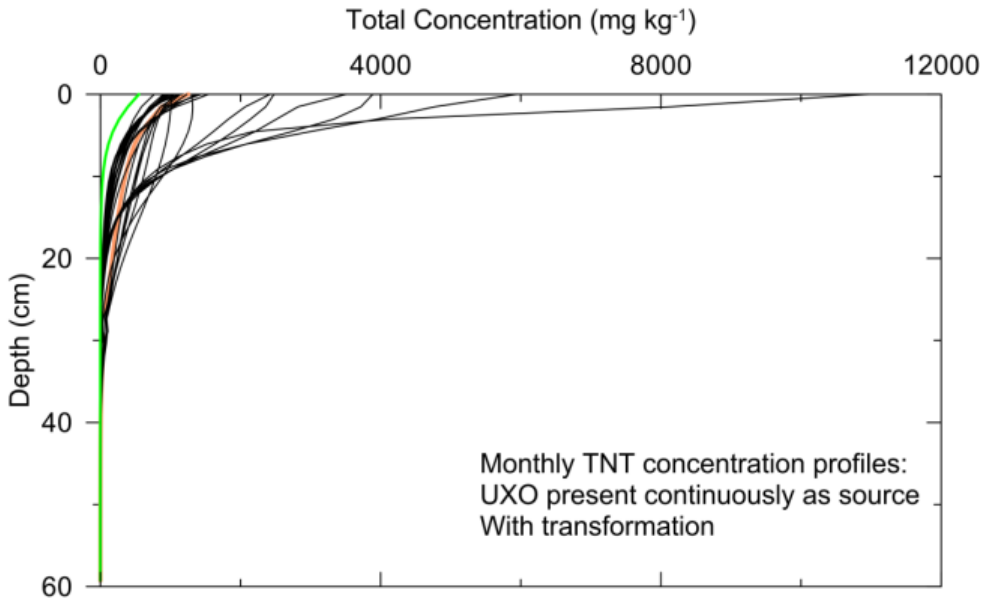

Figure 60. Simulations of TNT concentration profiles from a UXO that has been leaking HE for 2.5 years. Each line represents the concentration profile at the end of a month during the 30-month simulation. The first month (green, day 29) has low concentration because the soil was initially HE free; the last month (orange) shows a profile with lower concentrations than those seen during the large HE input pulse that occurred during the middle of the study period (day 479 of 893). Below 90 cm (not shown), TNT drops below detection limits (0.02 mg kg^{-1}) for all 30 simulations.

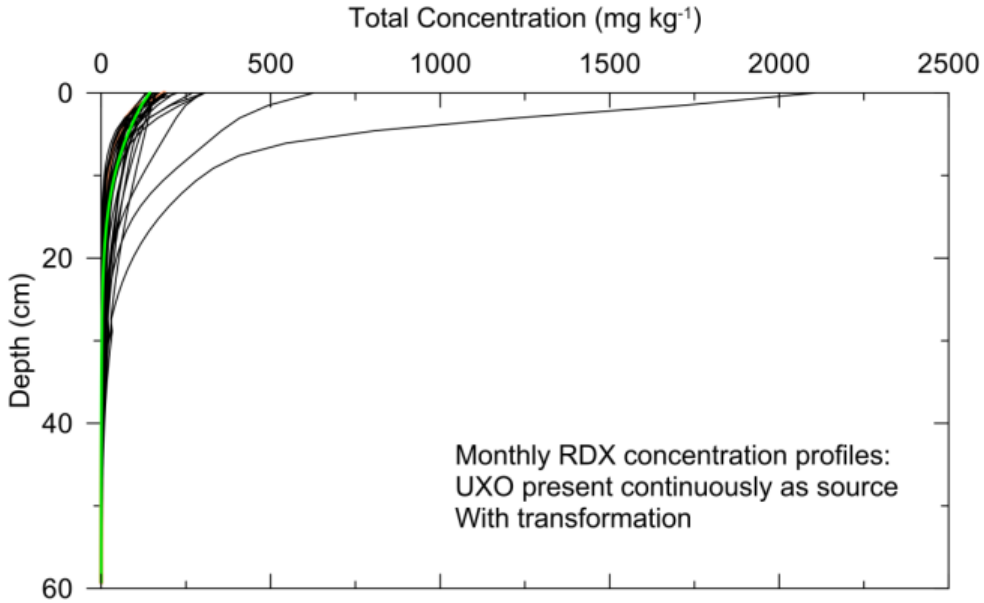

Figure 61. Simulations of RDX concentration profiles from a UXO leaking HE for 2.5 years. Each line represents the concentration profile at the end of a month during the 30-month simulation. The first month's profile (green, day 29) is more similar to the last month's (not visible) than is the case for TNT (Figure 60). Below 89 cm, RDX remains below detection (0.02 mg kg^{-1}) for all 30 simulations.

The concentrations vary significantly at the surface and decrease rapidly with depth. Neither solute was found to be above detection limits of 0.02 μg g^{-1} (0.02 mg kg^{-1}) at the bottom of the

soil profile (152 cm) during the time of the simulation. The profile with the highest concentrations of HE appears on a day that combines high potential evapotranspiration and precipitation. In the thirteen days during the study period with potential evapotranspiration over 0.5 cm day^{-1}, this day was the only one in which precipitation also occurred, and this combination may have led to a spike in the surface concentration of HE. Apart from the soil surface, the locations in which marked changes in concentration occurred were associated with the presence of the clay layer (29 cm to 54 cm) or the bottom of the root zone (60 cm), but these changes were small in comparison to those in the upper 20 cm of the soil profile. These results appear to overestimate surface concentrations as compared to the field measurements, which may be a result of using conservatively high dissolution rates, may indicate that significant irreversible sorption occurs, or may indicate that actual transformation rates are higher than those used in the simulation. However, the shapes of the concentration profiles generally mimic those found in the field. Of the total concentrations presented in these diagrams, most HE were found in the sorbed state. Dissolved concentrations as a percent of total concentrations range from 3 to 7% for TNT and from 13 to 22% for RDX.

Whether simulated concentrations of HE at the bottom of the soil profile would increase over time if the UXO were left in place as a source depends largely on the transformation parameters used. Figure 62 and 63 show the effect of a single pulse of HE due to dissolution during a single 8.6 cm rain event when transformation is not active. This mimics the situation of a UXO that is removed after one dissolution event. If transformation is simulated to be inactive, then the highest speed at which the TNT concentration peak moves through the soil profile is 0.022 cm day^{-1}. At this rate, the peak of the concentration profile would take a minimum of 19 years to reach the bottom of the 152-cm soil profile, ignoring the clay layer, and over this period even low transformation parameters become significant. For RDX, weaker sorption implies more rapid passage of the concentration peak through the profile (Figure 63), at an average rate of 0.090 cm day^{-1}. At this rate, the peak of the RDX could reach the bottom of the soil profile in approximately 4.5 years; thus similar transformation rates would have less time to attenuate RDX.

Transformation rates are not well constrained but prove important. Inclusion of transformation in the simulation significantly lowers HE concentrations at depth (Figures 64 and 65). With transformation, the same pulse simulation (representing a UXO that was removed immediately following one precipitation event) shows a significant flattening of the concentration profile over 893 days. The transformation coefficients used were derived from a small sample set (n=1 to 3), from laboratory tests of different (but hydraulically similar) soils, and varied widely, ranging from 0 to a value over twenty times the median value (this anomalous value was discarded). Laboratory testing of soil columns from the study site may help to better constrain transformation parameters for a particular location. The transformation coefficients for the explosives in question might be the single most useful piece of field information needed to estimate dissolved explosive transport through range soils on military ranges.

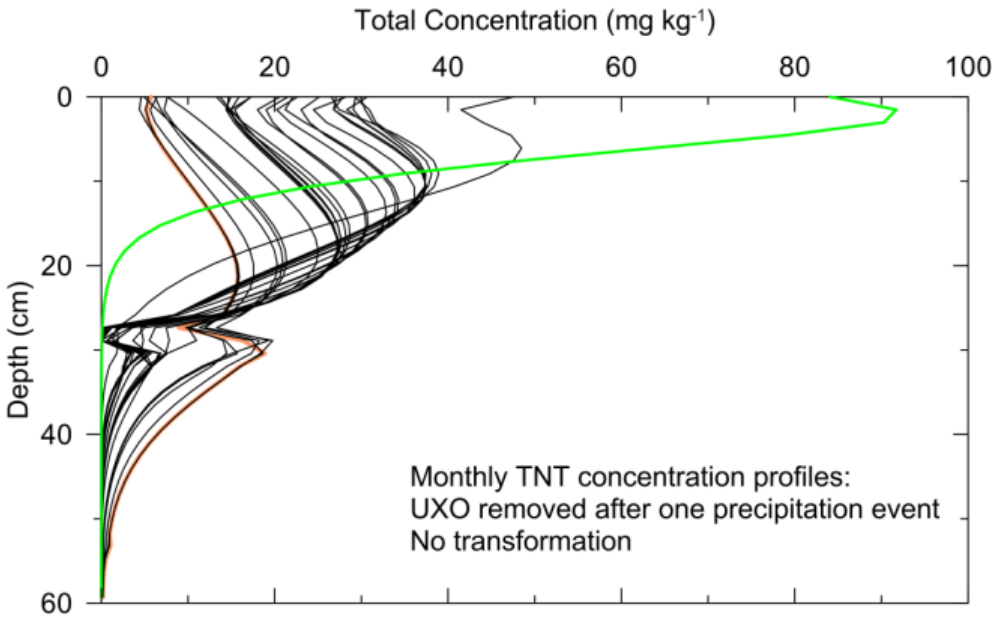

Figure 62. For a single TNT pulse input, the progression of TNT through the soil profile shows a secondary spike due to higher sorption of TNT on the clay layer beginning at 28 cm. When transformation is assumed to be insignificant, the concentration profile spreads out as time passes but does not attenuate, from the first month (green, day 29) through the end of the simulation (orange, day 893).

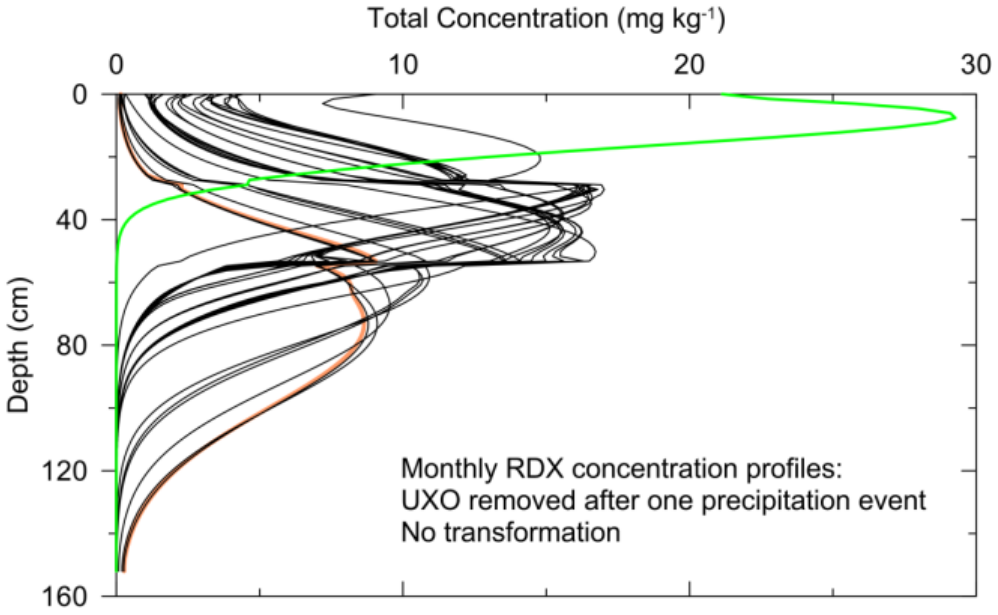

Figure 63. For a single pulse input of RDX in the absence of transformation, the concentration profile is clearly influenced by higher sorption in the clay layer (28 to 54 cm) and retention in the root zone (ending at 60 cm).

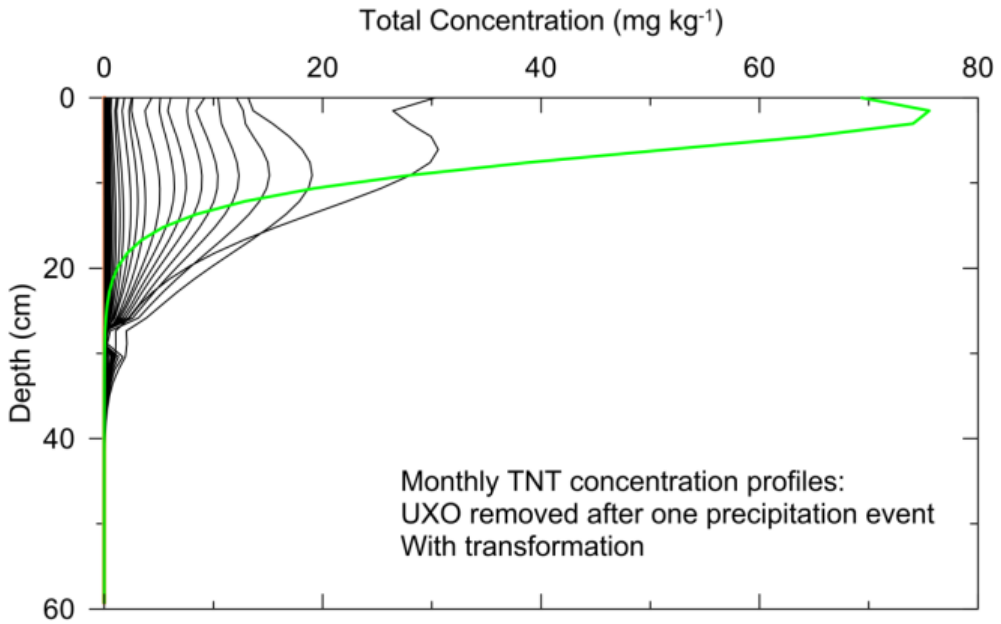

Figure 64. With active transformation, the passage of a single pulse of TNT is strongly attenuated from the end of the first month (green, day 29) to the end of the 30-month period (not visible).

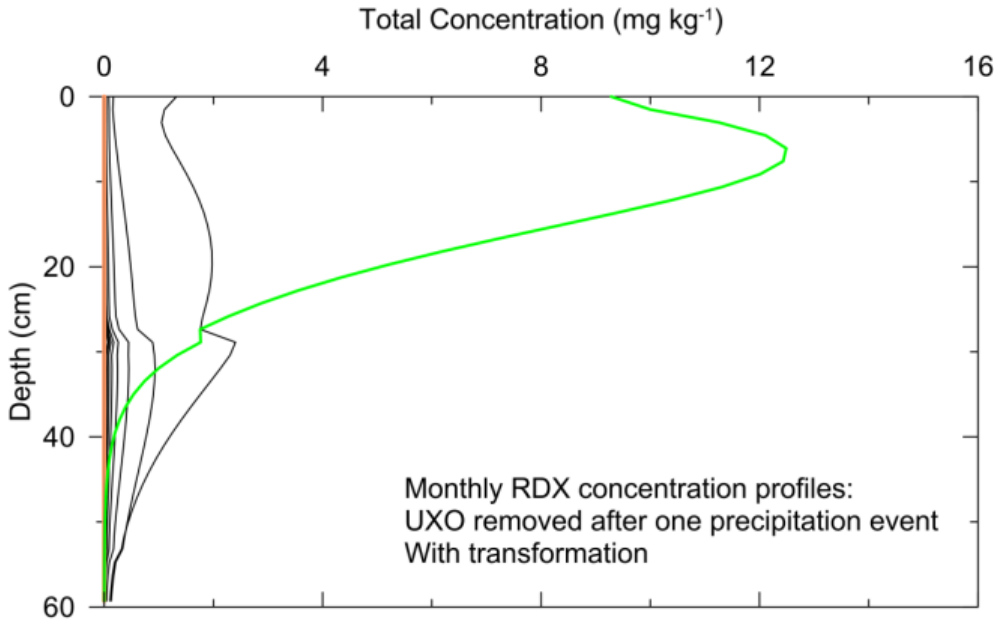

Figure 65. With active transformation, a single pulse of RDX is strongly attenuated from the first month (green, day 29) through the last month (not visible) of the 30-month simulation.

The simulation shows that while dissolved HE levels are well above EPA drinking water standards (2.2 µg L^{-1} for TNT and 0.6 µg L^{-1} for RDX) at the soil surface near a breached UXO, these levels are orders of magnitude below drinking water standards at the bottom of the AmC2 soil profile. UXOs on shallower soil profiles or those with preferential pathways for flow, such

as clays prone to cracking, are more likely to allow TNT and RDX to be transported to the groundwater. UXO removal could be prioritized by soil type, with Cm, DcE2, DeE2, and rock land profiles (Figure 56) presenting a more immediate risk of transmission of HE through the soil profile.

Discussion

Figure 66 shows the fates possible for a fired round (Taylor et al. 2004). Of the muntions manufactured only a certain percentage are used for training on US ranges. Of these some will detonate high-order, some will partially detonate and some will dud. Most rounds will detonate high order leaving very little explosive-containing residue (Dauphin and Doyle 2000, 2001). Although partial detonations are rare (0.06%) they release all their HE into the environment. A rough estimate of the HE load from this outcome can be obtained by multiplying the number and type of rounds fired by their partial detonation rates (Dauphin and Doyle 2000, 2001) and the mass of HE they contain (eg. 10000, 155mm projectiles fired, × 7 kg Comp B per projectile × 0.06 chance of scattering HE= 4200 kg of Comp B scattered).

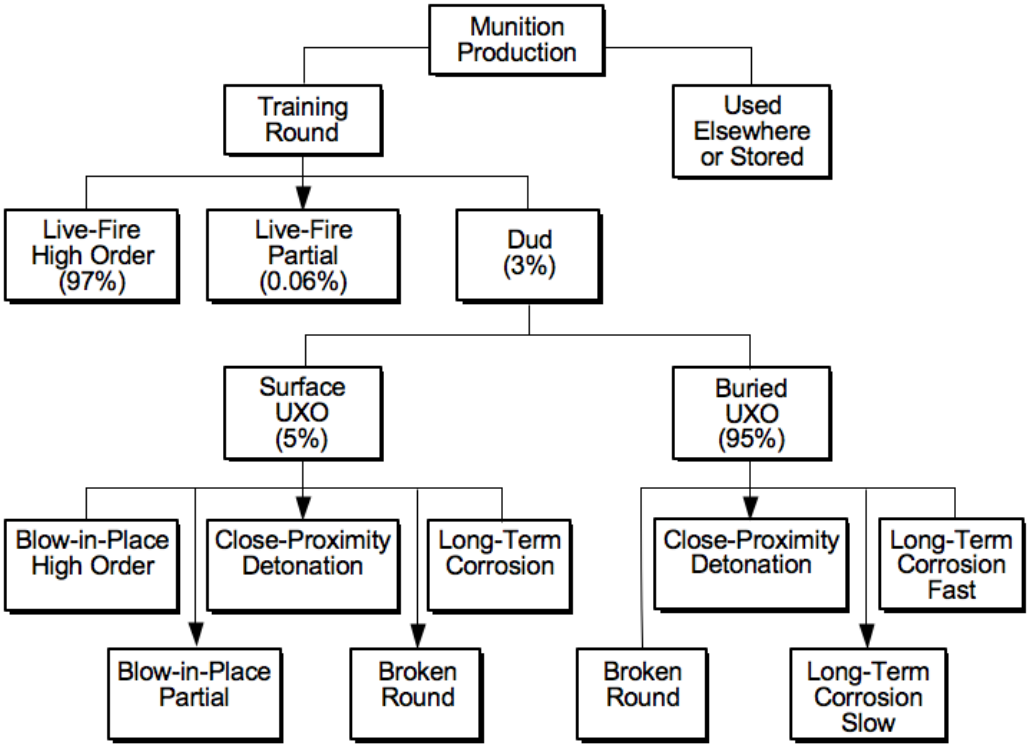

Figure 66. Possible fates of a fired round (Taylor et al. 2004).

For the 3% of fired rounds that become UXO, most are buried and corrode in place. Although buried UXO corrode more quickly than surface UXO they are less likely to be pierced by fragments from nearby detonations if they are covered by a few centimeters of soil (Walsh et al. 2011). Of the buried UXO an unknown number will have broken upon impact exposing HE to

pore water coursing through the soil. In arid regions dissolution of the HE will take a long time but in high rainfall areas it will be much faster. Similarly, corrosion of the buried UXO will depend on the moisture content as well as the acidity and conductivity of the soil. At all three of our sites, the part of UXO in contact with the soil was very corroded.

At Vieques and Camp Luis Osbispo we found that the UXO casing failed not because of pitting but because the metal casing oxidized and swelled. This process formed circumferential and longitudinal cracks that allowed large pieces of the casing to slough off exposing the HE fill. Taylor et al (2004) and Nalbandian and Kalikian (2007) both concluded that damage rounds (partial detonations, broken or holed by nearby high order detonations) are the greatest source of dissolved HE. We now add rapid and complete failure of the casing due to corrosion to this list.

Once released from the casing, the amount of HE dissolved during a given time depends on the collective surface area of exposed UXO, precipitation, and temperature. Of these three variables, the size distribution of the HE pieces has largest effect on solute flux entering the soil. Given pieces of UXO, mass varies with the cube of the length and dissolution of an individual cube varies with the cross-sectional area or the square of the length. Consider three sets of a dissolvable substance, each of which has equal mass: one cube 10 cm on a side, a second set of 1000 cubes 1 cm on a side, and a third set of 1,000,000 cubes 0.1 cm on a side. The precipitation will determine a dissolution rate, which in the case of TNT is equivalent to 0.219 mg cm^{-2} of surface area. For the 10 cm cubes, one 10 mm rain would dissolve 21.9 mg or approximately $1/75{,}000^{th}$ of the mass of the cube, so ~ 75,000 10-mm rain events would be required to dissolve the cube completely, disregarding changes in the surface area during this process. For the set of cubes 1 cm on a side, over 7500 rain events would be required, and for the 1 mm cubes, only 755 events. For example, if there are on the order of 100 rain events in a year, then these fragments could require approximately 750, 75, and 7.5 years to dissolve, respectively. This indicates that depending on the site history, percentage of the land with exposed HE, and cleanup objectives, fragments of HE smaller than a centimeter in diameter may need to be included as an integral part of long-term cleanup measures.

Once the HE is dissolved, the solute transport velocity is determined both by the sorptive properties of the soil and by the frequency of precipitation events larger than evapotransporation. Hydrus-1D is useful for estimating both the timing and concentration of HE with soil depth given the HE mass on the surface. We ran the simulations for TNT and RDX but similar studies could be conducted with other HE compounds, e.g. HMX. Our modeling results show that in the absence of transformation, HE will reach the base of a 152-cm soil profile on Vieques while if transformation occurs the HE will not travel that far. The transformation coefficients used, however, were not well constrained as they were derived from a small number of studies on soils not located at the study site. The transformation coefficients for the explosive in question might be the single most useful piece of field information needed to estimate if the dissolved explosive will reach groundwater. Consequently determining this parameter for soils at the field site would help calibrate the model and increase its accuracy.

Summary

Of the 42 corroded rounds sampled, seven of them (16%) had detectable levels of energetic compounds in the underlying soil. The rounds found to be leaking were 60 mm (3), 81 mm (1), 106 mm (1), 4.2 in (1), and 155 mm (1) in size. Based on dry sample weights, one round (a 60 mm) had soil energetic concentrations in the range > 0.10 but < 1.00 mg kg^{-1}, three rounds (a 60 mm, a 106 mm, and a 155 mm) had soil energetic concentrations in the range > 1.00 but < 10.0 mg kg^{-1}, and three others had soil samples with concentrations > 10.0 mg kg^{-1} (a 60 mm, an 81 mm, and a 4.2 in). We also sampled below a partially detonated round that had spread HE pieces nearby. This round had the highest soil concentrations, measuring 26,000 mg kg^{-1}; however, soils with these high concentrations likely included particles of energetic compounds.

The relative concentrations of RDX, HMX, TNT, and TNT transformation products in soil provide information both on the type of explosive fill present (TNT or Comp B) and a measure of how long the explosives have been in the environment. For example, Comp B particles should approximate the 55% RDX, 5% HMX and 39% TNT ratio of the formulation, whereas once in solution, TNT rapidly degrades leaving RDX and HMX behind. Furthermore, with time RDX will preferentially dissolve over HMX changing the ratio from 10:1 to parity or more HMX than RDX.

Some of the rounds were so corroded that we were surprised that they were not leaking explosives. We think the laboratory tests on the metal casings provide a plausible explanation: iron oxides quickly seal any small holes. However, if the holes are large enough—such as cm-sized perforations caused by fragmentation hits—they cannot be sealed by oxides. In these cases dissolution of the fill would occur. Furthermore, we would expect explosive fill near a hole to dissolve over time creating an ever-larger cavity and increasing the surface area of the fill available for dissolution. Such cavities were observed in our gypsum-filled Nalgene bottle tests and seen in sectioned gypsum-filled practice rounds.

Both at Camp Luis Obispo and at Vieques we found that oxidation of the metal casing caused the metal to swell, forming both longitudinal and circumferential cracks in the casing. At Vieques, many of these rounds had shed their metal casing leaving their entire HE fill exposed. Often the HE cores were quite smooth and not pitted suggesting that the casing failed quickly. In a few instances we saw cracks in the casing reflected in the underlying fill, indicating that water had penetrated and dissolved some of the HE.

Our Hydrus-1D results are useful for estimating both the timing and concentration of TNT and RDX traveling through the vadose zone. Our simulations, using conditions encountered at Vieques and for a simulation time of 2.5 yrs, suggest that none of the HE exits the base of the soil column. These results are very sensitive to the soil parameters used, particularly the transformation rates of the explosive compounds by biological or chemical processes. Determining the transformation rates of explosives in soils at the field site would help calibrate the model and increase its accuracy.

References

Arthur D. Little, 1994. *Phase II Remedial Investigation for Cold Regions Research and Engineering Laboratory (CRREL), Hanover, New Hampshire. Final Remedial Investigation Report*. DAAA15-91-D-0016. Delivery Order 0003. Cambridge, MA: Arthur D. Little, Inc.

Baker Environmental. 1999. *Results of the hydrogeologic investigation Vieques Island, Puerto Rico.* Contract report prepared for the US Navy, Task Order No. 0138.

Best, E. P. H., S. L. Sprecher, S.L. Larson, H. L. Fredrickson, and D. F. Bader 1999. Environmental behavior of explosives in groundwater from the Milan Army Ammunition Plant in aquatic and wetland plant treatments: uptake and fate of TNT and RDX in plants. *Chemosphere* 39(12):2057–2072.

Bjella, K. L. 2005. *Pre-screening for explosives residues in soil prior to HPLC analysis utilizing Expray*. ERDC/CRREL Technical Note TN-05-2. Hanover, NH: Engineer Research and Development Center.

Brannon, J. M., and T. E. Meyers. 1997. *Review of fate and transport processes of explosives.* IRRP-97-2, Vicksburg, Miss.: U.S. Army Engineer Waterways Experiment Station, http://libweb.wes.army.mil/uhtbin/hyperion/TR-IRRP-97-2.pdf.

Brannon, J. M. and J. C. Pennington. 2002. *Environmental fate and transport process descriptors for explosives.* ERDC Technical Report TR-02-10. Vicksburg, MS: Engineer Research and Development Center.

Brannon, J. M., C. B. Price, S. L. Yost, C. Hayes, and B. Porter. 2005. Comparison of environmental fate and transport process descriptors of explosives in saline and freshwater systems. *Marine Pollution Bulletin* 50:247–251.

Carsel, R. F., and R. S. Parrish. 1988. Developing joint probability distribution of soil water retention characteristics. *Water Resources Research* 24(5):755–769.

CH2MHill. 2007. *Expanded Range Assessment and Phase I Site Inspection Report, Former Vieques Naval Training Range, Vieques, Puerto Rico.* Contract Task Order No. 047. Prepared for Department of the Navy, Naval Facilities Engineering Command Atlantic. Virginia Beach, VA: CH2MHill.

CH2MHill. 2009. *Non-time-critical removal action work plan surface munitions and explosives of concern at munitions response area-surface impact area munition response sites 1 through 7.* Contract Task Order No. 0211. Prepared for Department of the Navy, Naval Facilities Engineering Command Atlantic. Virginia Beach, VA: CH2MHill.

Chendorain, M. D., L. D. Stewart, and B. Packer. 2005. Corrosion of unexploded ordnance in soil – field results. *Environmental Science Technology* 39(8):2442–2447.

Dauphin, L., and C. Doyle. 2000. *Study of ammunition dud and low order detonation rates*. Technical Report written for U.S. Army Environmental Center. Aberdeen Proving Ground, MD: U.S. Army Defense Ammunition Center—Technical Center for Explosives Safety.

Dauphin, L., and C. Doyle. 2001. *Phase II study of ammunition dud and low order detonation rates*. Technical Report written for U.S. Army Environmental Center. Aberdeen Proving Ground, MD: U.S. Army Defense Ammunition Center—Technical Center for Explosives Safety.

Dontsova K. M., S. L. Yost, J. Šimunek, J. C. Pennington, and C. W. Williford. 2006. Dissolution and transport of TNT, RDX, and Composition B in saturated soil columns. *Journal of Environmental Quality* 35:2043–2054.

Furey, J. S., H. L. Fredrickson, M. J. Richmond, and M. Michel. 2008. Effective elution of RDX and TNT from particles of Comp B in surface soil. *Chemosphere* 70: 1175–1181.

Goyal, M. R. 1988. Potential evapotranspiration for Vieques Island, Puerto Rico, with the Hargreaves and Samani model. AGRIS Record number US8837831. *Journal of Agriculture of the University of Puerto Rico* 72(1):177–178.

Jordan, D. G. and O. J. Cosner. 1973. *A survey of the water resources of St. Thomas, Virgin Islands.* US Geological Survey, Water Resources Division, Caribbean District.

Kuechler, R., K. Noack, and T. Zorn. 2004. Investigation of gypsum dissolution under saturated and unsaturated water conditions. *Ecological Modeling* 176: 1–14.

Larson, S. L., A. Martin, B. L. Escalon, and M. Thompson. 2008. Dissolution, sorption, and kinetics involved in systems containing explosives, water and soil. *Environmental Science Technology* 42(3): 786–792.

Lever J., S. Taylor, L. Perovich, K. Bjella, and B. Packer. 2005. Dissolution of Composition B Residuals. *Environmental Science Technology* 39: 8803–8811.

Lugo, A. E., L. Miranda Castro, A. Vale, T. del M López, E. Hernández Prieto, A. García Martinó, A. R. Puente Rolón, A. G. Tossas, D. A. McFarlane, T. Miller, A. Rodríguez, J. Lundberg, J. Thomlinson, J. Colón, J. H. Schellekens, O. Ramos, and E. Helmer. 2004. *Puerto Rican karst – a vital resource.* General Technical Report WO-65, Washington, DC: USDA Forest Service.

Lugo-Lopez, M. A., J. A. Bonnet, and J. Garcia. 1953. *The soils of the island of Vieques.* University of Puerto Rico, Agricultural Experiment Station, Bulletin 108.

Lynch, J. C., J. M. Brannon and J. J. Delfino. 2002a. Dissolution rates of three high explosive compounds: TNT, RDX, and HMX. *Chemosphere* 47: 725–734.

Lynch, J. C., J. M. Brannon and J. J. Delfino. 2002b. Effects of component interactions on the aqueous solubilities and dissolution rates of the explosive formulations octol, composition B, and LX-14. *Journal of Chemical Engineering Data* 47: 542–549.

Maidment, D. R. 1993. *Handbook of hydrology*. New York: McGraw-Hill, Inc.

Manahan, S. 1994. *Environmental Chemistry*. Boca Raton, FL: Lewis Publishers.

McCormick, N. G., F. E. Feeherry, and H. S. Levinson. 1976. *Applied Environmental Microbiology* 31:1357–1374.

Monteil-Rivera, F., S. Deschamps, G. Ampleman, S. Thiboutot, and J. Hawari. 2010. Dissolution of a new explosive formulation containing TNT and HMH: Comparison with octol. *Journal of Hazardous Materials* 174:281–288.

Morley, C., H. Yamamoto, G. E. Speitel Jr., and J. Clausen. 2006. Dissolution kinetics of high explosives particles in a saturated sandy soil. *Journal of Contamination Hydrology* 85: 141–158.

Nalbandian, A., and R. Kalikian. 2007. Soil testing, on-site corrosion examinations and laboratory testing of corroded inert items removed from six test plots within the central impact area Massachusetts military reservation Cape Cod, Massachusetts. *Thielsch Engineering Report No. 12080*.

National Climatic Data Center (NCDC). 2011. National Environmental Satellite, Data, and Information Service. www.ncdc.noaa.gov/

National Climatic Data Center (NCDC). 2010. Climate Data Online http://cdo.ncdc.noaa.gov/CDO/cdo

Parsons. 2009. Draft final intrusive work plan, former Camp San Luis Obispo, San Luis Obispo, California. Huntsville, AL: Parsons.

Prak, D. J. L. and D. W. O'Sullivan. 2006. Solubility of 2,4-dinitrotoluene and 2,4,6-trinitrotoluene in seawater. *Journal of Chemical Engineering Data* 51(2):448-450.

Romanoff, M. 1957. *Underground corrosion*. National Bureau of Standards, Circular 579, Washington D.C.: U. S. Department of Commerce, National Bureau of Standards. 222 p.

Šimunek, J., M. Šejna, H. Saito, M. Sakai, and M. Th. van Genuchten. 2009. *The HYDRUS-1D software package for simulating the one-dimensional movement of water, heat, and multiple solutes in variably-saturated media, Users Manual.* Univ. of California Riverside. Dep. of Environmental Sciences.

Szklarska-Smialowska, Z. 1986. *Pitting corrosion of metals.* Houston, TX: National Association of Corrosion Engineers.

Taylor S., J. H. Lever, B. Bostick, M. R. Walsh, M. E. Walsh, and B. Packer. 2004. *Underground UXO: Are they a significant source of explosives in soil compared to low- and high- order detonations?* ERDC/CRREL Technical Report TR-04-23. Hanover, NH: Engineer Research and Development Center.

Taylor S., J. H. Lever, J. Fadden, N. Perron and B. Packer. 2009. Simulated rainfall-driven dissolution of TNT, Tritonal, Comp B and Octol particles. *Chemosphere* 75(8): 1074–1081.

Taylor, S., J. Lever, M. Walsh, J. Fadden, N. Perron, S. Bigl, R. Spanggord, M. Curnow, and B. Packer. 2010. *Dissolution rate, weathering mechanics, and friability of TNT, Comp B, Tritonal, and Octol.* ERDC/CRREL Technical Report TR-10-2. Hanover, NH: Engineer Research and Development Center.

Taylor, S., T. Jenkins, H. Rieck, S. Bigl, A. D. Hewitt, M. E. Walsh and M. R. Walsh. 2011. *MMRP Guidance Document for Soil Sampling of Energetics and Metals.* ERDC/CRREL TR-11-15. Hanover, NH: Engineer Research and Development Center.

Thompson, G.L. 1986. *Rainfall interception by mesquite on the rolling plains of Texas*. Ph.D. dissertation, Texas Tech University, December 1986.

Torres-Gonzalez, S. 1989. *Reconnaissance of the ground-water resources of Vieques Island, Puerto Rico.* US Geological Survey Water Resources Investigations, Report No. 86-4100.

U.S. Dept. of Agriculture (USDA). Web Soil Survey: http://websoilsurvey.nrcs.usda.gov/app/HomePage.htm

U.S. Environmental Protection Agency (US EPA). 2006. Method 8330B: Nitroaromatics, nitramines, nitrate esters by high performance liquid chromatography (HPLC). In *Test Methods for Evaluating Solid Waste, Physical/Chemical Methods, Office of Solid Waste and Emergency Response. SW-846*. Washington, DC.

Vanderborght, J., and H. Vereecken. 2007. One-dimensional modeling of transport in soils with depth-dependent dispersion, sorption and decay. *Vadose Zone Journal* 6(1):140–148.

van Genuchten, M. Th. 1980. A closed-form equation for predicting the hydraulic conductivity of unsaturated soils. *Soil Science Society of America Journal* 44:892–898.

Walsh, M. R., M. E. Walsh, C. A. Ramsey, R. J. Rachow, J. E. Zufelt, C. M. Collins, A. B. Gelvin, N. M. Perron, and S. P. Saari. 2006. *Energetic residues deposition from 60-mm and 81-mm mortars*. ERDC/CRREL TR-06-10. Hanover, NH: Engineer Research and Development Center.

Walsh, M. R., M. E. Walsh, S. Taylor, A. Hewitt, S. Bigl, K. Jones, K. Gagnon, C. Collins, N. Perron, A. Gelvin, K. Foley, R. Bailey, and A. Wagner. 2011. *Characterization and fate of gun and rocket propellant residues on testing and training ranges*. ERDC/CRREL TR-11-13. Hanover, NH: Engineer Research and Development Center.

Appendix A. Analysis of mines buried at CRREL

In 2001, the Night Vision lab buried 57, un-fuzed mines in a fenced in area at CRREL. CRREL is located on the east side of the Connecticut River in western central New Hampshire. The bedrock is overlain by unconsolidated, glacially deposited sediments that have eroded into stepped terraces (Arthur D. Little 1994). The soil at the study site, on the lower of two terraces, is an olive gray to yellowish brown silt inter-bedded with layers of fine sandy silt.

This area of New England has a humid continental climate with short, mild summers and cold winters. Average daytime summer and winter temperatures range between about 57–71 °F and 19–33 °F, respectively. The frost-free growing season is about 200 days. Precipitation averages 39 inches a year, with around 94 inches of snow.

This study site was an opportunity to leverage information regarding corrosion of mines that had been buried for nearly a decade. The mines served as ground-truth for geophysical instruments trying to find and identify the mines and characterize their explosive fill. For this reason, a variety of types and makes of mines were buried and they all contained high explosives (HE) (see Table A.1). A crew from AP Hill removed the mines on 7 July 2009. The casings on these mines were all plastic and although measuring HE leakage from mines was not in our original plan, we took advantage of this opportunity.

To check if these mines had leaked any HE into the soil, we checked their surfaces for explosive compounds using a field screening method (Bjella 2005). We brushed the soil off the bottom of each mine, dripped a small volume of acetone onto the mine surface which we then collected on filter paper. The paper was then sprayed with reagent 1 and 2 contained in the EXPRAY kit. These reagents respond to the presence of nitroaromatics, such as TNT and Tetryl, and nitramines, such as RDX and HMX, by turning the filter paper brown and bright pink, respectively. The acetone deposits and concentrates any dissolved HE on the filter paper and the EXPRAY solution highlight the presence of HE. For aqueous solutions, concentrations of about 20 ppm are needed to produce color changes while the neat explosive from the evaporated acetone is readily detectable.

The exhumed mines showed no signs of wear or corrosion (Figure A.1). They all looked intact and in good condition. We tested 49 of the 57 mines and none of the swabs changed color (Figure A.2) indicating that none were leaking explosives. Four M14s, three TS-50s and one TM62M were not tested because lightning in the area necessitated packing up the mines and removing them from the field.

Table A.1. Type and number of mines buried at CRREL (record sent to us), the number of each type found and the number of each sampled in July 09. Note that we found a small discrepancy between what was unburied and what was supposed to be buried (highlighted in red). The mines are either antipersonnel (AP) or antitank (AT) mines and were made in the USA, Soviet Union and Italy.

NAME	HE	# in record	# found	# sampled
MINE, M14 (USA AP)	TETRYL	8	8	4
MINE, M15 (USA AT)	COMP B	4	4	4
MINE, M19 (USA AT)	COMP B	5	5	5
MINE, PMN (SOVIET AP)	TNT	4	5	5
MINE, TM-62M (SOVIET AT)	TNT	4	4	4
MINE, TM-62P3 (SOVIET AT)	TNT	5	5	5
MINE, TS-50 (ITALIAN AP)	COMP B	8	8	5
MINE, VALMARA 69 (ITALIAN AP)	COMP B	4	4	4
MINE, VS-1.6 (ITALIAN AT)	COMP B	5	5	5
MINE, VS-2.2 (ITALIAN AT)	COMP B	5	5	5
MINE, VS-50 (ITALIAN AP)	RDX	5	4	4
Total Removed		57	57	50

Figure A.1. Photo of each type of exhumed mine. The TM-62P3 is not pictured but looks similar to the TM-62M.

Figure A.2. Acetone was dripped onto one of the TS 50 mines and collected on this filter paper. No reaction is seen after both reagents were sprayed onto the paper. This result is typical of what was found for the other mines.

Appendix B. Concentration of energetic compounds in collected soils

Table B.1. Results of high explosive (HE) analysis of soil samples collected at Eagle River Flats, Alaska.

Round Type	Sampling Date	Sample ID	Subsample	Vertical Profile	Lateral Sampling		Underneath Round		HE Concentration (mg kg^{-1})*					
				(cm)	0-15 cm	15-30 cm	0-1 cm	1-2 cm	HMX	RDX	TNT	2,4-DNT	2am-DNT	4am-DNT
60-mm	05/23/09	CS09-12	-01	0-5					2.42	10.2	0.309	0.042	0.054	0.131
			-02	5-10					0.140	0.242	0.052	<d **	<d	<d
			-03	10-15					0.066	0.136	0.023	<d	<d	<d
			-04				x		0.309	0.175	0.148	0.080	<d	<d
			-05					x	0.033	<d	0.020	<d	<d	<d
			-06		x				0.027	<d	<d	<d	<d	<d
			-07			x			<d	<d	<d	<d	<d	<d
60-mm	05/26/09	CS09-16	-01				x		0.930	3.19	0.288	0.028	<d	<d
			-02					x	0.070	0.384	<d	<d	<d	<d
			-03		x				0.136	0.390	0.020	<d	<d	<d
			-04			x			0.076	0.042	<d	<d	<d	<d

* Data are shaded as follows: yellow (value < 1); grey (1 < value < 10); pink (10 < value). ** <d – non detect.

Table B.2. Results of high explosive (HE) analysis of soil samples collected at San Luis Obispo, California.

Round Type	Sampling Date	Sample ID	Subsample	Vertical Profile	Lateral Sampling	HE Concentration (mg kg^{-1})*								
				(cm)	(cm)	HMX	1,3,5 TNB	RDX	1,3 DNB	TNT	Tetryl	2,4 DNT	2am-DNT	4am-DNT
60-mm (Korean)	08/04/09	CS09-75	-01	0-5		<d **	<d	<d	<d	<d	0.305	<d	<d	<d
			-02	5-10		<d	<d	<d	<d	<d	0.040	<d	<d	<d
			-03	10-15		<d	<d	<d	<d	<d	<d	<d	<d	<d
			-04		0-5	<d	<d	<d	<d	<d	0.055	0.022	<d	<d
			-05		5-10	<d	<d	<d	<d	<d	<d	<d	<d	<d
			-06		10-15	<d	<d	<d	<d	<d	0.026	<d	<d	<d
			-07		15-20	<d	<d	<d	<d	<d	<d	<d	<d	<d
			-08		20-25	<d	<d	<d	<d	<d	<d	<d	<d	<d

* Data are shaded as follows: yellow (value < 1); grey (1 < value < 10); pink (10 < value). ** <d – non detect.

Table B.3. Results of high explosive (HE) analysis of soil samples collected at Vieques, Puerto Rico.

Round Type	Sampling Date	Sample ID	Subsample	Vertical Profile (cm)	Lateral Sampling (cm)	HE Concentration (mg kg^{-1})*								
						HMX	1,3,5 TNB	RDX	1,3 DNB	TNT	Tetryl	2,4 DNT	2Am-DNT	4am-DNT
105-mm	06/17/09	CS09-41	-05		0-5	0.104	<d **	0.041	<d	<d	<d	<d	<d	<d
			-04		5-10	0.093	<d	0.027	<d	<d	<d	<d	<d	<d
			-03		10-15	<d	<d	0.029	<d	<d	<d	<d	<d	<d
			-02		15-20	0.059	<d	0.097	<d	<d	<d	<d	<d	<d
			-01		20-30	0.068	<d	0.303	<d	<d	<d	<d	<d	<d
			-06	0-5		<d	<d	<d	<d	<d	<d	<d	<d	<d
			-07	5-10		<d	<d	<d	<d	<d	<d	<d	<d	<d
			-08	10-15		<d	<d	<d	<d	<d	<d	<d	<d	<d
4.2-in	06/17/09	CS09-49	-05		0-5	<d	<d	0.034	<d	61.2	<d	0.301	2.33	2.39
			-04		5-10	<d	<d	<d	<d	1.88	<d	<d	0.531	0.493
			-03		10-15	<d	<d	<d	<d	1.11	<d	<d	0.060	0.067
			-02		15-20	<d	<d	<d	<d	2.43	<d	<d	0.047	0.066
			-01		20-30	<d	<d	0.030	<d	1.77	<d	<d	0.203	0.216
			-06	0-5		<d	<d	0.036	<d	1.60	<d	0.699	2.67	3.39
			-07	5-10		<d	<d	0.030	0.034	0.279	<d	0.218	0.667	0.976
			-08	10-16		<d	<d	<d	<d	0.165	<d	0.114	0.251	0.375
			-09	0-5		0.194	<d	<d	0.083	1.47	<d	1.25	8.68	12.2
			-10	5-10		<d	<d	<d	<d	0.151	<d	0.118	0.283	0.470
			-11	10-17		<d	<d	<d	<d	1.38	<d	0.105	0.420	0.573
			-12	0-3		0.035	0.010	0.025	0.021	49.1	<d	0.401	1.92	2.27
			-13	3-5		0.019	0.050	<d	0.052	8.73	<d	0.765	1.05	1.01
			-14	5-7		<d	<d	<d	0.016	2.47	<d	0.160	0.484	0.616
			-15	7-9		<d	<d	<d	0.014	2.11	<d	0.130	0.396	0.517
			-16	9-11		<d	<d	<d	<d	1.61	<d	0.137	0.392	0.404

* Data are shaded as follows: : yellow (value < 1); grey (1 < value < 10); light pink (10 < value < 1,000); dark pink (1,0000 < value). ** <d – non detect.

Table B.3 (cont.). Results of high explosive (HE) analysis of soil samples collected at Vieques, Puerto Rico.

Round Type	Sampling Date	Sample ID	Subsample	Vertical Profile (cm)	Lateral Sampling (cm)	HE Concentration (mg kg^{-1})*								
						HMX	1,3,5 TNB	RDX	1,3 DNB	TNT	Tetryl	2,4 DNT	2Am-DNT	4am-DNT
4.2-in (cont.)	06/17/09	CS09-49	-17	11-13		<d	<d	<d	<d	0.589	<d	0.062	0.202	0.094
			-18	13-16		0.051	0.032	<d	0.069	108	<d	0.978	2.48	1.36
			-19	16-19		<d	<d	<d	<d	0.400	<d	0.027	0.066	0.060
			-20	19-21.5		<d	<d	<d	<d	0.037	<d	0.042	0.121	0.103
			-21	21.5-23		<d	<d	<d	<d	<d	<d	<d	0.086	<d
106-mm	06/23/09	CS09-55	-05		0-5	0.434	<d	1.52	<d	<d	<d	<d	0.216	0.201
			-04		5-10	0.139	<d	0.306	<d	<d	<d	<d	<d	<d
			-03		10-15	0.098	<d	0.486	<d	<d	<d	<d	<d	<d
			-02		15-20	0.380	<d	1.83	<d	<d	<d	<d	<d	<d
			-01		20-30	0.223	<d	0.034	<d	<d	<d	<d	<d	<d
			-06	0-5		0.897	<d	2.58	<d	0.127	<d	0.047	1.63	0.884
			-07	5-10		0.717	<d	2.27	<d	0.084	<d	0.078	1.79	1.03
			-08	10-12		2.04	<d	11.0	<d	0.411	<d	0.170	3.44	1.83
			-09	12-15		42.1	<d	479	<d	331	<d	0.277	2.62	1.60
			-10	15-18		3.39	<d	19.6	<d	1.23	<d	0.123	2.64	1.51
			-11	18-21		5.55	<d	40.8	<d	1.27	<d	0.048	0.829	0.797
155-mm	09/14/10	CS10-11	-01	0-5		<d	<d	0.046	<d	0.179	<d	0.044	<d	<d
			-02	5-10		<d	<d	<d	<d	0.144	<d	0.033	<d	<d
			-03	10-15		<d	<d	<d	<d	<d	<d	<d	<d	<d
			-04		0-5	<d	<d	<d	<d	0.500	<d	0.033	<d	<d
			-05		5-10	<d	<d	<d	<d	0.230	<d	<d	<d	<d
			-06		10-15	<d	<d	<d	<d	1.90	<d	0.063	<d	<d
			-07		15-20	<d	<d	<d	<d	0.786	<d	0.042	<d	<d
			-08		20-25	<d	<d	<d	<d	0.284	<d	<d	<d	<d

* Data are shaded as follows: : yellow (value < 1); grey (1 < value < 10); light pink (10 < value < 1,000); dark pink (1,0000 < value). ** <d – non detect.

Table B.3 (cont.). Results of high explosive (HE) analysis of soil samples collected at Vieques, Puerto Rico.

Round Type	Sampling Date	Sample ID	Subsample	Vertical Profile (cm)	Lateral Sampling (cm)	HE Concentration (mg kg^{-1})*								
						HMX	1,3,5 TNB	RDX	1,3 DNB	TNT	Tetryl	2,4 DNT	2Am-DNT	4am-DNT
105-mm	09/15/10	CS10-16	-01		0-10	9.56	<d	74.3	<d	55.2	<d	<d	0.856	1.42
			-02		10-20	12.0	<d	85.2	<d	62.4	<d	<d	<d	<d
			-03		Chunks	3620	<d	25800	<d	11700	<d	<d	<d	<d
			-04	0-5		<d	<d	1.68	<d	0.057	<d	<d	<d	<d
			-05	5-10		<d	<d	0.304	<d	0.102	<d	<d	<d	<d
			-06	10-15		<d	<d	0.024	<d	0.018	<d	<d	<d	<d
			-07	15-20		<d	<d	<d	<d	<d	<d	<d	<d	<d
			-08	20-25		0.083	<d	0.235	<d	0.208	<d	<d	<d	<d
			-09	0-5		0.305	<d	7.48	<d	0.351	<d	<d	<d	<d
			-10	5-10		<d	<d	0.084	<d	<d	<d	<d	<d	<d
			-11	10-15		<d	<d	0.051	<d	0.071	<d	<d	<d	<d
			-12	15-20		<d	<d	<d	<d	<d	<d	<d	<d	<d
			-13	20-25		<d	<d	<d	<d	<d	<d	<d	<d	<d
			-14	0-5		<d	<d	0.862	<d	<d	<d	<d	<d	<d
			-15	5-10		<d	<d	0.043	<d	<d	<d	<d	<d	<d
			-16	10-15		<d	<d	<d	<d	<d	<d	<d	<d	<d
			-17	15-20		<d	<d	<d	<d	<d	<d	<d	<d	<d
			-18	20-25		<d	<d	<d	<d	<d	<d	<d	<d	<d
			-19	0-5		<d	<d	1.23	<d	0.222	<d	<d	<d	<d
			-20	5-10		<d	<d	0.056	<d	<d	<d	<d	<d	<d
			-21	10-15		<d	<d	<d	<d	<d	<d	<d	<d	<d
			-22	15-20		<d	<d	<d	<d	<d	<d	<d	<d	<d
			-23	20-25		<d	<d	0.034	<d	<d	<d	<d	<d	<d
81-mm	09/16/10	CS10-25	-01	0-5		<d	<d	<d	<d	<d	45.6	<d	<d	<d
			-02	5-10		<d	<d	<d	<d	<d	59.3	<d	<d	<d
			-03	10-15		<d	<d	<d	<d	<d	1.81	<d	<d	<d

* Data are shaded as follows: : yellow (value < 1); grey (1 < value < 10); light pink (10 < value < 1,000); dark pink (1,0000 < value). ** <d – non detect.

Table B.3 (cont.). Results of high explosive (HE) analysis of soil samples collected at Vieques, Puerto Rico.

Round Type	Sampling Date	Sample ID	Subsample	Vertical Profile (cm)	Lateral Sampling (cm)	HE Concentration (mg kg^{-1})*								
						HMX	1,3,5 TNB	RDX	1,3 DNB	TNT	Tetryl	2,4 DNT	2Am-DNT	4am-DNT
HE Dissolution Experiment	09/17/10	CS10-38	-01	0-5		0.034	<d	0.163	<d	0.091	<d	<d	<d	<d
			-02	5-10		<d	<d	0.205	<d	<d	<d	<d	<d	<d
			-03	10-15		<d	<d	0.065	<d	<d	<d	<d	<d	<d
			-04	15-20		<d	<d	0.083	<d	0.029	<d	<d	<d	<d
			-05	20-25		<d	<d	<d	<d	<d	<d	<d	<d	<d
			-06	0-5		10.4	<d	81.5	<d	25.0	<d	0.030	1.01	1.52
			-07	5-10		0.572	<d	5.31	<d	2.26	<d	<d	0.045	0.069
			-08	10-15		0.070	<d	0.375	<d	0.135	<d	<d	<d	<d
			-09	15-20		0.189	<d	1.70	<d	0.850	<d	<d	<d	<d
			-10	20-25		0.398	<d	2.32	<d	1.04	<d	<d	<d	<d

* Data are shaded as follows: : yellow (value < 1); grey (1 < value < 10); light pink (10 < value < 1,000); dark pink (1,0000 < value). ** <d – non detect.

Appendix C. Photographs of rounds sampled without energetic compounds in adjacent soils

Table C.1. Rounds sampled with no high explosive (HE) compounds in surrounding soils. Images of rounds are provided in subsequent figures (Figures C.1 – C.9).

Location*	Munition Type	# UXO Sampled	Round ID	Sampling Date	Condition
ERF	60-mm	7	CS09-04	5/22/2009	Thin corrosion layer on underside
			CS09-06		" "
			CS09-08		" "
			CS09-17	5/26/2009	Slightly rusty
			CS09-18		" "
			CS09-19		" "
			CS09-20		" "
SLO	60-mm (Korean)	4	CS09-79	8/11/2009	Very corroded, metal scaling
			CS09-81		" "
			CS09-84	8/12/2009	" "
			CS09-86		" "
Vieques	60-mm	5	CS10-5	9/13/2010	Very corroded, metal scaling
			CS10-24	9/16/2020	Corroded, longitudinal cracking
			CS10-32		Very corroded, metal scaling
			CS10-33		Corroded with dimpled texture
			CS10-34		Very corroded
	81-mm	8	CS10-4	9/13/2010	Slight corrosion
			CS10-26	9/16/2020	Very corroded
			CS10-27		" "
			CS10-28		" "
			CS10-30		" "
			CS10-31		" "
			CS10-35		" "
			CS10-36		" "
	90-mm	1	CS10-20	9/15/2010	Swollen, longitudinal cracking
	105-mm	5	CS09-34	6/16/2009	Very corroded
			CS09-47	6/18/2009	" "
			CS10-8	9/14/2010	" "
			CS10-18	9/15/2010	Broken open, empty
			CS10-19		Very corroded
	106-mm	1	CS09-44	6/17/2009	Corroded with blisters
	4.2 in.	1	CS10-12	9/14/2010	Corroded
	5 in.	1	CS09-52	6/22/2009	Swollen, flaking metal

* ERF – Eagle River Flats, AK; SLO – San Luis Obispo, CA.

Figure C.1. 60-mm rounds sampled at Eagle River Flats with no HE found in soils.

Figure C.1 (cont.). 60-mm rounds sampled at Eagle River Flats with no HE found in soils.

Figure C.2. 60-mm rounds sampled at San Luis Obispo with no HE found in soils.

Figure C.2 (cont.). 60-mm rounds sampled at San Luis Obispo with no HE found in soils.

Figure C.3. 60-mm rounds sampled at Vieques with no HE found in soils.

Figure C.3 (cont.). 60-mm rounds sampled at Vieques with no HE found in soils.

Figure C.4. 81-mm rounds sampled at Vieques with no HE found in soils.

Figure C.4 (cont.). 81-mm rounds sampled at Vieques with no HE found in soils.

Figure C.4 (cont.). 81-mm rounds sampled at Vieques with no HE found in soils.

Figure C.5 90-mm APHE round sampled at Vieques with no HE found in soils.

Figure C.6. 105-mm rounds sampled at Vieques with no HE found in soils.

Figure C.6 (cont.). 105-mm rounds sampled at Vieques with no HE found in soils.

Figure C.6 (cont.). 105-mm rounds sampled at Vieques with no HE found in soils.

Figure C.7. 106-mm round sampled at Vieques with no HE found in soils.

Figure C.8. 4.2-inch round sampled at Vieques with no HE found in soils.

Figure C.9. 5-inch round sampled at Vieques with no HE found in soils.